OCT - 5 1988

ORNL/Sub/88-SA706/5/V1

MAS

CONTAMINANT TRANSPORT MODEL VALIDATION, GEOHYDROLOGIC SITE CHARACTERIZATION, AND GROUNDWATER FLOW COMPUTER MODEL APPLICATION

Vol. 1

ORNL/Sub/88-SA706/5/V1

Energy Division

CONTAMINANT TRANSPORT MODEL VALIDATION, GEOHYDROLOGIC SITE CHARACTERIZATION, AND GROUNDWATER FLOW COMPUTER MODEL APPLICATION

Report Prepared by
GOLDER ASSOCIATES, INC.
3730 Chamblee Tucker Road
Atlanta, GA 30341
under
Subcontract No. 30X-SA706C

Date Published—September 1988

OAK RIDGE NATIONAL LABORATORY
Oak Ridge, Tennessee 37831-6285
operated by
MARTIN MARIETTA ENERGY SYSTEMS, INC.
for the
U.S. DEPARTMENT OF ENERGY
under
Contract No. DE-AC05-84OR21400

ABSTRACT

A geohydrologic site characterization is being completed in Bear Creek Valley in support of Martin Marietta's Low Level Waste Disposal, Development and Demonstration (LLWDDD) Program. Site characterization studies have included core logging and geohydrologic testing, hydraulic head data collection, groundwater geochemical sampling, contaminant transport model validation, and development of a site groundwater flow and contaminant transport conceptual and computer model. This report presents the results of the contaminant transport model validation study.

The objectives of the model validation study were to plan and execute field tests for the purpose of providing data for validation of contaminant transport computer model(s), to attempt to perform a computer model validation exercise, and to document the degree of success of the exercise.

The test was performed from April through June, 1988 near the geologic contact of the Nolichucky Shale and Maryville Limestone. The test area was located near an existing stream which would act as a likely discharge point for the tracer. The tracer test was completed using Rhodamine WT as the tracer and a series of multi-level piezometers with discrete zone samplers as monitoring points. All samples were analyzed in an on site laboratory using a fluorimeter.

Prior to tracer injection, the hydrogeology at the tracer test area was characterized through the use of rock core drilling, packer testing, and performance of two aquifer pump tests. Site characterization studies at the tracer test area revealed the presence of a seemingly continuous zone of structural deformation located about 60 to 70 feet below the Maryville/Nolichucky contact. Based on pump test results and other hydraulic tests (packer tests and slug tests) it was decided that the tracer would be injected at the water table and the preliminary modeling would be based on a homogeneous anisotropic porous media approach.

After tracer injection it became obvious that the tracer movement was being structurally controlled. The model approach was then modified to simulate a heterogeneous anisotropic porous media. The revised model was successfully calibrated to the observed hydraulic heads and tracer breakthrough curves. The model was then used to predict tracer arrival at more distant points.

Steadily declining water levels throughout the test caused by unusually dry conditions resulted in a non-steady flow field and a reduction in the driving hydraulic gradient at the tracer test well field. Consequently, the steady state modeling approach did not result in a successful model validation.

TABLE OF CONTENTS

Cover Letter

Abstract i
Table of Contents - Volume I of IV iii
- List of Tables - Volume I of IV vi
- List of Figures - Volume I of IV vii
- List of Plates - Volume I of IV ix

Table of Contents - Volume II of IV x
Table of Contents - Volume III of IV xi
Table of Contents - Volume IV of IV xii

SECTION PAGE

1.0 INTRODUCTION 1
1.1 Task 5 Objectives 2
1.2 Task 5 Scope of Work 2

2.0 FIELD TEST PLANNING 7
2.1 Selection of Tracer Test Area 7
2.2 Geologic Description of Tracer Test Area ... 8
2.3 Selection of Tracer 10

3.0 ROCK CORE DRILLING AND LOGGING GW-404, GW-454, GW-455, AND GW-471 14
3.1 Objectives and Scope 14
3.2 Methods and Results 14

4.0 PACKER TESTING OF COREHOLES GW-404, GW-455 AND GW-471 17
4.1 Objectives and Scope 17
4.2 Selection and Description of Packer Test Intervals 17
4.3 Methods of Analysis 18
4.3.1 Field Data Reduction 18
4.3.2 Analytical Methods 20
4.4 Packer Testing Results 22
4.4.1 Hydraulic Head 22
4.4.2 Hydraulic Conductivity 24
4.4.3 Wellbore and Equipment Compressibility and Skin Factors 25
4.5 Discussion of Results 26

5.0 TRACER AREA PUMP TEST DESIGN AND PLANNING 35
5.1 Objectives and Scope 35
5.2 Site Selection and Pumping Test Design 35

TABLE OF CONTENTS
(CONT'D)

6.0 DRILLING AND INSTALLATION OF PUMPING/OBSERVATION AND MONITORING WELLS 41
6.1 Objectives and Scope 41
6.2 Drilling and Installation of Pumping/Observation Wells 42
6.3 Drilling and Installation of Tracer Test Wells 44

7.0 WELL DEVELOPMENT 54
7.1 Objectives and Scope 54
7.2 Discussion of Results 56

8.0 SLUG TESTING 59
8.1 Objectives and Scope 59
8.2 Reduction and Interpretation of Slug Test Data 59
8.3 Discussion of Results 60
8.4 Comparison of Slug Test Results with Pump and Packer Test Results 62

9.0 TRACER AREA PUMPING TESTS 66
9.1 Objectives and Scope 66
9.2 Data Collection and Reduction 67
9.3 Potentiometric Surfaces and Gradients..... 69
9.4 Deep Tracer Pump Test 70
9.4.1 Deep Test - Observed Drawdown Behavior 70
9.4.2 Deep Tracer Pump Test Results 73
9.5 Shallow Tracer Pump Test 79
9.5.1 Shallow Test - Observed Drawdown Behavior 79
9.5.2 Shallow Tracer Pump Test Results 80
9.6 Summary of Tracer Area Pump Test Results ... 84

10.0 FIELD TRACER TEST 101
10.1 Objectives and Scope 101
10.2 Test Design and Planning 101
10.2.1 Injection Depth Selection 101
10.2.2 Injection Well Location 102
10.3 Sampling Equipment and Procedures 103
10.4 Analytical Procedures and Data Collection .. 104
10.5 Field Data and Results 105
10.5.1 Tracer Injection 105
10.5.2 Tracer Detection 106

TABLE OF CONTENTS
(CONT'D)

11.0 TRACER AREA GROUNDWATER FLOW AND SOLUTE TRANSPORT MODELING 115
11.1 Objectives and Scope 115
11.2 Model Setup and Calibration 115
11.2.1 General 115
11.2.2 Mesh Generation 116
11.2.3 Boundary Conditions 117
11.2.4 Groundwater Flow Calibration 118
11.3 Solute Transport Modeling 126
11.3.1 Initial and Boundary Conditions 126
11.3.2 Solute Transport Calibration 127
11.4 Model Validation 135

12.0 DISCUSSION OF RESULTS AND CONCLUSIONS 141
12.1 Final Model Validation 141
12.2 Model Uncertainties and Deficiencies 142
12.3 Conclusions 144

REFERENCES 150

LIST OF TABLES

		PAGE
TABLE 3.1	- Corehole and formation Contact Summary	16
TABLE 4.1	- Description of Packertest Intervals, Tracer Area	30
TABLE 4.2	- Core Hole GW-404, Summary of Packer Test Results	31
TABLE 4.3	- Core Hole GW-455, Summary of Packer Test Results	32
TABLE 4.4	- Core Hole GW-471, Summary of Packer Test Results	33
TABLE 4.5	- Summary of structural Zone Locations, Descriptions, and Hydraulic Conductivity	34
TABLE 6.1	- Construction/Sample Point Summary of Tracer Area Wells	47
TABLE 6.2	- Tracer Area Well Survey Data	50
TABLE 7.1	- Well Development Data, Pumping/Tracer Test Wells	57
TABLE 8.1	- Rising Head Test Summary	64
TABLE 8.2	- Comparison of Slug Test Hydraulic Conductivity Values	65
TABLE 9	- Deep Pumptest/Tracer Area Summary of Drawdown and Recovery Analyses	86
TABLE 9.2	- Shallow Pumptest/Tracer Area Summary of Drawdown and Recovery Analyses	87
TABLE 9.3	- Deep and Shallow Tracer Pumptest Papadopulos Anisotropic Analysis Results	88
TABLE 9.4	- Deep and Shallow Tracer Pumptest Summary of Results and Gringarten-Witherspoon Analysis	89
TABLE 11.1	- Groundwater Flow Model Hydraulic Head Calibration	136
TABLE 11.2	- Solute Transport Calibration After 27 Days	137
TABLE 12.1	- Summary of Tracer Area Water Level Data	146

LIST OF FIGURES

		PAGE
FIGURE 1.1	- Site Location Plan	6
FIGURE 2.1	- General Site Location of Tracer Test Area	13
FIGURE 5.1	- Tracer Pump Test Well and Cross Section Location Plan	39
FIGURE 5.2	- Tracer Pump Test Geologic Section B-B'	40
FIGURE 6.1	- Grain Size Distribution, Coarse Sand	52
FIGURE 6.2	- Grain Size Distribution, Fine Sand	53
FIGURE 9.1	- Tracer Area - Deep Well Potentiometric Contour Map	90
FIGURE 9.2	- Tracer Area - Intermediate Well Potentiometric Contour Map	91
FIGURE 9.3	- Tracer Area - Shallow Well Potentiometric Contour Map	92
FIGURE 9.4	- Tracer Area - Deep Test Drawdown in Deep Wells After Pumping 24 Hours	93
FIGURE 9.5	- Tracer Area - Deep Pump Test Drawdown in Intermediate Wells After Pumping 24 Hours	94
FIGURE 9.6	- Tracer Area - Deep Pump Test Drawdown in Shallow Wells After Pumping 24 Hours	95
FIGURE 9.7	- Tracer Deep Pump Test Transmissivity Vectors From Papadopulos Anisotropic Analysis	96
FIGURE 9.8	- Tracer Area - Shallow Pump Test Drawdown in Intermediate Well After Pumping 24 Hours	97
FIGURE 9.9	- Tracer Area - Shallow Pump Test Drawdown in Shallow Wells After Pumping 24 Hours	98
FIGURE 9.10	- Tracer Area - Shallow Pump Test Drawdown in Deep Well After Pumping 24 Hours	99
FIGURE 9.11	- Tracer Shallow Pump Test Transmissivity Vectors From Papadopulos Anisotropic Analysis	100
FIGURE 10.1	- Tracer Test Well Location Map	109
FIGURE 10.2	- Well No. GW-484 Tracer Concentration Versus Time	110
FIGURE 10.3	- Well No. GW-481B Tracer Concentration Versus Time	111
FIGURE 10.4	- Well No. GW-486 Tracer Concentration Versus Time	112
FIGURE 10.5	- Well No. GW-487 Tracer Concentration Versus Time	113
FIGURE 10.6	- Well No. GW-493 Tracer Concentration Versus Time	114
FIGURE 11.1	- Field Observed Versus Model Predicted Break-Through Curves: GW-484	138

LIST OF FIGURES
(CONT'D)

PAGE

FIGURE 11.2 - Field Observed Versus Model Predicted Break-Through Curves: GW-487 139
FIGURE 11.3 - Field Observed Versus Model Predicted Break-Through Curves: GW-493 140
FIGURE 12.1 - Tracer Area Potentiometric Map, 4/18/88 148
FIGURE 12.2 - Tracer Area Potentiometric Map, 6/17/88 149

LIST OF PLATES

PLATE 1 - Tracer Area Location Plan and Geologic Cross-Section A-A'
PLATE 2 - Finite Element Mesh
PLATE 3 - Material Property Regions
PLATE 4 - Model Generated Potentiometric Map
PLATE 5 - Solute Concentrations After 27 Days

TABLE OF CONTENTS

VOLUME II OF IV

APPENDIX A - ROCK CORE LOGS, GW-404, GW-454, GW-455, and GW-471

APPENDIX B - PACKER TEST DATA AND ANALYSES GW-404, GW-455 AND GW-471

APPENDIX B1 - Arithmetic Transducer Plots
APPENDIX B2 - Reduced Field Data
APPENDIX B3 - Gringarten Log-Log Plots and Data
APPENDIX B4 - Horner Semi-Log Plots

APPENDIX C - FIELD BORING AND WELL INSTALLATION

TABLE OF CONTENTS

VOLUME III OF IV

APPENDIX D - SLUG TEST DATA AND ANALYSES

APPENDIX E - TRACER AREA PUMP TEST DATA AND ANALYSES

APPENDIX E1 - Deep Pump Test Field Data
APPENDIX E2 - Deep Pump Test Arithmetic Plots
APPENDIX E3 - Deep Pump Test Drawdown and Recovery Analyses

TABLE OF CONTENTS

VOLUME IV OF IV

APPENDIX E - Tracer Area Pump Test Data and Analyses

APPENDIX E4 - Shallow Pump Test Field Data
APPENDIX E5 - Shallow Pump Test Arithmetic Plots
APPENDIX E6 - Shallow Pump Test Drawdown and Recovery Analyses

APPENDIX F - TRACER FIELD DATA

1.0 INTRODUCTION

Martin-Marietta Energy System's (MMES) Low Level Waste Disposal, Development and Demonstration (LLWDDD) Program is in the process of developing new low-level radioactive waste disposal methods for use on the DOE Oak Ridge Reservation. Activities are in progress to develop and demonstrate new disposal technologies such as above ground disposal facilities similar to the French "Tumulus" Disposal concept. MMES has retained Golder Associates to perform a geohydrologic site characterization and groundwater flow computer model for a proposed LLWDDD site.

The proposed site (Figure 1.1) is located in Bear Creek Valley (hereafter, referred to as the site) at the Oak Ridge Reservation (ORR) and has been selected by Martin-Marietta for demonstration and possible operational scale development of this disposal technology. Development and operation of new low-level radioactive waste disposal facilities and any future operational scale disposal activities by the Department of Energy, requires preparation of an Environmental Impact Statement (EIS). The EIS must include an analysis of all potential radionuclide migration pathways. For waste disposal facilities located in a humid climate, such as the proposed facility, surface and groundwater pathways are most likely to represent pathways for migration of radionuclides. Consequently, characterization of the site hydrogeology is paramount for the preparation of the EIS.

The program to characterize the hydrogeology of the site has been structured as a phased, yet integrated approach, such that subsequent tasks can be effectively planned from previous results. Therefore, the following seven tasks have been defined by Martin-Marietta for characterizing the hydrogeology of the site:

Task

1 Work Plan Development

2 Well Logging and Geohydrologic Testing

3 Hydraulic Head Data Collection

4 Groundwater Geochemical Sampling and Analysis

5 Contaminant Transport Model Validation

6 Groundwater Flow and Contaminant Transport Conceptual Model

7 Groundwater Flow and Contaminant Transport Computer Model

Golder Associates has previously submitted final reports to MMES on the Task 1 Final Workplan and on Task 2 Well Logging and Geohydrologic Testing dated November 3, 1987, and May 10, 1988, respectively (Reference 3). Tasks 3 and 4 were finalized and delivered to MMES dated September 14, 1988 and September 12, 1988, respectively (References 11 and 17). This report presents the technical approach, field data, interpretation of tests, and results of the Task 5 contaminant transport model validation.

1.1 Task 5 Objectives

As stated in the Final Workplan, the objectives of Task 5 were to plan and execute field tests for the purpose of providing data for validation of contaminant transport computer model(s), and attempt to perform a computer model validation exercise and document the degree of success of the exercise.

1.2 Task 5 Scope of Work

To meet the objectives of Task 5 the task was subdivided into the following 6 sub-tasks:

Sub-task

1 Field Test Planning

2 Tracer Area Drilling and Packer Testing Program

3 Installation of Monitoring Equipment

4 Preliminary Model Validation Runs

5 Test Performance, Modifications and Final Model Validation

6 Deliverables

The sub-tasks were structured such that work could be performed sequentially and that each successive sub-task would build upon the others. The scope of work for each sub-task is presented below. The remaining sections of this report present the details of each work item generally in a chronological order.

Field Test Planning

Planning of the Task 5 field test started very early in the geohydrologic program several months prior to the commencement of drilling and has continued throughout the completion of the remaining sub-tasks. Field test planning included selection of the test location, determination of the appropriate scale at which to complete the test, development of a detailed discrete zone monitoring network, selection of an appropriate tracer and associated monitoring and analysis equipment, and calculations of required tracer amounts and monitoring frequencies.

Tracer Test Drilling and Packer Testing Program

Drilling at the tracer area included rock coring for subsequent packer testing, drilling and installation of shallow system pumping/observation wells for completion of aquifer pumping tests, and drilling and installation of additional

monitoring wells for tracer detection. The scope of work for packer testing at the tracer area included the completion of 24 straddle packer tests in 3 coreholes to identify zones of high hydraulic conductivity that may serve as primary migration pathways.

Installation of Monitoring Equipment

The scope of work for the installation of monitoring equipment included the selection of the appropriate equipment and the actual field installation. Several alternatives were presented in the final Workplan with regard to in-situ monitoring equipment. The type that was employed for this test consisted primarily of small diameter multilevel piezometer completions within a single borehole. Dedicated suction-type sampling devices were then installed at each location.

Preliminary Model Validation Runs

The scope of work for the preliminary model validation runs included model setup, grid development and calibration of the simulated steady state field to the observed hydraulic heads measured in each well. Once the model was calibrated to the flow field the observed tracer migration was used to calibrate the model with regard to solute transport. The calibrated model was then used to predict tracer arrival at more distant points in the flow field.

Test Modifications and Final Model Validation

It was anticipated in the Workplan that, as the tracer moved through the geologic strata toward the more distant wells, it may encounter several flow paths that could cause variations in the local flow direction and subsequent variable dispersion and retardation during tracer movement. In a worst case

scenario, the tracer could move in an entirely unanticipated direction. The scope of work for test modifications and final model validation included provisions for these possibilities. In addition, this sub-task included final model validation runs.

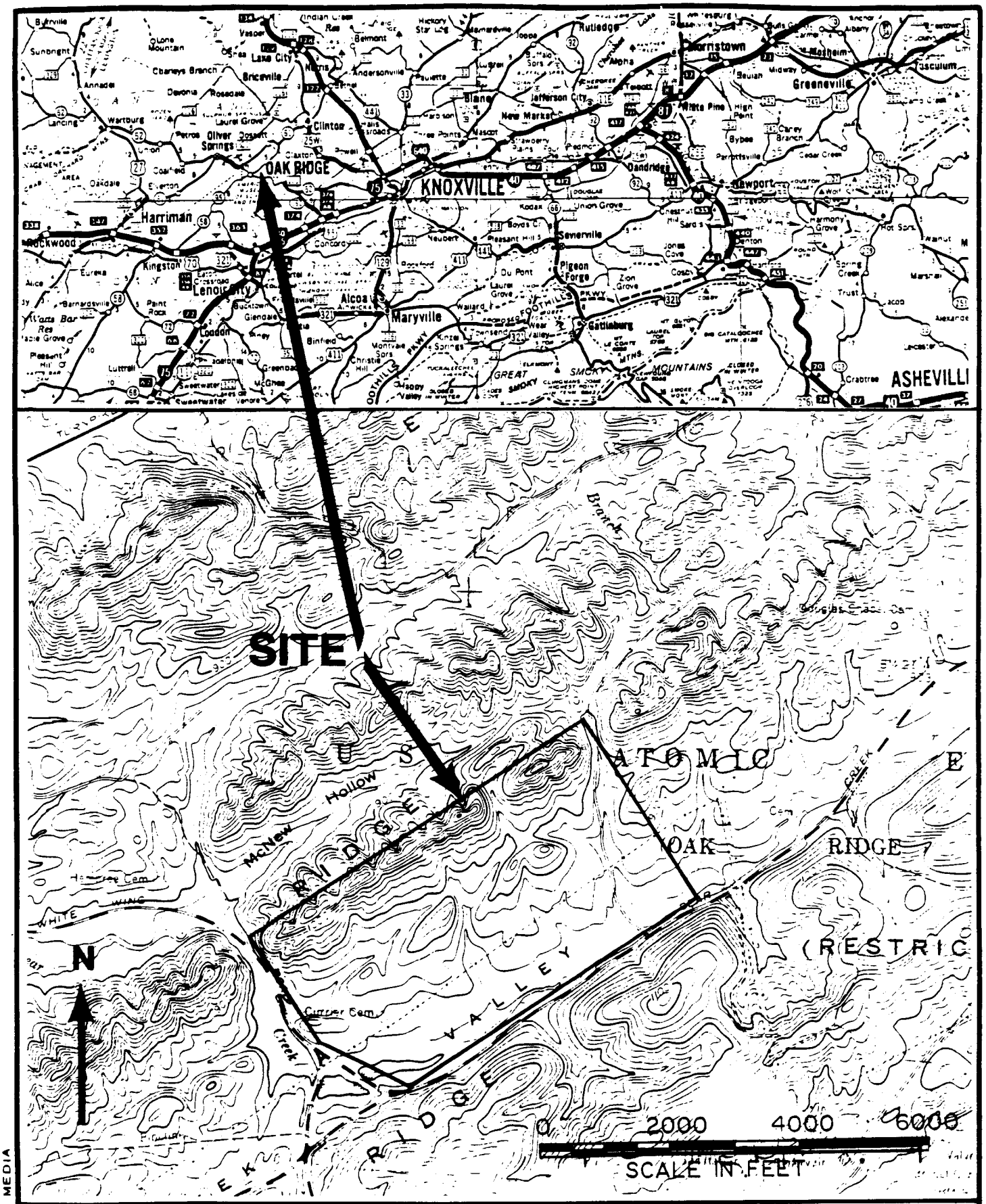

JOB NO. 873-3512.26	SCALE AS SHOWN	SITE LOCATION PLAN	
DRAWN WGG	DATE 3/9/88		
CHECKED RP	DWG NO. 7		
Golder Associates		MARTIN MARIETTA ENERGY SYSTEMS, INC.	FIGURE 1.1

GAF DRAFTING MEDIA

2.0 FIELD TEST PLANNING

As previously stated, the scope of work for field test planning included the selection of the test location, determination of the appropriate scale at which to complete the test, development of a detailed discrete zone monitoring network, and selection of an appropriate tracer. Field test planning was an interactive process. The following presents a narrative explanation of the planning process and a description of resulting tracer test location and the tracer selection. The details of planning and designing the discrete zone monitoring system for the field tracer test are presented in Section 10.0.

2.1 Selection of Tracer Test Area

Selection of the appropriate location to complete the tracer test was dependent upon several factors. First, it was desirable to complete the test under natural gradients with a potential for discharge to a local stream in a reasonable time frame. Consequently, the selected area would have to exhibit a rather high hydraulic gradient (relative to the overall site) and relatively high hydraulic conductivity so as to allow the tracer movement to be fast enough to complete the test within this reasonable time frame. Second, it was desirable for the test to be conducted in a well defined flow field that would minimize the potential for the tracer to move in some unanticipated direction. Third, it was considered appropriate that the geology and general rock structure around the tracer site be characterized in detail with a core drilling and core logging program. Finally, although not of paramount importance, it was desirable for the test to be completed in an area of the site where a potential contaminant leak might occur, i.e. a plausible leak scenario.

The location that was selected to perform the tracer test is presented on Figure 2.1. The selected area meets all of the above criteria. In particular, the local gradient is relatively high, the nearby creek to the west provides a likely local discharge point for the tracer, and the area is located at the geologic contact of two formations that underlie most of the site, namely the Nolichucky Shale and the Maryville Limestone. The following section presents a detailed geologic description of the tracer test site.

2.2 Geologic Description of Tracer Test Area

The tracer test area is located near the central portion of the site, along the formational contact of the Maryville Limestone and Nolichucky Shale which forms a prominent east-west ridge line running along geologic strike, and on the flank of a small valley carved through the ridge line by a local stream (Plate 1). The tracer observation wells are screened in residuum and in rock of the Maryville Limestone or Nolichucky Shale. The location of the tracer well field with respect to the geology of the area is illustrated on the geologic cross section A-A' (Plate 1). This section shows the close proximity of the well field to the Limestone and Shale contact, the approximate thickness of the saprolite, and the relatively steep dip (about 40 to 45 degrees) of the rock strata. Depth to rock in the tracer area ranges from zero, where outcrops occur in the creek bed to the west, to approximately 20 to 25 feet near the crest of the stream valley to the east.

The Maryville Limestone in the tracer area consists of gray limestone and interbedded grayish-black mudstone and shale, with the percentage of limestone being greater than 50%. Fractures in the Maryville predominantly occur along bedding planes with a frequency that may range from 0 to over 10 fractures per foot, but with an average frequency of roughly

5 fractures per foot at depths less than 200 feet. The majority of fractures appear tight and mechanically induced when reviewing rock core. However, some fractures do appear open with secondary calcite infilling or solutioning, and other fractures have slickensided surfaces, indicating bedding plane or dip slip movement.

Zones of more intense structural deformation, such as tight folding and shearing are also found within the Maryville Limestone in the tracer area. A zone of such deformation was observed in coreholes GW-404, GW-455 and GW-471 at depths of approximately 60 to 70 feet below the Nolichucky/Maryville contacts, as shown in Plate 1. A similar feature is present in corehole GW-403 at depths of about 67 to 95 feet below the Nolichucky/Maryville contact. The presence of this structural zone at an approximately similar stratigraphic level in all of the previously mentioned coreholes, suggests the zone may be locally continuous, with the top of bedrock trace of the zone probably lying beneath residuum exposed in the tracer area.

A thin layer of saprolite overlies the bedrock in the immediate vicinity of the tracer test area and ranges from approximately 4 to 25 feet in thickness. The thickness of the saprolite varies according to the degree of weathering of the parent rock. Weathering is controlled by the rock type, the degree of fracturing and groundwater flow characteristics. The saprolite consists of residual soil formed from the in-place decomposition of the parent rock. Saprolite in the tracer area ranges in composition from clay to sandy silt, and contains pieces of intensely to partially weathered rock. The saprolite exhibits a similar residual structure as the rock from which it was derived; therefore, residual bedding of the saprolite also strikes approximately north 56 degrees east, and dips generally 40-45 degrees south. However,

apparent dips of residual saprolite structure generally appear more steep with greater variability in dip near the surface; approximately 45 to 65 degrees.

2.3 Selection of Tracer

One of the major components of planning the field tracer test was the selection of an appropriate tracer. Ideally, the selected tracer should be easily detectable, environmentally safe, readily available, and should possess physical characteristics, such as density and viscosity, that would allow it to move through the geologic media in a manner that would simulate likely contaminant movement. For the purposes of this test, however, the tracer was required to be relatively non-sorbing and easily dissolved or soluble in water.

Several tracers were considered. Initially, Golder Associates recommended using a radioactive tracer such as Iodine-131, Bromine-88 or Strontrium-85. The intent was that this type of tracer would ideally simulate a realistic leak scenario, would be relatively non-sorbing, and could easily be detected using downhole in-situ instrumentation. However, this type of tracer does pose significant complications with regard to handling, permitting and environmental impact. Consequently, radioactive tracers were considered not feasible and an alternative tracer type was sought.

Other tracers that were considered included ion specific solutions such as sodium chloride, and potassium chloride. These tracers, although environmentally safe and easily detectable with downhole in-situ instrumentation, pose serious problems with regard to density contrasts. Typically, the high concentration of these solutions that is required, results in tracer migration that is not typical of natural groundwater flow paths.

The third class of tracers that were considered were dyes of the colorimetric type. These tracers are well suited for the required application with the one exception that they are not easily detectable with downhole in-situ instrumentation. It is necessary to obtain a sample of water from the well for each analysis.

Rhodamine WT was selected as the tracer for this test. Rhodamine WT is a dye that was developed specifically for tracer work (Reference 16) and can be detected in very small quantities using a fluorimeter. The minimum detectability of Rhodamine WT, according to Reference 16, is 0.013 ug/liter (0.013 ppb), where the minimum value is taken as a reading 10% in excess of background fluorescence for distilled water or 1 scale unit. The fluorimeter type used for the above work, however, was not the same as that used for this test. As described later in Section 10.3, the instrument used in the test described in this report is capable of routine detection limits of about 0.1 ppb, although it can be used for lower values.

The emission fluorescence of Rhodamine WT is not affected by pH values when a specific excitation warelength is used. Site groundwater pH values are typically higher than 6.0 which further stabilizes the emmission intensity and, hence, produces concentrations that are not pH sensitive. The dye fluorescence is, however, affected by temperature variations. Although the groundwater temperatures during the test were not expected to have much variation, care had to be taken in the analysis stage. All samples were transferred from the field to the on-site laboratory and in general, were at the same temperature of the calibration standards. Similarly, the dye fluorescence is affected by highly saline waters, however, these water types are not present at the tracer area.

Rhodamine WT is not the ideal tracer from the point of view of adsorbing properties on natural materials. It may be expected to lose up to 35% of its fluorescence in sediment loaded waters, particularly where limestone and kaolinite materials are present. However, there is a marked decrease in percentage of dye loss with increasing dye concentration. The dye is also considered to have negligible toxicity properties compared with other dyes such as Rhodamine B. The dye is thus environmentally safe, readily available, and has physical characteristics not too dissimilar to water.

Dedicated automatic samplers were installed at selected wells to obtain water samples for analysis. All samples were then analyzed using a fluorimeter capable of detecting the dye at concentrations in the parts-per-billion range. The samplers and analytical methods are discussed in more detail in Section 10.0.

A F 20440C D

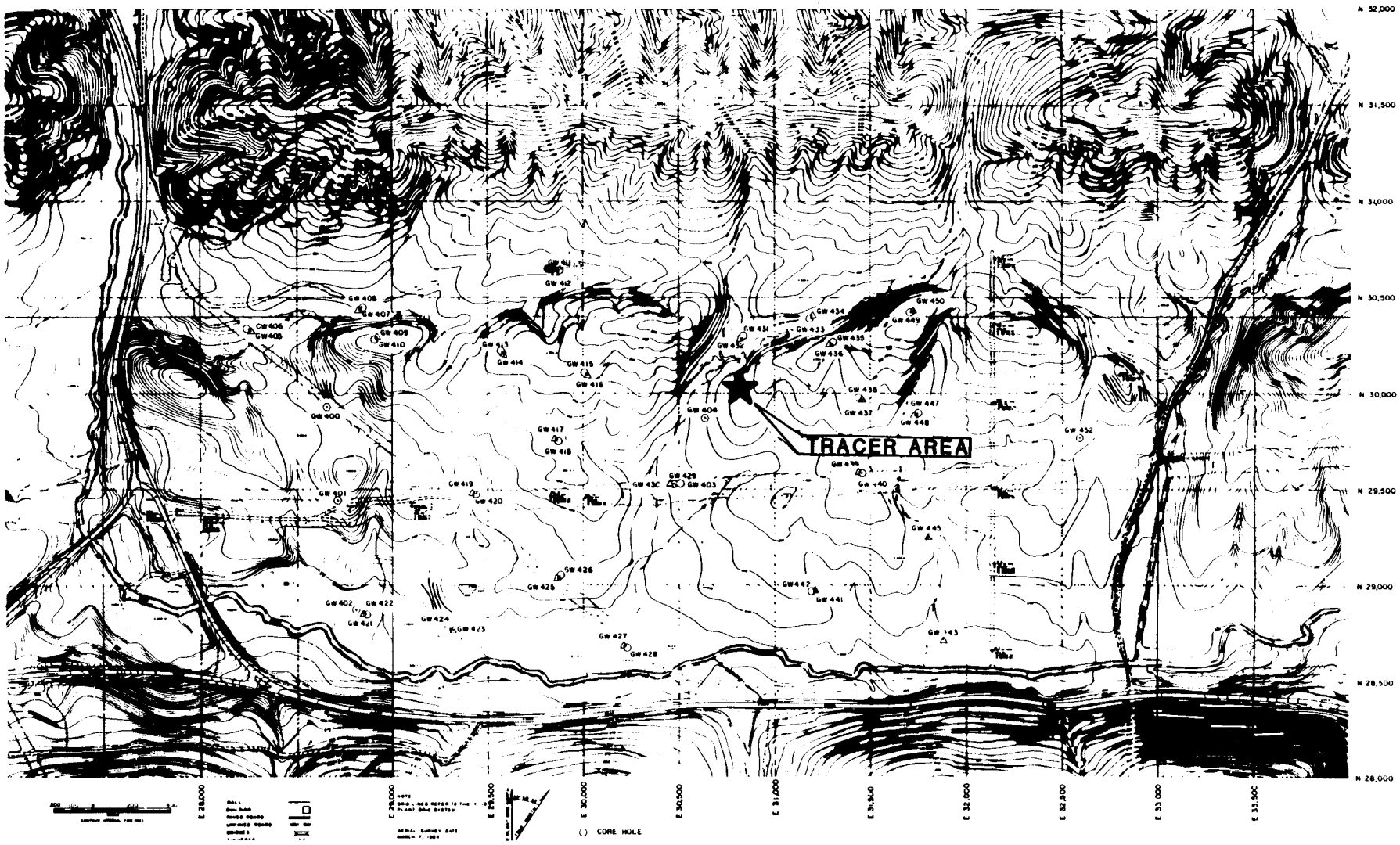

JOB NO. 873-3512	SCALE AS SHOWN	GENERAL SITE LOCATION OF TRACER AREA	
DRAWN	DATE 6/7/88		
CHECKED	DWG. NO 47		
Golder Associates		MARTIN MARIETTA ENERGY SYSTEMS, INC.	FIGURE 2.1

3.0 ROCK CORE DRILLING AND LOGGING GW-404, GW-454, GW-455, AND GW-471

3.1 Objectives and Scope

The primary purpose of drilling and logging coreholes in the Model Validation Area was to provide data for more effective planning of the field tracer test program. The corehole data were used to better define subsurface geologic controls on groundwater flow, and to provide information that was used for selecting zones for packer testing. Corehole data and subsequent packer test results were used to plan and design the tracer field test drilling program and to supplement the overall site characterization program.

A total of 401 feet of rock was logged under Task 5.2 from the following coreholes: GW-404, GW-454, GW-455 and GW-471. Total depths of coreholes and associated cased intervals are presented in Table 3.1. Corehole GW-454 was terminated and abandoned at a depth of 57.8 feet due to poor drilling conditions. A new corehole GW-455, was completed approximately 5 feet northeast of GW-454 to a depth of 293.0 feet. All coreholes, with the exception of GW-404, were logged at the drilling site by a Golder Associates geologist. Corehole GW-404 was previously drilled by Martin Marietta, and was logged by a Golder geologist in the core shed. The locations of these coreholes are illustrated on Plate 1.

3.2 Methods and Results

The coreholes were drilled by Martin Marietta subcontractors in general accordance with the drilling procedures presented in Appendix A2 of the Task 2 report (Reference 3). One significant exception was that a double tube core barrel was used instead of a triple tube barrel as originally specified in the work plan. Using the double tube barrel led to repeated problems in removing the core from the barrel, particularly when the lithology consisted largely of

mylonitic shale which swelled upon recovery. In order to remove such core the barrel was tapped with a hammer, while pushing on a rod inserted behind the core. In many cases, the resultant quality of the core was poor and may not be fully representative of subsurface conditions.

A Golder geologist was assigned to the drill rig during the coring of additional holes GW-454, GW-455, and GW-471. All core was logged immediately at the drilling site and placed in properly labeled boxes by the geologist in accordance with the procedures presented in Appendix A1 of the Task 2 report (Reference 3). All rock core was logged in detail for the same lithologic, structural, and geohydrologic information as the logging of existing rock core under Task 2. All core logs were reviewed and checked by a project level geologist.

Field log data were entered into a computer log format (Goldlog-Seatlog) in the Atlanta office, and are presented in Appendix A. Copies of original field logs have been forwarded to MMES in Quarterly data packages (References 5 and 6). Data obtained from the logging of core was used for determining stratigraphic contacts. All formation contacts (Table 3.1) were agreed upon in the field by the Golder geologist and MMES personnel.

TABLE 3.1

COREHOLE AND FORMATION CONTACT SUMMARY

HOLE NO.	TOTAL DEPTH (ft)	HOLE CASED TO (ft)	DOWNHOLE DEPTHS OF FORMATION CONTACTS (ft) RM	PV	RT	RG	MR	NL	MD
GW-136(1)	800.0	39.0					580	*	
GW-137	1000.0	40.0					911	236	*
GW-138	1095.0	35.0						977	532
GW-400(1)	1251.5	24.0	1056	680	558	465	26(G)		
GW-401(1)	862.8	74.0					451	*	
GW-402(1)	600.0	75.0						110	*
GW-403(1)	612.9	80.5					311		
GW-404	200.0	21.0					11(G)		
GW-453(1)	810.8	60.4	745	347	221	70	*		
GW-454	57.8	11.4							
GW-455(2)	293.0	10.2					109	*	
GW-468	500.5	27.0						80	*
GW-471(1)	104.7	18.8					10		

NUMBERS INDICATE DEPTHS TO FORMATION CONTACTS SPECIFIED IN DRILLED HOLE (FT. BELOW GROUND SURFACE).

* - INDICATES THE HOLE IS COLLARED IN THIS FORMATION.

G - CONTACT PICKED BASED BASED ON GEOPHYSICAL LOG.

NOTES: (1) COREHOLE COMPLETED AS A ONE-INCH PVC OBSERVATION WELL.
(2) COREHOLE COMPLETED AS A TWO-INCH PVC OBSERVATION WELL.

FORMATION ABBREVIATIONS: RM - ROME FORMATION; PV - PUMPKIN VALLEY SHALE; RT - RUTLEDGE LIMESTONE RG - ROGERSVILLE SHALE; MR - MARYVILLE LIMESTONE; NL - NOLICHUCKY SHALE; MD - MAYNARDVILLE. LIMESTONE.

REFERENCE: GEOLOGIC CONTACTS BASED ON VERBAL COMMUNICATION WITH MR. RICHARD LEE AND MR. RICHARD KETELLE OF MARTIN MARIETTA ENERGY SYSTEMS INC.

4.0 PACKER TESTING OF COREHOLES GW-404, GW-455 AND GW-471

4.1 Objectives and Scope

The objective of the packer testing program at the model validation area was to identify zones of hydraulic conductivity that may act as primary migration pathways. In addition, the hydraulic head estimates were used to help characterize the local flow system at the tracer area.

All packer tests were completed in accordance with the procedures outlined in Appendix A3 of the Task 2 Final report (Reference 3). A total of 24 tests were completed in coreholes GW-404, GW-455, and GW-471.

4.2 Selection and Description of Packer Test Intervals

In general, selection of packer test sections was based on review of the rock core logs, presented in Appendix A. Coreholes GW-404 and GW-471, however, were tested throughout their entire length with a 12-foot packer spacing.

The objective of such back-to-back testing was to provide bench-mark values of hydraulic conductivity and hydraulic head at depth at the tracer area. The test sections in corehole GW-455 were selected as zones that were expected to exhibit high hydraulic conductivity. Because of the relatively shallow depth of this corehole and the number of tests completed, for practical purposes the corehole was tested throughout its entire depth. It should be noted, however, that no tests could be completed below about 175 feet in corehole GW-455 due an offset or blockage in the corehole that would not allow the packers to pass. Table 4.1 presents the depth and geologic formation of each tested zone.

4.3 Methods of Analysis

Methods of analysis of packer test data generally fall into two categories, semi-log or conventional analyses, and log-log type-curve analyses. Data obtained may be suitable for one type of analysis, both, or in a few cases neither. For this project, semi-log methods were used in the field to provide preliminary estimates and to help guide the field program. In the office, however, log-log procedures were used to reevaluate which tests were suitable for semi-log methods. In the office, the analysis procedure consisted of data reduction, followed by log-log curve matching, followed by semi-log analysis, and completed with specialized analyses such as pressure slug decay, boundary, and sensitivity analyses. For the twenty-four tests completed at the tracer area, none were suitable for pressure slug decay or boundary analyses.

4.3.1 Field Data Reduction

An arithmetic plot of the transducer readings for each test is provided in Appendix B1 of this report. The field data are presented in Appendix B2. The first step in data reduction was to reduce the transducer readings to total hydraulic head. This was accomplished by expressing the transducer pressure as feet of water and adding it to the elevation above mean sea level of the transducer position in the borehole. For example, a transducer located at 600 FT. MSL with a reading of 100 psi would be equivalent to about 830 feet of total hydraulic head. The hydraulic head values, presented in Appendix B2, are expressed in terms of a fresh water head; density gradients due to salinity and temperature variations are assumed to be negligible. Geochemical analyses as part of Task 4 (Reference 17) indicated the presence of elevated chloride content in many of the groundwater samples, possibly a result of mixing with saline waters. However,

specific gravity tests indicated that hydraulic head variations due to density contrasts would be negligible. Also, it should be noted that the transducer elevations presented in Appendix B2 are based on survey data that were available at the time of field testing. In some instances, there may be a slight (less than 0.3 ft.) discrepancy between the ground surface elevations presented in Appendix B2 and on Table 6.2. Table 6.2 supersedes Appendix B2 elevation data.

The second step of data reduction was to calculate the flow rate and the elapsed shut-in time data. Shut-in data refers to the transducer pressure readings obtained immediately after a flow period. During the flow period, the downhole valve is open and water is allowed to flow from the formation into the rods through the perforated sections. The rate of rise of water in the N-size rods (i.e. the slope of the arithmetic plot of the pressure in the test section vs. time) is used to calculate the flow rate. Once the valve is shut, the flow period ends and the shut-in period begins.

Appendix B2 presents the shut-in data and flow rates. In determining the exact time of shut-in, a 30 second valve delay was used. The actual valve delay was calculated for over 100 cases and ranged from about 25 seconds to 40 seconds. Note that for the preliminary field analyses valve delay was assumed to be zero. The shut-in data are designated in Appendix B2 under the column "test status" by the numbers 4 and 6 for first and second shut-in, respectively. The actual data used in the flow rate calculation, described above, are denoted with a "*" and "**" for the first and second flow periods, respectively.

4.3.2 Analytical Methods

Log-Log Analysis - All tests were analyzed according to a procedure outlined by Gringarten et al. (Reference 7). The Gringarten procedure is a type curve procedure in which a log-log plot of residual drawdown (hydraulic head at some time after shut-in minus hydraulic head at shut-in) verses elapsed shut-in time is constructed. The log-log plot is then superimposed against a family of type curves. The residual drawdown plots, type curve, and field data are presented in Appendix B3. For a more detailed theoretical discussion of the Gringarten method, see Reference 7.

This method results in an estimate of hydraulic conductivity, wellbore compressibility, and a dimensionless skin factor. In addition, the procedure provides an indication of when the front-end effects i.e., skin and storage have dissipated and when the semi-log straight line data should occur. The Gringarten et al. type curves are presented in Appendix B3 as Figure B2-1.

Wellbore Storage and Skin Effects - Wellbore storage and skin effects generally manifest themselves in the early time data of pressure build-up. Immediately after shutting in a producing well, a small amount of flow may still be occurring at the corehole face, often referred to as after-flow. This volume of water may be stored in the wellbore due to compliance in the rock mass immediately surrounding the borehole and in the down hole equipment such as packers and plastic tubing. As a result, the pressure in the tested interval may not build as rapidly as would be expected.

Skin effects are a result of damage to the corehole face during drilling. The face can become smeared, fractured, or filled with fine cuttings, etc. As a result, the early pressure response during shut-in may be more representative

of the hydraulic characteristics at the corehole face rather than the geologic formation itself. Skin effects can be either positive or negative and may cancel or compound wellbore storage effects. For these reasons, the early shut-in time data may be misleading.

Semi-Log Analysis - The shut-in data presented in Appendix B2 were analyzed (where applicable) according to the method described by Horner (Reference 9). The Horner method is a semi-log method in which the head (or pressure) is plotted against the log of the ratio of the duration of the flow period (T), plus the elapsed shut-in time (t'), to the elapsed shut-in time i.e.

$$H \text{ vs. } \text{Log } [(T + t')/t']$$

Where: H = Total Hydraulic Head (FT MSL)
T = Duration of Flow Period (Min)
t' = Elapsed time since shut-in (Min)

It can be seen from the above that, as the elapsed shut-in time (t') increases, the log [(T + t')/t'] will decrease. Consequently, for convenience, the function is often plotted on a reversed X-axis i.e. decreasing to the right. For computational convenience, this was done by plotting head verses minus the Log [(T + t')/t']. Also note that as the shut-in time increases the value of [(T + t')/t'] will approach unity and the log will approach zero.

According to Horner, a portion of the shut-in data plotted as described will fall on a straight line. However, the early and late data may deviate from the straight line due to wellbore storage and skin, or boundary effects, respectively. The slope of the identified straight line portion can be used to calculate the hydraulic conductivity of the tested interval.

In addition to hydraulic conductivity, the Horner plot can be used to estimate the static head of the tested interval. As previously stated, as the elapsed shut-in time (t') increases, the value of log [(T + t')/t'] will approach zero. Consequently, the straight line portion of the Horner plot can be extrapolated to log [(T + t')/t'] = 0 which will correspond to large values of elapsed shut-in time (t').

The Horner analysis method presented above is essentially the same as the Theis recovery method (Reference 12). Both methods are based on the solution to the partial differential equation governing groundwater flow.

The Horner method assumes a constant flow rate during the flow period and does not quantitatively consider the effects of wellbore storage, skin, or boundary effects. The Horner Analyses are presented in Appendix B4. For more detailed procedures and theory regarding the Horner analysis, see References 9 and 12.

4.4 Packer Testing Results

4.4.1 Hydraulic Head

Plate 1 and Tables 4.2 through 4.4 present the results of the packer tests completed in coreholes GW-404, 455, and 471, respectively. The tables present the estimated static head for each tested zone, the semi-log and log-log hydraulic conductivity estimates, as well as estimates of wellbore compressibility and skin factors. It should be noted that all results presented in Tables 4.2 through 4.4 are based on the second shut-in period only unless otherwise noted. For comparative purposes Appendix B2 does include the semi-log estimates of hydraulic conductivity based on the first shut-in period. These results are in general agreement with

the second shut-in period results. Each of the hydraulic parameters presented in Tables 4.2 through 4.4 are discussed below.

The hydraulic head estimates in GW-404 (ground surface = 852.30 ft. MSL, Table 4.2) ranged from a low value of about 846 ft. MSL to about 857 ft. MSL. While there is variability in head values down the length of the borehole, the presence of higher heads at the bottom of the borehole, compared with the top of the borehole, indicate vertically upward gradients are probable. In addition, the borehole had been noted to flow under artesian conditions, further confirming this analysis.

The hydraulic head estimates in GW-455 (ground surface = 853.44 ft. MSL, Table 4.3) ranged from about 846 ft. MSL to about 850 ft. MSL. It is difficult to assess the overall head conditions of this corehole in that only five tests were conducted and no tests were completed below 175.0 feet, although upward gradients seem to prevail.

In general, the head distribution in GW-471 (ground surface = 864.14 ft. MSL, Table 4.4) appears to be in hydrostatic equilibrium at about 852 ft. MSL.

In summary, the distribution of shallow heads in corehole GW-404, GW-455 and GW-471, as estimated from packer tests, indicate that the tracer test area is underlain by a local discharge zone, discharging to the nearly stream. The deeper heads can be interpreted as a second flow system that may pass under the stream. This interpretation is consistent with the Task 2 initial modeling effort.

4.4.2 Hydraulic Conductivity

The hydraulic conductivity estimates for GW-404, expressed as mean values of semi-log and log-log analyses, range from about 1.7×10^{-4} cm/s to about 2.8×10^{-6} cm/s. Most estimates, however, exhibited hydraulic conductivities in the 5×10^{-6} cm/s to 5×10^{-5} cm/s range. The highest value of 1.7×10^{-4} cm/s was found at depths of 110.0 to 122.0 feet.

Of the five tests completed in corehole GW-455, all were near 10^{-5} cm/s, with the exception of the 4.6×10^{-7} cm/s estimate at 109.0 to 131.0 feet. Again, it is difficult to assess the complete range in hydraulic conductivity in this corehole since only five tests were completed and none were completed below about 175.0 feet. A zone from 175 to 195 feet in depth was anticipated to be a significant flow zone, since the rock core exhibited significant structural deformation with some bedrock solutioning evident. Unfortunately, this zone could not be tested due to hole blockage. The location of this structural zone relative to the packer test intervals is clearly shown in Plate 1.

Corehole GW-471, in the Maryville Limestone, appears to indicate an overall trend of decreasing hydraulic conductivity with depth. The hydraulic conductivity range is from about 3.0×10^{-4} cm/s to about 5.0×10^{-6} cm/s. The two extreme values occurred between 33.0 to 45.0 feet and between 81.0 to 93.0 feet, respectively. The bottom 3 feet of the corehole, however, showed evidence of high hydraulic conductivity (7.1×10^{-5} cm/s); however, data from this test may be suspect as detailed review of the data suggests there may have been a poor lower packer seal. Field personnel confirmed that the packer tool become repeatedly stuck in and near this zone which may have caused crimping of the packer inflation

line. However, a piezometer installed in this zone produced a hydraulic conductivity of about 1 x 10^{-5} cm/s from both slug and pumping test results.

4.4.3 Wellbore and Equipment Compressibility and Skin Factors

Wellbore compressibility factors for all tests range from 0.002 cm^2 to 7.59 cm^2. However, the geometric mean value for coreholes GW-404, 455, and 471 were 0.05, 0.07, and 0.34 cm^2, respectively. The full range of wellbore compressibility values range from equivalent to the compressibility of water to 4000 times higher than can be attributed solely to the compressibility of water. The compressibilities are attributable to that of water and either the rock mass or equipment compliance or a combination of both, with the rock mass becoming dominant as the compressibility rises due to fracture compression and expansion. In subsequent equipment compliance testing, in a rigid 4 inch diameter steel casing, there was no evidence of significant packer equipment compliance.

Skin factors ranged from 3.0 to 28. Normal skin factors range from about -5 for a highly developed zone to positive infinity for a zone that is too damaged to produce. Generally, skin factors values that exceed 10 would be considered severely damaged by near-hole sealing. The average skin factor values for coreholes GW-404, 455 and 471 are, 17.3, 7.3, and 14.02, respectively. Note that all skin factors were positive.

4.5 Discussion of Results

As stated in Section 4.1, the primary objective of the packer testing program was to identify zones of high hydraulic conductivity that may act as migration pathways for contaminants. Additionally, it was desirable to identify these potential zones of migration as part of planning the field tracer test.

Results of the core drilling program had indicated the presence of a seemingly continuous zone of structural deformation between coreholes GW-404, GW-455, and GW-471 at about 60 to 70 feet below the Maryville/Nolichucky Contact and GW-403 at about 67 to 95 feet below the contact. Table 4.5 summarizes the description, locations, and depths at which the zone of structural deformation was noted. The structure zone is depicted in Plate 1.

To evaluate the flow potential of the structural zone, several packer tests were completed in coreholes GW-404, GW-471, GW-455, within the zone and above and below the zone. The results of these tests are included in Table 4.5.

In corehole GW-404 the structural zone was tested at a depth of 74.0 to 86.0 feet and yielded a hydraulic conductivity of 4.3×10^{-5} cm/s. The tested sections immediately above and below the zone yielded hydraulic conductivities of 7.0×10^{-6} cm/s and 5.42×10^{-6} cm/s, respectively (Table 4.2). It is noted, however, that several tested sections beneath the structural zone gave higher values of hydraulic conductivity even though there was no indication that they contained structural deformations of the type noted at 74 to 86 feet depth. It is also noted that a test in a deeper section with similar structural deformation features (134.0 to 146.0 feet) yielded a hydraulic conductivity of 5.86×10^{-5} cm/s, while a

more shallow test again with similar structural deformation (50-62 ft.) yielded a hydraulic conductivity of 9.36 x 10^{-6} cm/s.

In corehole GW-471, along strike from GW-404, the structural zone was tested at depths of 81.0 to 93.0 feet and 84.4 to 96.4 feet and yielded hydraulic conductivities of 5.39 x 10^{-6} cm/s and 7.1 x 10^{-5} cm/s, respectively. These tests were in overlapping sections with the latter (deeper) test very close to a second zone of deformation at the bottom of the corehole. Thus, the deeper test may have tapped into this deeper zone of deformation, since it was observed that the lower packer may not have sealed correctly, possibly due to intense fracturing. The very bottom of corehole GW-471 was not straddle packer tested but the entire bottom section was comleted as a pump test observation well and yielded a hydraulic conductivity of 1.28 x 10^{-5} cm/s, thus, confirming the apparent high value indicated by packer testing.

In corehole GW-455, packer testing could not be completed beneath a depth of 174.8 feet due to an offset in the corehole which would not allow the packers to pass. A zone of structural deformation is evident beneath this depth which corresponds to the depth beneath the Maryville/Nolichucky contact where deformation was noted in corehole GW-404 (Table 4.5).

In corehole GW-403 two packer tests were completed in sections which contained structural deformation (Table 4.5). The shallow test was just beneath the Maryville/Nolichucky contact and yielded a low hydraulic conductivity of 4.9 x 10^{-8} cm/s. The deeper test was about 80 to 100 feet beneath the contact and yielded a low hydraulic conductivity of 1.37 x 10^{-7} cm/s. This latter section lies deeper in the formation than the zone tested in GW-404 and may not be related. The low value of hydraulic conductivity could be

caused by the greater depth beneath ground surface which might indicate a fracture closing phenomena caused by higher stresses.

Based on review of these results, the following observations are made:

- In general, packer tests indicate the zone of structural deformation in coreholes GW-404 and GW-471 has hydraulic conductivity values of about 5 x 10^{-5} cm/s. Similar zones in GW-455 could not be tested but were highly fractured and those in GW-403 were hydraulically tight, probably due to higher stresses caused by greater depth.

- It is noted that hydraulic conductivities on the order of 10^{-4} cm/s to 10^{-5} cm/s were observed at locations that were not identified as structural or shear zones.

Based on packer test results, it is concluded that the discrete zone of structural deformation does possess discrete sections with high hydraulic conductivity. The flow path continuity and relative size of the flow paths could not, however, be determined by this packer test program since the packer spacing is too large and borehole interconnectivity tests were not performed during packer testing.

Overall, the packer testing was effective in evaluating the location of possible migration pathways within the rock. The results also allowed identification of zones of high permeability and delineated the sub-horizontal layered nature of the aquifer system that exists at the area. In addition, the hydraulic head results were used to characterize the local flow system at the tracer area and confirmed that the area was most likely a discharge area to the nearby stream, at least in the upper 100 feet.

The results of the packer testing program were used to plan the field pump test and tracer test in terms of sections of rock to isolate with screens in order to determine, in greater detail, the nature of the flow paths within both the shallow (top of bedrock) and deeper (structural zone) systems.

TABLE 4.1
DESCRIPTION OF PACKER TEST INTERVALS
TRACER AREA

TEST NO.	TESTED ZONE (FT BELOW GS)	FORMATION TESTED
GW-404-1	26.5 to 38.5	UPPER MARYVILLE
GW-404-2	38.0 to 50.0	UPPER MARYVILLE
GW-404-3	50.0 to 62.0	UPPER MARYVILLE
GW-404-4	62.0 to 74.0	UPPER MARYVILLE
GW-404-5	74.0 to 86.0	UPPER MARYVILLE
GW-404-6	86.0 to 98.0	UPPER MARYVILLE
GW-404-7	98.0 to 110.0	UPPER MARYVILLE
GW-404-8	110.0 to 122.0	UPPER MARYVILLE
GW-404-9	122.0 to 134.0	UPPER MARYVILLE
GW-404-10	134.0 to 146.0	UPPER MARYVILLE
GW-404-11	146.0 to 158.0	UPPER MARYVILLE
GW-404-12	158.0 to 170.0	MIDDLE MARYVILLE
GW-404-13	170.0 to 182.0	MIDDLE MARYVILLE
GW-455-1	87.0 to 109.0	LOWER NOLICHUCKY
GW-455-2	109.0 to 131.0	CONTACT NOLICHUCKY
GW-455-3	138.0 to 160.0	UPPER MARYVILLE
GW-455-4	152.8 to 174.8	UPPER MARYVILLE
GW-455-5	65.0 to 87.0	LOWER NOLICHUCKY
GW-471-1	57.0 to 69.0	UPPER MARYVILLE
GW-471-2	69.0 to 81.0	UPPER MARYVILLE
GW-471-3	81.0 to 93.0	UPPER MARYVILLE
GW-471-4	84.4 to 96.4	UPPER MARYVILLE
GW-471-5	45.0 to 57.0	UPPER MARYVILLE
GW-471-6	33.0 to 45.0	UPPER MARYVILLE

NOTE: UPPER, MIDDLE AND LOWER REFER TO DEPTH WITHIN EACH GEOLOGIC FORMATION AND IS NOT INTENDED TO INFER STRATIGRAPHIC MEMBERS.

TABLE 4.2

CORE HOLE GW-404
SUMMARY OF PACKER TEST RESULTS

TEST NO.	TESTED ZONE BELOW G.S. (FT) (G.S.= 852.30 FT MSL)	ESTIMATED STATIC HEAD (FT MSL)	HYDRAULIC CONDUCTIVITY SEMI-LOG METHOD (CM/S)	HYDRAULIC CONDUCTIVITY LOG-LOG METHOD (CM/S)	GEOMETRIC MEAN HYDRAULIC CONDUCTIVITY (CM/S)	WELLBORE COMPRESSIBILITY (CMCM)	SKIN FACTOR DIMENSIONLES
GW-404-1	26.5 to 38.5	847.00 (2)	(1)	1.90E-05	1.90E-05	0.05	8.65
GW-404-2	38.0 to 50.0	847.00 (2)	(1)	9.40E-06	9.40E-06	0.01	14.02
GW-404-3	50.0 to 62.0	847.00	5.84E-06	1.50E-05	9.36E-06	0.01	27.83
GW-404-4	62.0 to 74.0	851.00 (2)	(1)	7.00E-06	7.00E-06	0.01	5.71
GW-404-5	74.0 to 86.0	850.60	3.24E-05	5.70E-05	4.30E-05	0.26	6.66
GW-404-6	86.0 to 98.0	851.20	5.75E-06	5.10E-06	5.42E-06	0.01	14.29
GW-404-7	98.0 to 110.0	850.10	5.40E-05	8.00E-05	6.57E-05	0.08	8.42
GW-404-8	110.0 to 122.0	847.10	1.55E-04	1.90E-04	1.72E-04	0.29	5.47
GW-404-9	122.0 to 134.0	848.20	2.41E-05	3.50E-05	2.90E-05	0.04	4.11
GW-404-10	134.0 to 146.0	848.70	2.86E-05	1.20E-04	5.86E-05	0.07	38.40
GW-404-11	146.0 to 158.0	856.10	1.14E-06	2.60E-05	5.44E-06	0.02	39.05
GW-404-12	158.0 to 170.0	846.00	6.89E-06	2.40E-04	4.07E-05	0.47	37.46
GW-404-13	170.0 to 182.0	857.10	1.01E-06	7.60E-06	2.77E-06	0.09	15.27

(1) DATA NOT SUITABLE FOR HORNER ANALYSIS

(2) HEAD ESTIMATED FROM ARITHMETIC PLOTS

TABLE 4.3

CORE HOLE GW-455
SUMMARY OF PACKER TEST RESULTS

TEST NO.	TESTED ZONE BELOW G.S. (FT) (G.S.= 853.44 FT MSL)	ESTIMATED STATIC HEAD (FT MSL)	HYDRAULIC CONDUCTIVITY SEMI-LOG METHOD (CM/S)	HYDRAULIC CONDUCTIVITY LOG-LOG METHOD (CM/S)	GEOMETRIC MEAN HYDRAULIC CONDUCTIVITY (CM/S)	WELLBORE COMPRESSIBILITY (CMCM)	SKIN FACTOR DIMENSIONLES
GW-455-5	65.0 to 87.0	845.90	5.58E-05	7.50E-05	6.47E-05	0.11	3.57
GW-455-1	87.0 to 109.0	848.00 (1)	(2)	1.60E-05	1.60E-05	0.02	16.23
GW-455-2	109.0 to 131.0	849.60	2.76E-07	7.80E-07	4.64E-07	0.002	5.98
GW-455-3	138.0 to 160.0	849.00	2.61E-05	2.60E-05	2.61E-05	0.07	7.61
GW-455-4	152.8 to 174.8	849.90	3.73E-05	1.10E-04	6.41E-05	5.75	3.12

(1) Hydraulic head estimated from arithmetic plots

(2) Data not suitable for Horner analysis

TABLE 4.4

CORE HOLE GW-471
SUMMARY OF PACKER TEST RESULTS

TEST NO.	TESTED ZONE BELOW G.S. (FT) (G.S.= 864.14 FT MSL)	ESTIMATED STATIC HEAD (FT MSL)	HYDRAULIC CONDUCTIVITY SEMI-LOG METHOD (CM/S)	HYDRAULIC CONDUCTIVITY LOG-LOG METHOD (CM/S)	GEOMETRIC MEAN HYDRAULIC CONDUCTIVITY (CM/S)	WELLBORE COMPRESSIBILITY (CMCM)	SKIN FACTOR DIMENSIONLES
GW-471-6	33.0 to 45.0	851.90	3.09E-04	(1)	3.09E-04	(1)	(1)
GW-471-5	45.0 to 57.0	852.20	8.30E-05	6.30E-04	2.29E-04	7.59	13.04
GW-471-1	57.0 to 69.0	850.50	1.33E-05	1.60E-04	4.61E-05	2.81	11.23
GW-471-2	69.0 to 81.0	853.60	4.67E-06	7.20E-06	5.80E-06	0.02	16.05
GW-471-3	81.0 to 93.0	852.50	4.34E-06	6.70E-06	5.39E-06	0.03	15.75
GW-471-4	84.4 to 96.4	851.70	7.10E-05 (2)	(1)	7.10E-05	(1)	(1)

(1) Data not suitable for log-log analysis

(2) TEST RESULTS MAY BE ERRONOUS DUE TO IMPROPER SEAL OF LOWER PACKER. HYDRAULIC CONDUCTIVITY CALCULATED BASED ON TESTED INTERVAL LENGTH OF 20.35 FT. TESTED LENGTH CALCULATED AS DISTANCE FROM BOTTOM OF UPPER PACKER TO BOTTOM OF COREHOLE.

TABLE 4.5

SUMMARY OF STRUCTURAL ZONE LOCATIONS, DESCRIPTIONS, AND HYDRAULIC CONDUCTIVITY

LOCATION	DEPTH (FT BELOW GS)	CORE LOG DESCRIPTION	PACKER TEST RESULTS TEST NO.	DEPTH (FT BELOW GS)		HYDRAULIC CONDUCTIVITY (CM/S)
GW-403	320.2 - 325.5	Bedding near vertical and distorted along high angle shear - calcite filled fractures - displacement of bedding	GW-403-5	306.0 - 328.0		4.90E-08
	380.8 - 408.5	Zone of steep bedding, contorted bedding brecciation, mylonitization, and numerous calcite filled fractures	GW-403-6	387.0	409.0	1.37E-07
GW-455	177.0 - 178.0	Near vertical shear with approx. 0.2' displacement, badly broken	NO TESTS COMPLETED BELOW 174.8 FEET			
	220.0 - 226.0	Zone of complex structure, shear zone distorted beds and calcite filled fractures				
	233.0 - 233.5	Shear/mylonitized zone broken with calcite infilling; weathered				
GW-404	50.0 - 51.4	Bedding slightly contorted along near vertical joint shear.	GW-404-3	50.0	62.0	9.36E-06
	81.2 - 82.1	Bedding contorted along near vertical shear. Some calcite infilling, some fractures possibly open.	GW-404-5	74.0	86.0	4.30E-05
	134.4 - 135.3	Near vertical joint.	GW-404-10	134.0	146.0	5.86E-05
	138.5 - 156.5	Core broken along high angle shear w/ numerous calcite filled fractures - some calcite is pitted (solutioned) and some mylonitization.	GW-404-10 GW-404-11	134.0 146.0	146.0 158.0	5.86E-05 5.44E-06
GW-471	84.0 - 86.0	Intense zone of deformation with abundant folding shears with offsets	GW-471-3 GW-471-4	81.0 84.4	93.0 96.4	5.39E-06 7.10E-05
	90.2 - 90.6	Shear zone	GW-471-4	84.4	96.4	7.10E-05
	99.0 - 104.7	Deformation throughout run with shearing	NO TEST COMPLETED BELOW 96.4 FEET			

5.0 TRACER AREA PUMP TEST DESIGN AND PLANNING

5.1 Objectives and Scope

As part of Task 5, two pump tests were performed within selected zones of the tracer test area shallow aquifer system (<100 feet) to better define the aquifer characteristics and degree of anisotropy (Tmax vs. Tmin) of the Maryville Limestone and to effectively plan and design the field tracer test. Results from the tests were also evaluated to determine bulk hydraulic conductivity, storativity, vertical leakage components, and to identify potential hydraulic boundaries. The general location of the tracer pump test area is shown in Figure 2.1, with a detail location plan presented in Figure 5.1.

The scope of work for the two pump tests, designated deep and shallow, consisted of pumping each test well for 24 hours, followed by monitoring of the recovery period until greater than 90% recovery was achieved. The tests were performed using a small submersible pump powered by a 5 kw generator. Pumping rates for the tests were maintained at very low flow to prevent total dewatering of the pumping well if depletion of fracture storage was observed. The deep test was performed at a flow rate of 0.59 gallons per minute (gpm), and the shallow test was performed at 0.42 gpm.

5.2 Site Selection and Pumping Test Design

Selection of the tracer test site was based upon the desired conditions described in Section 2.1 of this report. The pump tests were performed at the tracer area to provide information regarding the hydrologic characteristics of the tracer area.

The pump tests were designed with a dual purpose in mind, the primary purpose was to fulfill the hydrologic characterization objectives previously described and secondly, to be able to utilize the pumping/observation wells as monitoring points during the field tracer test.

In order to better characterize the hydraulic characteristics of the shallow system, two pumping wells were installed in the same well field at different depths so that separate pumping tests could be performed in selected zones as defined by packer test results. A deep pumping well with an open interval from 68 to 94 feet, and a shallow pumping well from 26.3 to 44.5 feet in depth were installed about 3 feet apart along strike.

The deep pumping well (GW-473), as depicted in Figure 5.2, was designed to intercept the updip projection of the structural zone that was observed in wells GW-471, GW-404, and GW-455. It was desirable to stress this zone to provide a better understanding of its hydraulic characteristics in order to assess its potential as a migration pathway or control. The shallow pumping well (GW-474), as depicted in Figure 5.2, was designed to stress the material overlying the structural zone to evaluate its hydraulic characteristics in terms of its potential to act a confining aquitard over the structural zones. The pumping tests were designed to achieve both a qualitative and quantitative assessment of the following characteristics:

- Degree of anisotropy (Tmax vs. Tmin) and how it varies with depth;
- General aquifer characteristics including transmissivity, storativity, hydraulic conductivity and their degree of uniformity with depth and along bedding;

- Degree of vertical leakage (v) across bedding and structural planes, and from weathered rock (saprolite) zones;
- Anisotropy of the shallow flow system with respect to fracture flow characteristics (fracture direction and length); and
- The vertical distribution of hydraulic head.

The pumping test design was generally based on corehole data (Appendix A) and packer test results from coreholes GW-404, GW-455, and GW-471. These packer test results are presented in section 4.0 and primarily consist of the vertical distribution of hydraulic head and hydraulic conductivity. In particular, the test was designed from corehole data and packer test results derived from GW-471 as this corehole was drilled very near Tracer Area and packer tested back-to-back with a 12-foot spacing to provide detailed site-specific (near field) information for the pump test and tracer test design. Packer test results from coreholes in the tracer test vicinity are presented in section A-A' (Plate 1). Packer test results for GW-471, in addition to the vertical distribution of multi-level pump test well completions, are shown on section B-B' (Figure 5.2).

The observation well field was designed for the placement of wells along geologic strike (about north 56° east) from the pumping wells and at locations and depths corresponding to up and down dip correlation, assuming a 45° dip, of the specific stratigraphic and structural zones as delineated by rock core logs and packer test results from GW-471. The core logs, packer test data, and previous pump tests performed in the Nolichucky Shale, suggested that the orientation of transmissivity would be both strike and dip controlled. Core logging suggested that the predominant fracture orientation is along

bedding plane partings, whereas previous pump tests performed in the Nolichucky Shale (Reference 3) suggest that the principal direction of transmissivity is oriented along strike. Thus, the well field layout could test both factors.

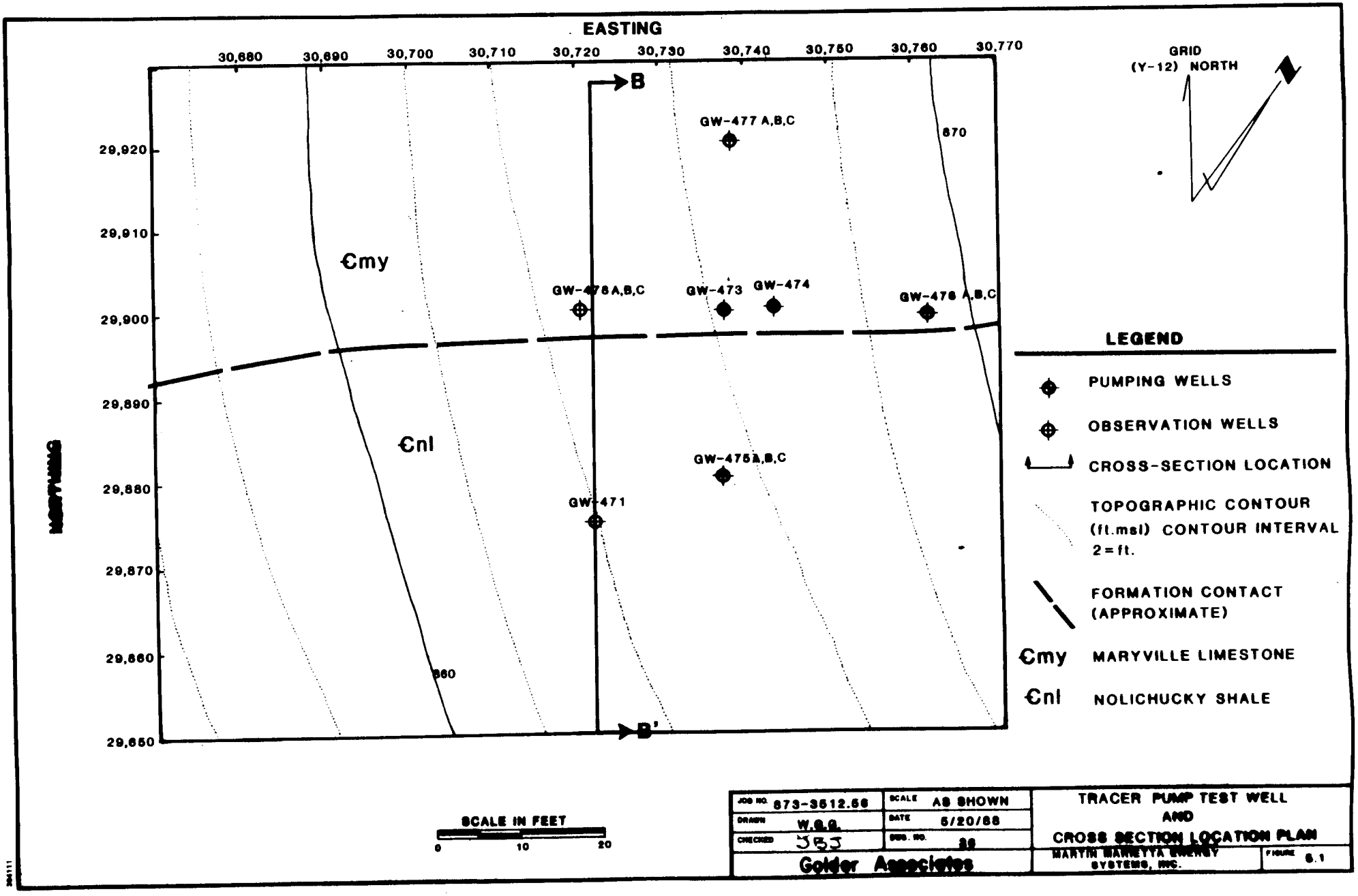
EASTING
30,680
30,690
30,700
30,710
30,720
30,730
30,740
30,750
30,760
30,770
NORTHING
29,920
29,910
29,900
29,890
29,880
29,870
29,860
29,850
B
B'
GW-477 A,B,C
GW-476 A,B,C
GW-473
GW-474
GW-478 A,B,C
GW-475 A,B,C
GW-471
Ꞓmy
Ꞓnl
870
860
GRID
(Y-12) NORTH
LEGEND
PUMPING WELLS
OBSERVATION WELLS
CROSS-SECTION LOCATION
TOPOGRAPHIC CONTOUR
(ft.msl) CONTOUR INTERVAL
2=ft.
FORMATION CONTACT
(APPROXIMATE)
Ꞓmy MARYVILLE LIMESTONE
Ꞓnl NOLICHUCKY SHALE
SCALE IN FEET
0
10
20
JOB NO. 873-3512.56
SCALE AS SHOWN
DRAWN W.G.G.
DATE 5/20/88
CHECKED JBJ
SUB. NO. 38
Golder Associates
TRACER PUMP TEST WELL
AND
CROSS SECTION LOCATION PLAN
MARTIN MARIETTA ENERGY
SYSTEMS, INC.
FIGURE 5.1

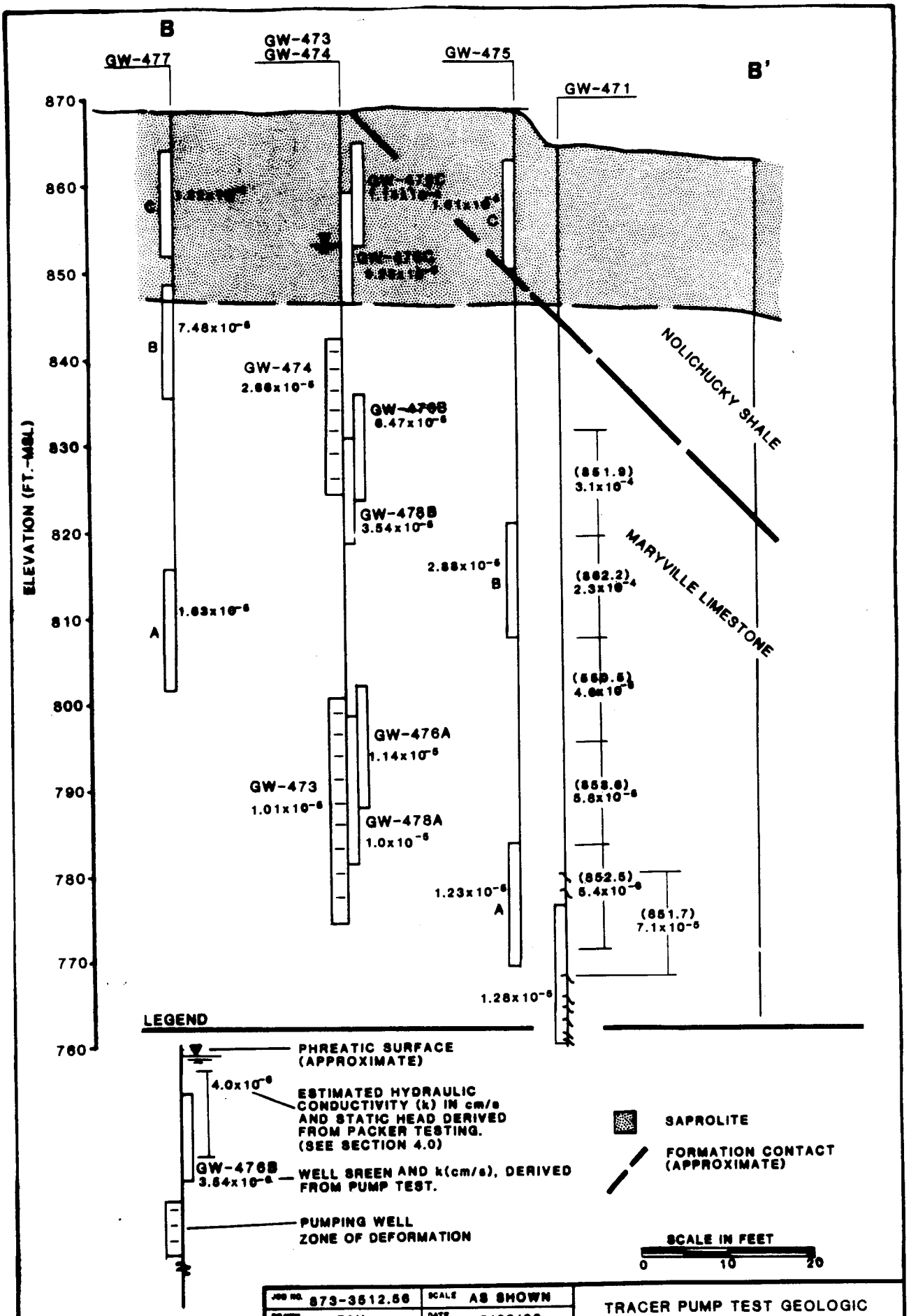

JOB NO. 873-3512.56	SCALE AS SHOWN	TRACER PUMP TEST GEOLOGIC CROSS SECTION B-B'	
DRAWN EAH	DATE 5/20/88		
CHECKED JBJ	DWG. NO. 36		
Golder Associates		MARTIN MARIETTA ENERGY SYSTEMS, INC.	FIGURE 5.2

6.0 DRILLING AND INSTALLATION OF PUMPING/OBSERVATION AND MONITORING WELLS

General - Three separate stages of well installation were performed at the tracer test area. The first stage consisted of wash rotary drilling and installation of pump test and observation wells. Upon completion of the aquifer pumping tests, the second stage of well installation began, which included the installation of additional tracer detection wells. The third stage consisted of the progressive installation of tracer observation wells during the tracking of the tracer migration.

6.1 Objectives and Scope

The primary objective of well installation in the field tracer test area was to provide an appropriate monitoring network for the tracer test. Field tracer test wells were installed using methods that would cause minimal damage and disturbance to the aquifer system. In particular, once through wash rotary techniques were used to minimize the potential for cuttings to infill the fractures. Wells were designed so that the screened intervals isolated specific zones of interest, in addition to providing an effective hydraulic connection for tracer monitoring purposes.

The three stages of well installation in the tracer area, described above, produced the following number of wells:

1. Pump Test Wells - A total of four multi-level well completions (3 two-inch PVC wells per completion), and two 4-inch PVC pumping wells were installed in the tracer area using wash rotary methods.

2. Tracer Injection/Observation Wells - A total of three multi-level well completions (3 one-inch PVC wells per completion) -similar to those installed for the pump test - and 3 single 2-inch wells were installed using either wash rotary or augering methods. These field tracer wells supplemented the existing well field used for pump testing.

3. Ongoing Tracer Detection Wells - After tracer injection and initial tracer detection, a total of 26 shallow observation wells were installed during performance of the field tracer test. Boreholes for these wells were drilled using solid stem auger methods in order to minimize external influences on tracer migration. The installation of these wells was necessary for greater far field coverage of tracer movement as the test progressed. In addition, MMES installed 5 shallow observation wells using hand or power auger techniques.

6.2 Drilling and Installation of Pumping/Observation Wells

Two pumping wells and 12 observation points in four wells were installed in the Maryville Limestone and saprolite (shallow wells) for the performance of the aquifer pump tests. The drilling details are presented in this section, the pump tests and results are described in Section 9.0.

Appendix C includes the well installation logs for all wells in the tracer pump test area. The tracer pump test wells were drilled by Highland Drilling Company from January 6, 1988, to January 29, 1988. Golder Associates provided QA/QC supervision during the drilling and well installation operation. All holes were drilled with an Ingersoll/Rand XL750 drill rig employing once through wash rotary techniques. Upon reaching the desired depth, a bentonite gel slurry was circulated through each hole to facilitate the removal of cuttings not evacuated during the wash rotary procedure. This process was followed immediately by the circulation of clean potable water through the hole to remove the remaining bentonite gel.

The two pumping wells, GW-473 and GW-474, were both completed within the Maryville Limestone. The deep pumping well GW-473, was drilled to approximately 94.0 feet below ground surface, penetrating nearly 70 feet into the limestone bedrock and intercepting the structural zone previously described. The shallow pumping well GW-474, was drilled to approximately 44.5 feet below ground surface and was completed about 20

feet into the Maryville Limestone. Both wells were constructed using 4-inch diameter, schedule 40 PVC riser and .010 slot well screen. The open intervals for GW-473 and GW-474 are 68.0 to 94.0 feet and 26.3 to 44.5 feet below ground surface, respectively.

Four 9.5-inch wash rotary holes were drilled to depths ranging from 67.0 to 99.4 feet below ground surface for multi-level well completions. The installations consisted of a deep, intermediate, and shallow observation well installed in each hole. The shallow wells (designated as "C" wells) were completed as water table wells in saprolite and were generally screened from approximately 11.0 to 13.0 feet below ground surface (depth to center of screened interval). The intermediate wells (designated as "B" wells) were completed in the upper Maryville Limestone or at the contact between the saprolite and bedrock. The depth range within which the intermediate wells were screened varies from 26.5 to 55.4 feet below ground surface (depth to center of screened interval). All deep observation wells (designated as "A" wells) were completed well within the Maryville Limestone. These wells were installed to intercept and monitor the up and down dip projection of the same structural zone that the deep pumping well was screened in. The screened intervals for deep observation wells range from 60.0 to 92.0 feet below ground surface (depth to center of screened interval).

All pump test observation wells are constructed of 2-inch schedule 40 PVC riser and .010 slot well screen. Seals between multi-level completions consisted of both bentonite pellets and cement grout. After sufficient time was allowed for bentonite pellet hydration, cement was tremied directly above the bentonite under gravity flow. After the cement had sufficiently cured, the borehole was thoroughly flushed with

fresh water to remove cement residue. A bentonite seal was again placed above the cement to isolate shallow or intermediate wells from cement grout.

Two additional observation wells were constructed in coreholes GW-455 and GW-471. The piezometer constructed in GW-455 consists of 2-inch, Schedule 40 PVC with 20 feet of 0.01 inch machine slotted screen. This piezometer is screened in the Maryville Limestone from 162.5 to 182.5 feet below ground surface. Well GW-471 is screened from 91.5 to 101.5 feet below ground surface about 80 feet into the Maryville Limestone. The well is constructed of 1-inch schedule 40 PVC riser and hand slotted screen. Table 6.1 presents the well construction details for all wells described in this section. Well installation logs along with installation notes are presented in Appendix C.

6.3 Drilling and Installation of Tracer Test Wells

As discussed in section 6.1, tracer observation wells were drilled in two separate phases upon completion of the tracer pump test. After reviewing the tracer pump test results, three multi-level piezometers and three single well completions - two background wells and one injection well - were installed in the tracer area to supplement the existing tracer well field. These wells were installed in boreholes that were drilled by Highland drilling using a Drilltek DL rig with 6-1/8 inch or 8-1/4 inch rotary wash bit. Highland Drilling operated under contract to Martin Marietta Energy Systems (MMES). Golder Associates provided QA/QC supervision during the drilling and installation of all wells. Each borehole was drilled to approximately 2 feet below desired depth with cuttings washed from the hole using clean potable water. To minimize the potential of damaging or altering the hydraulic connection of these wells to the aquifer, no bentonite slurry was used to remove cuttings. Consequently,

sounding of the hole was delayed approximately 1/2 hour giving time for any drill cuttings to settle. Table 6.1 presents the well construction summary for the tracer test wells. Field boring logs and well installation logs for these wells are presented in Appendix C.

Wells GW-480A, B, C, GW-481A, B, C and GW-482A, B, C were installed as multi-level piezometers using 1 inch, schedule 40, threaded PVC with a 3 foot screen. The deepest piezometers were sealed in rock, while the intermediate piezometers were installed at the rock/soil interface. The shallow piezometers were installed with about one-half of the 3 feet section of screen below groundwater. This determination was made by the Golder Associates Engineer at site during the drilling. At this time, some of the shallow piezometers installed are dry due to recent drought conditions.

Well GW-479 was drilled using an 8-1/4 inch rotary wash bit while GW-483 and GW-484 used a 6-1/4 inch rotary wash bit. All 3 wells were installed using a 2 inch threaded PVC (schedule 40) and 10 feet of screen. For well GW-484, a 10 feet section of screen was hand slotted, while GW-479 and GW-483 were machine slotted (0.01-inch slots). The sand pack in wells GW-483 and GW-484 consisted of 1/4 to 1/16 inch coarse sand, while all other sand packs were installed using 20/40 sand. Figures 6.1 and 6.2 present the grain size distribution for the coarse and fine sand, respectively. The coarse sand was used to maximize the hydraulic connection for the injection and background wells.

After installation of the above mentioned wells at the tracer area, well development was performed with the methods discussed in Section 7. Field parameters, including pH, conductivity, salinity, and temperature were recorded during the development of each well (Table 7.1).

The next phase of observation well installation occurred during the course of the tracer test, with 10 additional wells installed with the intent of model calibration and 16 subsequent wells installed at a later time for model validation. Boreholes for these wells were drilled using auger techniques. Boreholes for the 10 wells installed for additional model calibration (GW-485 through GW-494) were drilled to auger refusal and ranged in depth from 14.1 to 20.5 feet. The wells consisted of 2 inch schedule 40, threaded PVC with a 10 foot section of machine slotted (0.01-inch) screen. The 10 additional calibration wells were drilled from April 22, 1988 to May 16, 1988 using the same QA/QC procedures presented in Appendix A5 of the Task 2 report (Reference 3). The construction summary for these additional 10 wells is also presented in Table 6.1.

The 16 additional wells installed for tracer validation or detection were drilled and installed on May 20, 1988, and June 28 through June 30, 1988. These 16 wells include: GW-495 through GW-499, GW-499A, and GW-499G through GW-499P. Boreholes for these wells were drilled to auger refusal and completed with 2-inch, Schedule 40 threaded PVC riser and 3 feet sections of machine slotted 0.01-inch screen. The total depth of the wells ranged from 4.0 to 13.2 feet below ground surface.

SEPTEMBER 1988

TABLE 6.1

873-3512.56

CONSRUCTION/SAMPLE POINT SUMMARY
OF TRACER AREA WELLS
(PAGE 1 of 3)

WELL NO.	ELEVATIONS TOP/PVC (FT MSL)	ELEVATIONS GROUND (FT MSL)	WELL DIAMETER (IN)	DEPTHS BELOW GROUND SURFACE: DEPTH TO ROCK	HOLE DEPTH	TOP OF SAND PACK	TOP OF SCREEN	BOTTOM OF SCREEN	OPEN INT. LENGTH (FT)	BOREHOLE DIAMETER (IN)	APPROX DEPTH TO WATER (FT. BMP)	APPROX WATER COLUMN (FT)	SAMPLE INTAKE DEPTH (FT)
GW-455	855.75	853.44	2.0	10.2	293.2	155.4	162.5	182.5	37.6	3.70	FLOWING	184.81	NA
GW-471	865.18	864.14	1.0	18.7	104.7	88.8	91.5	101.5	15.0	3.70	6.35	96.2	110.0
GW-473	868.93	868.60	4.0	25.0	94.0	68.0	70.1	90.0	26.0	8.75	11.55	78.8	81.0
GW-474	870.03	868.87	4.0	25.0	44.5	26.3	28.8	43.8	18.3	8.75	14.68	30.2	39.1
GW-475A	870.20	868.63	2.0	25.0	99.4	85.0	87.0	97.0	14.4	9.50	13.81	84.8	93.5
GW-475B	870.70	868.63	2.0	25.0	--	48.0	50.4	60.4	13.0	9.50	15.26	47.2	58.4
GW-475C	870.83	868.63	2.0	25.0	--	6.0	8.0	18.0	12.5	9.50	16.37	3.8	25.0
GW-476A	871.86	869.91	2.0	25.0	82.0	67.9	70.0	80.0	13.1	9.50	14.3	67.7	76.4
GW-476B	872.72	869.91	2.0	25.0	--	34.0	36.0	46.0	12.5	9.50	16.68	32.1	44.3
GW-476C	873.45	869.91	2.0	25.0	--	5.0	6.2	16.2	11.7	9.50	18.88	0.9	19.6
GW-477A	870.13	868.33	2.0	25.0	67.0	53.0	55.0	65.0	14.0	9.50	12.58	54.2	70.0
GW-477B	870.75	868.33	2.0	25.0	--	20.0	21.5	32.1	12.6	9.50	16.03	17.9	30.6
GW-477C	871.39	868.33	2.0	25.0	--	4.5	6.0	16.0	11.9	9.50	16.75	2.3	25.0
GW-478A	865.20	863.27	2.0	20.0	82.0	65.0	68.0	78.0	15.4	9.50	8.17	71.8	74.5
GW-478B	865.40	863.27	2.0	20.0	--	33.0	34.5	44.5	12.0	9.50	10.36	36.3	41.2
GW-478C	865.55	863.27	2.0	20.0	--	4.5	6.0	16.0	12.0	9.50	11.91	6.4	19.1

SEPTEMBER 1988 TABLE 6.1 873-3512.56

CONSRUCTION/SAMPLE POINT SUMMARY
OF TRACER AREA WELLS
(PAGE 2 of 3)

WELL NO.	ELEVATIONS TOP/PVC (FT MSL)	ELEVATIONS GROUND (FT MSL)	WELL DIAMETER (IN)	DEPTHS BELOW GROUND SURFACE: DEPTH TO ROCK	HOLE DEPTH	TOP OF SAND PACK	TOP OF SCREEN	BOTTOM OF SCREEN	OPEN INT. LENGTH (FT)	BOREHOLE DIAMETER (IN)	APPROX DEPTH TO WATER (FT. BMP)	APPROX WATER COLUMN (FT)	SAMPLE INTAKE DEPTH (FT)
GW-479	873.04	870.61	2.0	23.0	26.0	11.0	13.0	23.0	12.5	8.75	17.87	7.6	22.8
GW-480A	871.28	868.67	1.0	28.0	42.5	31.0	32.0	34.5	4.0	6.12	16.68	20.4	35.6
GW-480B	871.93	868.67	1.0	28.0	--	25.5	26.5	29.0	4.0	6.12	17.73	14.5	31.5
GW-480C	871.84	868.67	1.0	28.0	--	12.0	13.0	15.5	4.0	6.12	18.16	0.5	---
GW-481A	871.13	868.61	1.0	25.0	39.0	28.9	29.5	32.0	4.0	6.12	15.97	18.5	33.3
GW-481B	870.50	868.61	1.0	25.0	--	22.5	23.5	26.0	4.0	6.12	15.62	12.3	28.5
GW-481C	870.87	868.61	1.0	25.0	--	11.5	12.5	15.0	3.9	6.12	16.33	0.9	14.7
GW-482A	871.18	869.21	1.0	26.0	40.5	30.8	31.8	34.3	4.0	6.12	15.87	20.3	34.7
GW-482B	871.46	869.21	1.0	26.0	--	23.8	24.8	27.3	4.0	6.12	16.34	13.2	29.8
GW-482C	871.96	869.21	1.0	26.0	--	11.8	12.8	15.3	4.0	6.12	17.86	0.1	16.5
GW-483	874.28	870.98	2.0	24.0	26.0	11.4	13.7	23.7	13.8	6.12	17.81	9.2	23.5
GW-484	871.55	869.33	2.0	26.0	26.0	10.4	12.1	21.1	13.4	6.12	16.47	6.8	19.6
GW-485	864.30	863.81	2.0	20.5	20.5	8.3	9.5	19.5	12.2	6.00	12.75	7.2	17.5
GW-486	866.32	863.01	2.0	16.8	16.8	5.0	6.8	16.8	11.8	6.00	14.67	5.4	14.8
GW-487	865.25	862.98	2.0	21.0	21.0	6.0	8.0	18.0	12.0	6.00	13.38	6.9	16.0
GW-488	866.81	863.14	2.0	17.0	17.0	5.0	6.3	16.3	11.3	6.00	15.37	4.6	14.3
GW-489	867.27	863.22	2.0	21.5	21.5	8.0	10.5	20.5	12.5	6.00	15.70	8.8	18.5
GW-490	863.83	861.55	2.0	19.0	19.0	6.0	8.0	18.0	12.0	6.00	12.35	7.9	17.0
GW-491	864.69	861.12	2.0	17.0	17.0	4.5	6.5	16.5	12.0	6.00	13.02	7.1	14.5
GW-492	862.85	860.69	2.0	14.1	14.1	3.1	4.1	14.1	11.0	6.00	11.76	4.5	12.1
GW-493	863.99	861.10	2.0	19.3	19.3	4.0	6.8	16.8	14.5	6.00	12.27	7.4	16.5
GW-494	863.75	861.34	2.0	16.5	16.5	3.0	4.2	14.2	11.2	6.00	12.10	4.5	12.2
GW-495	855.08	852.24	2.0	7.7	7.7	2.3	3.3	6.3	4.0	6.00	7.91	1.2	5.3
GW-496	854.68	852.03	2.0	6.7	6.7	2.0	3.0	6.0	4.0	6.00	7.61	1.0	5.0

TABLE 6.1

CONSRUCTION/SAMPLE POINT SUMMARY
OF TRACER AREA WELLS
(PAGE 3 of 3)

WELL NO.	ELEVATIONS TOP/PVC (FT MSL)	ELEVATIONS GROUND (FT MSL)	WELL DIAMETER (IN)	DEPTH TO ROCK	HOLE DEPTH	TOP OF SAND PACK	TOP OF SCREEN	BOTTOM OF SCREEN	OPEN INT. LENGTH (FT)	BOREHOLE DIAMETER (IN)	APPROX DEPTH TO WATER (FT. BMP)	APPROX WATER COLUMN (FT)	SAMPLE INTAKE DEPTH (FT)
				**********	**********	DEPTHS BELOW GROUND SURFACE	**********	**********	**********	**********	**********	**********	**********
GW-497	854.57	851.87	2.0	8.2	8.2	2.7	3.7	6.7	4.0	6.00	6.06	3.3	5.7
GW-498	854.48	852.03	2.0	5.1	5.1	1.1	1.6	4.6	3.9	6.00	5.42	1.6	3.6
GW-499	854.85	852.15	2.0	5.0	5.0	1.0	1.0	4.0	4.0	6.00	6.62	0.1	3.0
GW-499A	854.69	852.35	2.0	6.2	6.2	2.0	2.6	5.6	4.2	6.00	7.47	1.2	4.6
GW-499B	855.50	852.85	NA	NA	NA	NA	NA	NA	NA	NA	NA	NA	NA
GW-499C	855.98	853.03	NA	NA	NA	NA	NA	NA	NA	NA	NA	NA	NA
GW-499D	855.93	852.56	NA	NA	NA	NA	NA	NA	NA	NA	NA	NA	NA
GW-499E	855.47	852.33	NA	NA	NA	NA	NA	NA	NA	NA	NA	NA	NA
GW-499F	853.44	852.15	NA	NA	NA	NA	NA	NA	NA	NA	NA	NA	NA
GW-499G	859.76	857.74	2.0	14.0	14.0	5.3	7.8	12.8	8.7	6.00	7.08	7.7	11.8
GW-499H	859.77	857.57	2.0	12.5	12.5	2.7	4.7	9.7	8.3	6.00	9.03	2.9	8.7
GW-499I	859.75	857.41	2.0	10.5	10.5	2.7	4.0	9.0	6.3	6.00	10.00	1.3	8.0
GW-499J	859.60	857.15	2.0	10.0	10.0	3.0	3.6	8.0	5.0	6.00	8.78	1.7	7.6
GW-499K	862.32	859.44	2.0	12.3	12.3	4.0	5.0	10.0	6.0	6.00	NA	NA	9.0
GW-499L	862.26	859.62	2.0	15.0	15.0	3.8	7.0	12.0	8.2	6.00	NA	NA	11.0
GW-499M	862.35	859.39	2.0	12.3	12.3	4.3	6.6	11.6	7.3	6.00	NA	NA	10.6
GW-499N	862.27	859.32	2.0	13.0	13.0	4.0	7.0	12.0	8.0	6.00	NA	NA	11.0
GW-499O	862.63	859.20	2.0	13.0	13.0	4.0	6.3	11.3	7.3	6.00	NA	NA	10.3
GW-499P	860.87	859.37	2.0	15.0	15.0	4.0	8.2	13.2	9.2	6.00	NA	NA	12.2

NOTES: 1. WELLS GW-455 TO GW-478A,B,C WERE UTILIZED FOR BOTH THE PUMP AND TRACER TEST
2. WELLS GW-455 TO GW-484 DEPTH TO WATER TAKEN 3/20/88
3. WELLS GW-499A TO GW-499J DEPTH TO WATER TAKEN 6/17/88
4. WELLS GW-499B TO GW-499F ARE MMES WELLS. NO QA/QC BY GOLDER ASSOCIATES.

SEPTEMBER 1988

TABLE 6.2
(1 of 2)
TRACER AREA WELLS
SURVEY DATA

WELL NO.	AS BUILT COORDINATES NORTHING	EASTING	ELEVATIONS GROUND	T/PROT. CASING	T/STEEL CASING	T/PVC CASING	MEASURE POINT
GW-404	29870.29	30636.05	852.30		852.81		
GW-455	29765.95	30676.25	853.44			855.75	855.75
GW-471	29875.29	30721.63	864.14		865.46	865.18	
GW-473	29900.16	30737.60	868.60			868.93	
GW-474	29900.64	30743.32	868.87			870.03	
GW-475 A	29880.60	30737.01	868.63		869.07	870.20	
B						870.70	
C						870.83	
GW-476 A	29899.50	30761.82	869.91		870.45	871.86	
B						872.72	
C						873.45	
GW-477 A	29920.10	30738.54	868.33		868.57	870.13	
B						870.75	
C						871.39	
GW-478 A	29900.61	30720.30	863.27		863.47	865.20	
B						865.40	
C						865.55	865.55
GW-479	29889.73	30773.29	870.61		870.96	873.04	873.04
GW-480 A	29890.25	30737.11	868.67		868.81	871.28	871.28
B						871.93	871.93
C						871.84	871.84
GW-481 A	29910.66	30738.09	868.61		869.09	871.13	871.13
B						870.50	870.50
C						870.87	870.87
GW-482 A	29900.41	30747.28	869.21		870.15	871.18	871.18
B						871.46	871.46
C						871.96	871.96
GW-483	29908.58	30773.45	870.98		871.15	874.28	874.28
GW-484	29911.80	30751.92	869.33		869.43	871.55	871.55
GW-485	29987.86	30718.88	863.81			864.30	864.30
GW-486	29908.82	30713.65	863.01			866.32	866.32
GW-487	29914.27	30708.68	862.98			865.25	865.25
GW-488	29902.43	30711.37	863.14			866.81	866.81
GW-489	29922.49	30706.85	863.22			867.27	867.27
GW-490	29921.53	30692.75	861.55			863.83	863.83
GW-491	29915.19	30693.65	861.12			864.69	864.69
GW-492	29908.18	30694.68	860.69			862.85	862.85
GW-493	29912.84	30694.15	861.10			863.99	863.99
GW-494	29917.50	30693.18	861.34			863.75	863.75

SEPTEMBER 1988

TABLE 6.2
(2 of 2)
TRACER AREA WELLS
SURVEY DATA

WELL NO.	AS BUILT COORDINATES NORTHING	EASTING	ELEVATIONS GROUND	T/PROT. CASING	T/STEEL CASING	T/PVC CASING	MEASURE POINT
GW-495	29920.31	30639.44	852.24			855.08	855.08
GW-496	29917.51	30639.11	852.03			854.68	854.68
GW-497	29914.47	30639.84	851.87			854.57	854.57
GW-498	29911.65	30640.30	852.03			854.48	854.48
GW-499	29908.62	30640.74	852.15			854.85	854.85
GW-499A	29923.23	30638.43	852.35			854.69	854.69
GW-499B	29898.85	30643.12	852.85				855.50
GW-499C	29890.16	30642.22	853.03				855.98
GW-499D	29882.73	30639.27	852.56				855.93
GW-499E	29875.26	30636.15	852.33				855.47
GW-499F	29903.81	30641.31	852.15				853.44
GW-499G	29916.11	30667.88	857.74				859.76
GW-499H	29913.72	30666.85	857.57				859.77
GW-499I	29910.31	30665.71	857.41				859.75
GW-499J	29907.68	30664.70	857.15				859.60
GW-499K	29919.73	30680.58	859.44				862.32
GW-499L	29922.96	30681.85	859.62				862.26
GW-499M	29916.41	30679.86	859.39				862.35
GW-499N	29913.23	30679.66	859.32				862.27
GW-499O	29910.03	30681.70	859.20				862.63
GW-499P	29907.35	30683.35	859.37				860.87

NOTES: 1) T/STEEL CASING OR T/PVC CASING REPRESENTS THE "NOTCH" OR "MEASURE POINT" LOCATED ON THE INNER CASINGS OF THESE WELLS.

2) * INDICATES ELEVATION TAKEN AT TOP OF CONCRETE (NO PROTECTIVE CASING FOR THESE WELLS).

3) # INDICATES ELEVATION TAKEN AT TOP OF ELBOW.

GRAIN SIZE DISTRIBUTION

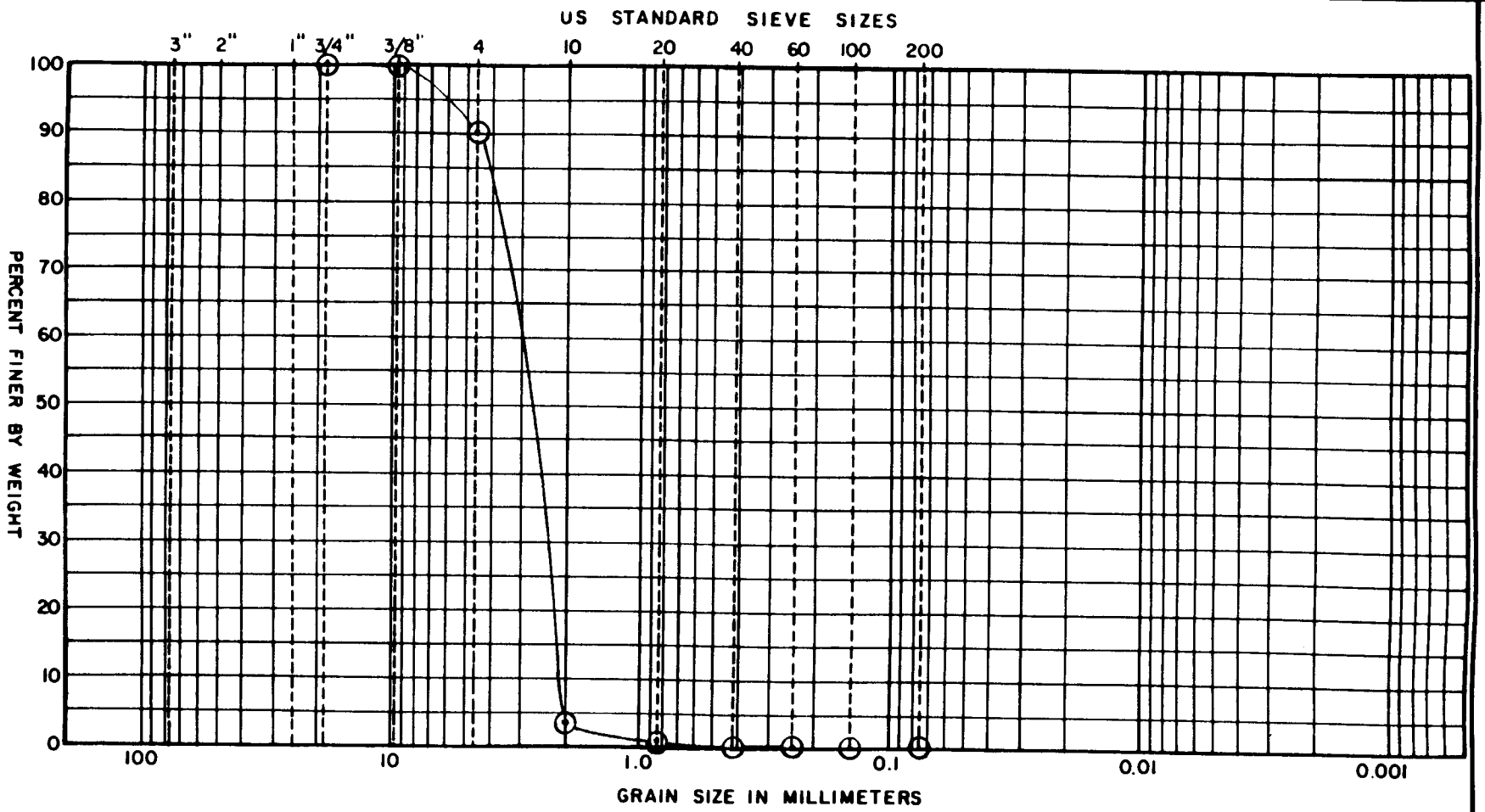

COBBLES	GRAVEL		SAND			FINES
	COARSE	FINE	COARSE	MEDIUM	FINE	SILT OR CLAY

BORING NO.	ELEV. OR DEPTH	W_n	W_L	W_p	I_p	DESCRIPTION OR CLASSIFICATION
—	—	—	—	—	—	TAN, COARSE TO MEDIUM SAND, LITTLE FINE GRAVEL, (SP)

FIGURE 6.1

Golder Associates

Date 7/23/88
Job No. 873-3512

Drawn JLW
Checked JEE
Reviewed

GRAIN SIZE DISTRIBUTION

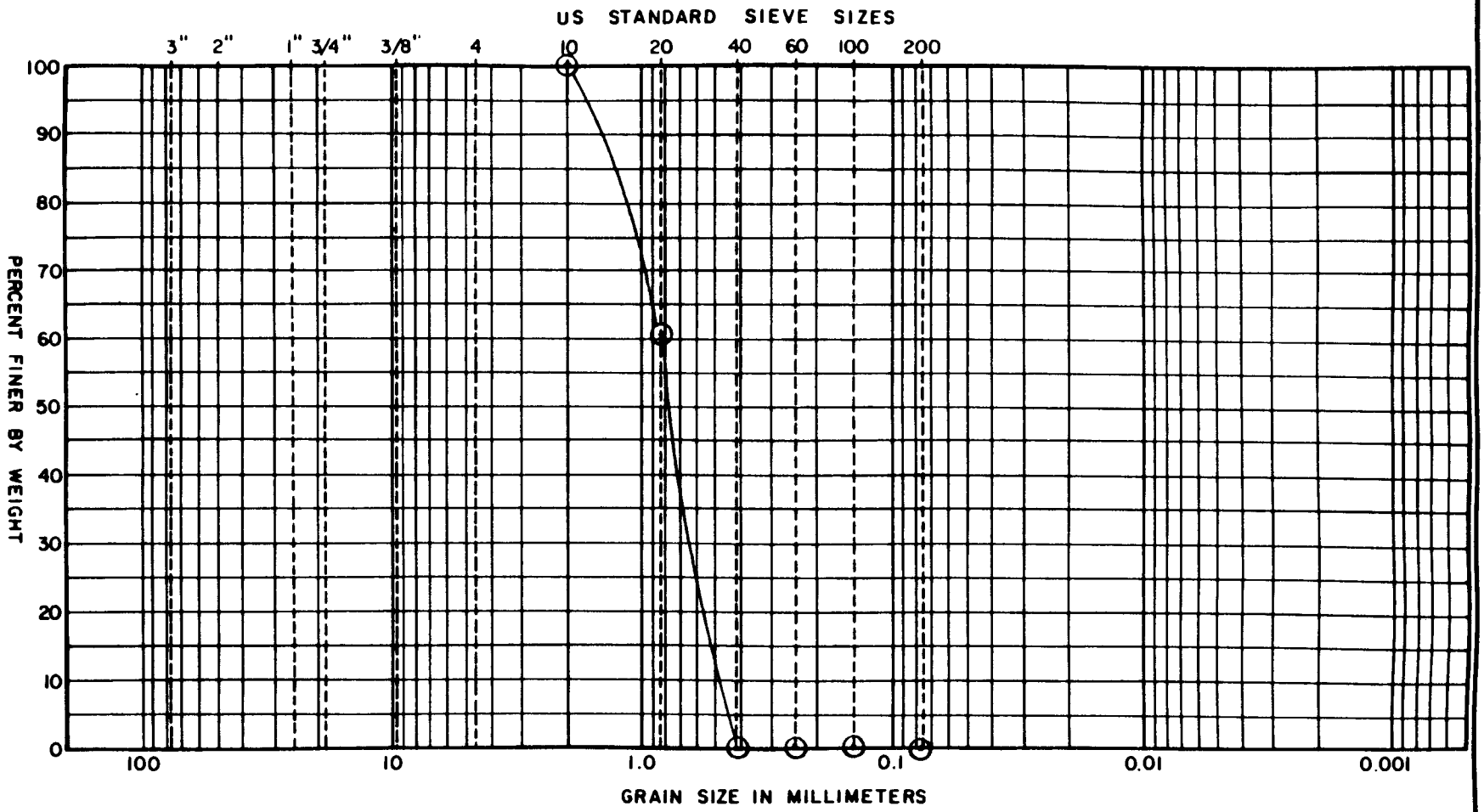

COBBLES	GRAVEL		SAND			FINES
	COARSE	FINE	COARSE	MEDIUM	FINE	SILT OR CLAY

BORING NO.	ELEV. OR DEPTH	W_n	W_L	W_p	I_p	DESCRIPTION OR CLASSIFICATION
—	—	—	—	—	—	TAN, MEDIUM SAND, (SP)

FIGURE 6.2

Golder Associates

Date 7/23/88
Job No. 873-3512

Drawn JLW
Checked
Reviewed

7.0 WELL DEVELOPMENT

7.1 Objectives and Scope

Pump test and observation wells were developed prior to the pump test and field tracer test to remove drilling fluids, to remove sediment associated with installation, to develop a filter pack to help prevent the migration of fines into the screened interval, and to provide an effective hydraulic connection between the formation and well screen. After these objectives were accomplished, representative data could then be obtained for field permeability tests and the well could be used as an effective observation well for pump tests or as a monitoring point for tracer detection. No well development was performed on wells installed subsequent to tracer injection, so as not to alter the aquifer hydraulics or tracer migration near these wells.

Development of wells was accomplished with the following methods: air-lift with either an air compressor or bottled nitrogen, pumping with a submersible pump, or by hand bailing. Well development was performed in general accordance with the procedures stated in Appendix A7 of the Task 2 Report (Reference 3). Wells were generally developed until the well produced representative formation water. Water developed from these wells was deemed representative of the formation when values of specific conductance, pH, and visual clarity remained relatively stable. Wells were developed for a minimum of four hours, or until water representative of the formation was produced. Wells completed in formations of low permeability could frequently not be developed continuously, nor could a sufficient volume of water be removed within a reasonable time frame. Development in these wells often required that they be purged until dry, and then subsequently re-purged after many hours or even days.

In general, a minimum of three well volumes was removed from each well completed in intervals possessing sufficient yield characteristics.

Data obtained during well development, including field parameter measurements, were summarized and are presented in Table 7.1.

In wells developed by air-lift methods, a one-inch eductor pipe with a one-way check-valve was utilized in conjunction with either an oil-less air compressor or pure grade nitrogen. New, clean polyethylene tubing was used to introduce air or nitrogen into the eductor pipe. The line was inserted approximately two feet above the foot valve.

Hand bailers were used predominately in wells completed in intervals of low permeability, or in cases where there was little standing water present in the well. Bailers consisted of a five or ten foot section of PVC pipe, with a one-way foot valve. Wells were bailed as continuously as possible, depending upon the recovery rate of the well.

Submersible pumps were used exclusively for the development of four inch pump test wells. The use of submersible pumps in these wells allowed for the efficient removal of large volumes of water. Submersible pumps used to develop pumping wells also facilitated in determining a desirable flow rate for the test, as well as observing the likely aquifer response to pumping. All submersible pumps used for well development were capable of producing at least 3 gpm.

Well and piezometer development data was collected and reported in accordance with the data management procedures set forth in Appendix A8 of the Task 2 Report (Reference 3). A summary of the data is presented in Table 7.1.

7.2 Discussion of Results

In general, deep and intermediate wells were developed until representative groundwater was obtained with respect to stable values of pH and specific conductance. Stable "background" and field parameters for the tracer area consisted of pH values of approximately 8.0 and specific conductance values of about 200 to 400 micromhos/cm.

Typically, the shallow (C) wells contained inadequate supplies of water to facilitate proper development. These wells could not be developed until representative water was produced, and thus, pH and specific conductance values for these wells are rather high. These high pH and conductance values are probably due to cement grout contamination which occurred in the screened interval during well installation. However, the high values would have no effect on tracer fluorescence, as previously discussed.

TABLE 7.1

WELL DEVELOPMENT DATA
PUMPING TEST AND TRACER TEST WELLS (2)

WELL NO.	DATE	CUMULATIVE VOLUME REMOVED (GALS)	pH	TEMP. (C)	SPECIFIC CONDUCTANCE	REMARKS
GW-473	2-3-88	43	7.83	23.0	340	
	2-3-88	100	7.93	24.4	315	
	2-3-88	145	8.07	22.9	305	
	2-3-88	175 (1)	7.92	28.8	305	
GW-474	2-3-88	20	8.07	21.0	265	
	2-3-88	40	8.05	19.9	265	
	2-3-88	70	8.36	21.3	275	
	2-3-88	100 (1)	8.51	21.2	265	
GW-475A	1-26-88	5	7.94	12.5	295	Turbid
	1-26-88	15	8.40	11.4	261	Clear
	1-26-88	17	7.99	11.6	275	
	2-1-88	23	9.76	14.2	362	
	2-1-88	27	9.36	14.9	370	
	2-1-88	32 (1)	9.34	20.1	345	
GW-475B	2-1-88	5	12.48	14.9	980	O2 = 8.2
	2-1-88	20	7.84	18.8	1,120	
	2-1-88	30	11.85	18.7	700	
	2-1-88	50	11.50	19.8	440	
	2-1-88	90 (1)	9.29	19.6	175	
GW-475C	1-29-88	2	NA	13.0	390	O2 = 10.6
	1-29-88	4	NA	13.0	385	O2 = 11.2
	2-1-88	5.5	11.97	14.0	1,100	O2 = 8.2
	2-1-88	7.5	11.86	13.4	810	O2 = 7.2
	2-1-88	8.5	12.06	12.5	1,600	O2 = 9.0
	2-2-88	13.5	9.73	11.0	275	
	2-2-88	18.5	10.10	8.5	260	
	2-2-88	21.5 (1)	10.75	12.5	315	
GW-476A	2-1-88	5	9.89	13.0	360	
	2-1-88	10	9.58	14.9	362	
	2-1-88	15.5	9.84	14.8	425	
	2-1-88	20.5	9.48	14.5	415	
	2-1-88	30.5	9.13	19.8	370	
	2-1-88	40.5	8.86	20.2	362	
	2-1-88	43.0 (1)	8.82	19.0	342	
GW-476B	1-29-88	3	NA	15.0	275	O2 = 9.8
	1-29-88	18	NA	15.5	265	O2 = 9.8
	1-29-88	28	NA	14.0	260	O2 = 9.7
	1-29-88	38	NA	14.0	260	O2 = 8.9

TABLE 7.1
(2 of 2)
WELL DEVELOPMENT DATA
PUMPING TEST AND TRACER TEST WELLS (2)

WELL NO.	DATE	CUMULATIVE VOLUME REMOVED (GALS)	pH	TEMP. (C)	SPECIFIC CONDUCTANCE	REMARKS
	2-5-88	78	8.85	17.9	230	
	2-5-88	88 (1)	8.36	16.7	235	
GW-476C	2-1-88	2.5 (1)	12.23	13.4	1,150	O2 = 8.6
GW-477A	2-1-88	10	9.36	13.4	265	O2 = 8.4
	2-1-88	20	8.49	14.7	280	O2 = 7.4
	2-1-88	25	8.46	14.7	282	O2 = 7.0
	2-1-88	35	7.80	14.1	270	
	2-1-88	45 (1)	8.21	19.8	260	
GW-477B	1-29-88	38	9.35	13.5	245	O2 = 9.8
	1-29-88	43	NA	13.2	265	O2 = 8.6
	2-1-88	66	NA	13.1	235	O2 = 9.5
	2-1-88	86	9.88	13.6	245	O2 = 8.0
	2-1-88	94	9.81	19.4	250	
	2-5-88	99	9.39	17.3	212	
	2-5-88	109	9.43	16.0	138	
	2-5-88	134	9.10	16.4	240	
	2-5-88	149	9.29	16.4	295	
	2-5-88	164 (1)	8.67	12.3	230	
GW-477C	2-1-88	3	10.30	14.1	270	O2 = 7.8
	2-1-88	6	10.36	14.4	285	O2 = 7.9
	2-1-88	7 (1)	10.30	14.2	280	
GW-478A	2-2-88	5	9.55	20.6	250	Slightly Turbid
	2-2-88	10	8.32	20.5	260	
	2-2-88	15	8.79	20.2	255	
	2-2-88	20 (1)	8.47	19.5	275	
GW-478B	2-1-88	2.5	11.94	14.4	800	O2 = 9.0
	2-1-88	7.5	11.28	13.1	420	O2 = 8.0
	2-1-88	10.5	10.94	14.8	315	O2 = 7.5
	2-1-88	13.5	10.77	14.5	360	O2 = 8.4
	2-1-88	16	10.76	13.3	255	O2 = 8.2
	2-5-88	26	10.10	11.0	230	
	2-5-88	36	8.96	13.5	250	
	2-5-88	51	9.78	14.3	155	
	2-5-88	61	10.03	13.0	165	
	2-5-88	76 (1)	9.62	13.2	225	
GW-478C	2-5-88	11 (1)	11.89	11.5	4,200	

NOTES: (1) This volume represents the total volume removed during development.

(2) Well development results for tracer wells GW-479 through GW-484 were not available at the time of the publication of this report.

(3) O2 Denotes dissolved oxygen content in mg/l.

8.0 SLUG TESTING

8.1 Objectives and Scope

The objective of the slug test program was to determine in-situ hydraulic conductivity values through the use of field rising head (slug) tests. Slug tests were performed in pump test/tracer test wells and in piezometer completions in coreholes GW-455 and GW-471, as part of QA/QC measures for comparing results of different field testing methods (i.e. packer and pump tests). Comparisons of slug test results with other methods are discussed in Section 8.4. Slug tests also served as a QA/QC check regarding proper well installation procedures, to establish if an effective hydraulic connection exists between the interval screened.

A total of 21 slug tests were performed. In cases where the well did not exhibit a sufficient standing water column, a rising head test was not attempted. Slug tests were performed subsequent to and upon completion of well development, in accordance with the procedures outlined in Appendix A8 of the Task 2 Report (Reference 3).

Rising head tests on corehole piezometer completions and development GW-455 and GW-471 were performed after the installation of 2 inch and 1 inch piezometers, respectively.

8.2 Reduction and Interpretation of Slug Test Data

Data obtained from rising head test measurements were recorded in the field on rising head test field forms. The field test data was transported to Atlanta and entered into a computer data management program.

Semi-log plots were generated from slug test field data for the interpretation and selection of points used for calculations. All calculations of hydraulic conductivity (K) were done in accordance with the procedure described by Hvorslev

(Reference 10). The Hvorslev method does not consider the effects of vertical flow components or system anisotropy. However, the radius of influence for standard rising head tests is relatively small and it is unlikely that the errors introduced are considerable. In general, rising head test results should be considered somewhat qualitative.

Interpretation of the semi-log plots attempted to distinguish between early and late recovery data. In shallow wells, or in wells with significant drawdown, there is potential for dewatering of the sand pack. When such a condition exists, early time recovery may represent sand pack draining, therefore, late time recovery data were selected for analysis because there were more representative of formation response. Conversely, in wells with a very short water column and a subsequent low driving head, the early time data were thought to be a more accurate indication of in-situ permeabilities. In such cases, the late time data experienced an insufficient head differential to effectively stress the aquifer.

The reduced field data and semi-log plots of recovery are presented in Appendix D. It should be noted that, to allow for the fact that flow to the wells is not truly radial nor spherical, the hydraulic conductivity calculations in Appendix D are based on an open interval length (L) which includes a maximum of 2 ft. of sand pack above the top of screen and 1 ft. of sand pack below the bottom of the screen, but not the entire sand pack length. Consequently, there are some differences in sand pack length indications between Appendix D, Table 6.1, and the well installation logs.

8.3 Discussion of Results

Table 8.1 summarizes the calculated values of rising head test horizontal hydraulic conductivities.

The deep pump test or "A" wells were typically completed 40 to 75 feet in depth into the Maryville Limestone, where a zone of structural deformation had been observed. Hydraulic conductivities for these wells ranged from 3.93×10^{-5} cm/s to 7.85×10^{-7} cm/s with a geometric mean of 7.72×10^{-6} cm/s. This moderate range of hydraulic conductivity values could be due to secondary fracture flow features, in conjunction with primary, lithologically controlled bedding features. Evidence from the pump test (Section 9.0) and tracer test (Section 10.0) indicate that these structural variations may indeed control the distributions of hydraulic conductivity within this area.

The intermediate pump test observation wells or "B" wells were typically completed in the upper 25 to 35 feet of the Maryville Limestone, in a zone which sits above the aforementioned structural zone. Hydraulic conductivities for these wells ranged from 7.96×10^{-5} cm/s to 1.12×10^{-5} cm/s, with a geometric mean of 3.45×10^{-5} cm/s.

The shallow pump test/tracer test wells (C-wells) completed in saprolite, had insufficient standing water columns at the time of field testing to produce slug test results of meaningful value.

The tracer test wells were generally completed in the saprolite or in the upper 10 feet of the Maryville Limestone. The hydraulic conductivity for these wells range from 1.82×10^{-6} to 1.81×10^{-4} cm/s with a geometric mean of 1.30×10^{-5} cm/s.

Rising head tests were performed in 2 wells completed in coreholes GW-471 and GW-455. Piezometer GW-471 (Total depth = 101.5 feet) was completed approximately 80 feet into the Maryville Limestone and yielded a hydraulic conductivity of 1.18×10^{-6} cm/s. Piezometer GW-455 (Total depth = 182.5

feet) was completed about 60 feet into the Maryville Limestone and exhibited a hydraulic conductivity of 4.57×10^{-5} cm/s.

The geometric mean for all wells completed in the Maryville Limestone within the pump test/tracer test area is 1.34×10^{-5} cm/s, which is consistent with the mean value (4.36×10^{-5} cm/s) obtained from a site-wide testing of shallow system wells completed in the Maryville Limestone (Reference 3).

8.4 Comparison of Slug Test Results with Pump and Packer Test Results

Hydraulic conductivity values determined from slug test results were compared with those calculated from pump test and packer test data (Table 8.2). Interpretation and reduction of packer test and pump test data are discussed in Sections 4.0 and 9.0, respectively. In cases where packer test intervals corresponded with screened intervals of adjacent wells (within one or two feet), direct comparisons could be made between slug test and packer test results from coreholes GW-471 and GW-455.

Comparisons of slug test results with pump test and packer test results demonstrated a high degree of consistency between these methods for determinations of hydraulic conductivity. In general, slug test results, for a given tested interval, were within one order of magnitude of pump test and packer test results.

It should be noted that packer test comparisons with slug test results were based on the up and down dip correlation of tested intervals from corehole GW-471, assuming a 45 degree dip; therefore, such comparisons should not be interpreted as common depth correlations. Nevertheless, the uniformity in

these results strongly suggests that hydraulic conductivity is not directly depth dependent, but is related to discrete bedrock zones.

Overall comparisons of slug test, pump test, and packer test methods for determination of hydraulic conductivity have demonstrated a high degree of consistency for the tracer area site.

SEPTEMBER 1988 TABLE 8.1 873-3512.

RISING HEAD TEST SUMMARY

WELL NO.	OPEN INTERVAL TOP OF SATURATED SAND (TOC-FT)	OPEN INTERVAL BOTTOM OF SAND PACK (TOC-FT)	FORMATION	K (cm/sec)
GW-455	157.7	185.8	MARYVILLE	4.57E-05
GW-471	89.7	103.4	MARYVILLE	1.18E-06
GW-473	68.4	94.4	MARYVILLE	3.93E-05
GW-474	27.9	45.1	MARYVILLE	3.33E-05
GW-475A	86.4	99.7	MARYVILLE	7.85E-07
GW-475B	49.9	62.9	MARYVILLE	6.96E-05
GW-476A	69.9	83.0	MARYVILLE	6.61E-06
GW-476B	36.9	49.4	MARYVILLE	7.96E-05
GW-477A	54.7	68.7	MARYVILLE	1.37E-05
GW-477B	22.3	34.9	MAY-SAP	1.12E-05
GW-478A	66.9	81.3	MARYVILLE	9.81E-06
GW-478B	35.2	47.2	MARYVILLE	2.35E-05
GW-479	18.4	25.9	SAPROLITE	2.48E-05
GW-480A	33.6	37.6	MARYVILLE	2.86E-06
GW-480B	28.6	32.6	MAY-SAP	5.23E-06
GW-481A	31.4	35.1	MARYVILLE	1.81E-04
GW-481B	28.6	32.6	MAY-SAP	6.76E-06
GW-482A	32.7	36.7	MARYVILLE	1.82E-06
GW-482B	26.2	30.2	MAY-SAP	2.29E-05
GW-483	18.4	28.0	MAY-SAP	3.27E-05
GW-484	17.1	24.3	SAPROLITE	1.75E-05

GEOMETRIC MEANS

ALL (incl SAP) = 1.37E-05
MARYVILLE (excl SAP) = 1.34E-05
SAPROLITE AND MAY-SAP CONTACT = 1.44E-05

* FORMATION ABBREVIATIONS: MAY = MAYNARDVILLE
MARY = MARYVILLE
SAP = SAPROLITE

TABLE 8.2

COMPARISON OF SLUG TEST HYDRAULIC CONDUCTIVITY (K) VALUES
WITH PUMP TEST AND PACKER TEST RESULTS

WELL NO.	TESTED INTERVAL (FT. BGS.)	SLUG TEST K (CM/SEC)	PUMP TEST (1) K (CM/SEC)	PACKER TEST (2) K (CM/SEC)
GW-455	157.7 to 185.8	3.61E-05	3.47E-06	4.07E-05
GW-471	89.7 to 105.6	1.05E-06	1.28E-05	NA
GW-473	68.4 to 94.4	3.93E-05	1.01E-05	5.39E-06 (1)
GW-474	27.9 to 45.1	3.33E-05	2.66E-05	4.61E-05 (1)
GW-475A	86.4 to 99.7	7.88E-07	1.23E-05	5.39E-06 (1)
GW-475B	49.9 to 62.9	6.96E-05	2.88E-05	4.61E-05 (1)
GW-476A	69.9 to 83.0	6.61E-06	1.14E-05	5.39E-06 (1)
GW-476B	36.9 to 49.4	7.96E-05	6.47E-05	4.61E-05 (1)
GW-477A	54.7 to 68.7	1.37E-05	1.63E-05	NA
GW-477B	22.3 to 34.9	1.12E-05	7.48E-05	NA
GW-478A	67.9 to 81.3	9.81E-06	1.00E-05	5.39E-06 (1)
GW-478B	35.2 to 47.2	2.35E-05	3.54E-05	4.61E-05 (1)
GW-479	18.4 to 25.9	2.70E-05	NA	NA
GW-480A	33.6 to 37.6	2.86E-06	NA	NA
GW-480B	28.6 to 32.6	5.23E-06	NA	NA
GW-481A	31.4 to 35.1	1.81E-04	NA	NA
GW-481B	28.6 to 32.6	6.76E-06	NA	NA
GW-482A	32.7 to 36.7	1.82E-06	NA	NA
GW-482B	26.2 to 30.2	2.29E-05	NA	NA
GW-483	18.4 to 28.0	3.27E-05	NA	NA
GW-484	17.1 to 24.3	1.75E-05	NA	NA

NOTES (1) PACKER TEST HRDRAULIC CONDUCTIVITY (K) DERIVED FROM COREHOLE GW-471. THE COMPARISON PACKER TEST K IS CORRELATIVE TO THE ALONG-DIP PROJECTION OF TESTED ZONES IN GW-471, ASSUMING A DIP OF 45 DEGREES SOUTH.

9.0 TRACER AREA PUMPING TESTS

9.1 Objectives and Scope

The objectives of the tracer area pumping tests were to perform a preliminary characterization of the aquifer characteristics to assist in the planning and design of the field tracer test. The deep test was designed to evaluate the hydraulic characteristics of the structural zone that was observed in coreholes GW-471, GW-404, and GW-455. The shallow test was designed to evaluate water table hydraulic parameters, and interconnection between zones.

In addition, at the time of the tests, the tracer injection depth and location were undecided and the two tests were intended to provide data to clarify the best injection point. The scope of work for the two tracer area pumping tests consisted of pumping each of the deep and shallow test wells for a period of 24 hours followed by monitoring of each recovery period until the majority of wells reached 90% recovery. The deep pumping test was performed from February 8 to February 9, 1988 with recovery in selected wells being monitored to February 16, 1988. The deep test was performed first based on the assessment that total recovery would be achieved faster, since the test was reasoned to likely behave as a confined or semi-confined system, and cause little, if any, dewatering of the more unconfined saprolite. The recovery portion of the deep test was continued until static conditions were reached.

The shallow test was performed by pumping from February 17 to February 18, 1988, and measuring recovery in some wells until February 25, 1988. All wells in the immediate vicinity of the tracer area were monitored during the pumping tests.

The methods of analysis for the pump tests were selected to examine several hydrogeological models for the site behavior ranging from homogeneous, isotropic, through leaky aquifer to discrete fracture models.

9.2 Data Collection and Reduction

Data Collection - The Tracer Test Area pump test field data are included in Appendices E1 and E4 of this report. Pumping and observation wells were monitored during the pumping tests either manually or with a transducer datalogger system. Water levels were initially measured in all wells manually using a SINCO electronic water level indicator and calibrated tape. Wells measured manually for the duration of the tests included the following: GW-404, 455, 476C, 477C and 478C. Wells monitored using vibrating wire transducers (10 and 50 psi) and datalogger systems include the following: GW-471, 473, 474, 475A, 475B, 475C, 476A, 476B, 477A, 477B, 478A, and 478B. Each transducer was calibrated to a known column of water in the well as derived from manual measurements.

Calibration checks were performed periodically during the pumping tests by comparing observed transducer pressure readings to manually measured (calculated) values. Pump discharge rates were measured using a Rockwell flow meter that is 99.9% accurate to flow rates between 0.25 and 10 gpm. Flow measurements were recorded manually by a Golder hydrogeologist. Barometric pressure readings were also obtained during pumping tests. Barometer fluctuations were minor and no significant changes in water levels were observed due to barometric effects.

Data Management and Reduction - All pump test data were entered or transferred into a computer data management program (Lotus version 2.0) and checked by the project hydrogeologist. Backup copies were made in the field of all

data recorded. Quarterly data transfers (References 5 and 6) included computer generated field data and plots used for analysis and reduction of values.

The first step in data reduction of the transducer data was to reduce the transducer readings to hydraulic head. This was accomplished by expressing the transducer pressure as feet of fresh water. Various formulas were written to reduce both time and pressure readings into the necessary format needed for plotting and analysis. Analytical methods used to evaluate and interpret the tracer area pump test data included both traditional radial, non-radial, isotropic, and anisotropic drawdown procedures. These procedures include the following: Theis drawdown (Reference 18) and recovery (Reference 12), Chow (Reference 1), Neuman delayed yield (Reference 14), Gringarten and Witherspoon fractured aquifer analysis (Reference 8), and Papadopulos anisotropic analysis (Reference 15). It should be noted that additional analyses such as the Hantush modified leaky aquifer system and partially penetrating analyses were investigated. These analytical procedures, however, either resulted in estimates of hydraulic parameters that were clearly inappropriate or could not be completed due to lack of sufficient field data.

All of the above analytical procedures are based on certain simplifying assumptions that are presented in their respective references. The aquifer systems at the tracer area do not ideally satisfy all of the assumptions for any one method. Consequently, each result must be interpreted with knowledge of the underlying assumptions. No one method is absolutely correct or incorrect, but rather must be considered as additional input in the overall assessment of the tracer area hydrogeology. Several methods of analysis were used, however, to determine which method best approximated the natural system.

9.3 Potentiometric Surfaces and Gradients

Prior to starting the pump test, water levels were obtained from each well at the tracer area. These levels, assumed to represent static conditions, were used to evaluate the potentiometric surfaces and vertical gradients at the tracer area for the deep, intermediate, and shallow aquifer systems.

Upon review of these data, it is evident that a strong upward vertical gradient exists in the tracer test area, confirming the previous packer testing data analyses. Figures 9.1 through 9.3 present the potentiometric contour maps of the deep, intermediate, and shallow aquifer systems, respectively. Vertical gradients between the deep (designated subscript A) and shallow (subscript C) wells range from approximately .031 ft./ft. between GW-475A and C, to 0.10 ft./ft. between GW-477A and C.

The potentiometric contours for the deep system indicated, just prior to the pump tests, that groundwater flow at the tracer pump test area was generally southwest, but with components to the west and south. The intermediate and shallow wells suggested a flow direction to the west.

It should be noted that the potentiometric contours presented in Figure 9.1 through 9.3 were from early data and were based on very few data points. They are presented to show the information available at the time. Consequently, the figures are qualitative and all flow directions were generalized. The most defensible conclusions that could be drawn at the time of measurement were that an upward gradient exists and that the generalized flow directions, although somewhat depth dependent, appear to be to the west or southwest.

9.4 Deep Tracer Pump Test

General - The deep pumping test was designed to effectively stress a specific stratigraphic and structural level within the Maryville Limestone. The open interval of the deep pumping well extends from 68.0 to 94.0 feet in depth, in contrast to the shallow pumping well which is open from 26.3 to 44.5 feet. The planning and design of the tracer pump tests are discussed in Section 5.0. Section 6.2 presents the drilling and installation of the pump test wells. Well construction details for these wells are presented in Table 6.1 with individual well installation logs presented in Appendix C.

9.4.1 Deep Test - Observed Drawdown Behavior

Arithmetic plots of water level versus time provide a convenient means of qualitatively evaluating drawdown response to pumping. Such plots for each well are provided in Appendix E2. Drawdown response to pumping was nearly immediate in all of the deep observation wells, a typical response for wells screened in a confined to semi-confined aquifer. The drawdown rate in deep (designated subscript A) observation wells was relatively steady for approximately the first five hours. After this time, the rate of drawdown decreased, with the majority of near field wells approaching steady state conditions after about 17 hours of pumping. One exception to this was well GW-475A, which continued to have a steady rate of drawdown throughout the pumping period and did not approach steady state conditions. This indicates that this observation well is screened in a zone of relatively high storage capacity, probably associated with the structural zone observed in GW-471.

Review of the drawdown data indicates a period of sharp decline in deep well drawdown after 13.4 hours of pumping. This was a result of discontinuation of pumping due to generator failure. Pumping was resumed approximately 14 hours into the test at a slightly increased pumping rate, which accounts for the slight offset in the late data, in comparison to early data which had approached steady state. The absence of a response in well GW-475A, due to the temporary pump shut-off indicates that this well may not be as effectively connected to the pumping well as other deep observation wells. This lack of sensitivity or response is probably related to the lack of significant fracture connection which may indicate a discontinuity in the structural zone between observation well GW-475A and the pumping well.

After pumping 24 hours, the maximum drawdown observed in the pump well GW-473 was 61.66 feet. The drawdown pattern observed in the deep wells at the end of pumping (24 hours) is presented as Figure 9.4. The drawdown pattern is non-radial and is elongated along the direction of strike. This orientation suggests anisotropic conditions with the direction of maximum transmissivity oriented along strike. This non-radial pattern was previously observed in the Nolichucky pump test (Reference 3) and is typical of steeply dipping, fractured sedimentary strata with the orientation of fractures parallel or sub-parallel to bedding.

Significant drawdown was also observed in the more distant corehole completion GW-455 (r = 150 ft.) and in the open corehole GW-404 (r = 105.8 ft.), even though these wells were flowing prior to the start of pumping. The maximum drawdown observed in GW-404 and GW-455 was greater than 5.0 and 0.9 feet, respectively. These observed drawdowns also suggest anisotropic conditions along and perpendicular to strike.

Significant drawdown at these distances, indicate that fracture sets are extensive. As illustrated in cross-section A-A' (Plate 1), the stratigraphic and structural level stressed by the deep pumping well correlates with the open interval of piezometer GW-455 and corehole GW-404. Drawdown observed in these wells was not used for contouring in Figure 9.4 because static levels were unknown (wells were flowing) and because their large distances from the pump test field would not lend itself to accurate contouring.

Drawdown observed in intermediate and shallow wells was minimal to negligible. Figure 9.5 presents the maximum drawdown observed in the intermediate wells (designated subscript B) at the end of pumping. Maximum drawdown observed in intermediate wells was very uniform, ranging from 0.72 to 0.89 feet. This consistent, yet small amount of drawdown, indicates that slight vertical leakage occurred between the zone effectively stressed by the deep pumping well and the zone monitored by the intermediate wells, 20 to 25 feet above the pumping well. The uniform distribution in drawdown of B wells suggests that major discrete fractures perpendicular or oblique to bedding are not prevalent.

The maximum drawdown observed in the shallow wells (designated subscript C) at the end of the pumping is presented in Figure 9.6. Drawdown observed in shallow wells during the deep test ranged from essentially zero feet in GW-477C to 0.33 feet in GW-478C. It should be noted, however, that observation well GW-477C actually indicated -0.11 ft. of drawdown. This may be an indication of non-steady conditions at the start of the test. The negligible to small amount of drawdown observed in the shallow wells also indicates that vertical leakage is slight to negligible.

9.4.2 Deep Tracer Pump Test Results

General - For completeness, all observation points were considered for aquifer test analysis of the deep pump test. All calculations are included in Appendix E-3. However, due to partial penetration of the deep pumping well and the fact that the well was designed to stress a selected zone, only the deep "A" wells and perhaps the corehole completions GW-471 and GW-455 and open corehole GW-404 can be considered to represent aquifer characteristics of the deep zone. The results presented in this section only include those values representative of the deep zone.

Transmissivity (T) and Storativity (S) - Analytical results from the deep pump test performed in the tracer area are presented in Table 9.1. In general, the analytical methods are in good agreement with each other. Transmissivity values of deep wells were calculated using the three methods referenced in Section 9.2 (References 1, 14 and 18). Drawdown and Recovery analyses are presented in Appendix E-3.

The geometric mean of transmissivity values derived from individual deep wells ranged from 1.07×10^{-5} ft^2/s (GW-477A) to 6.56×10^{-6} ft^2/s (GW-478A), indicating slight heterogeneity within the system (Table 9.1). The Transmissivity result for GW-455 (6.94×10^{-5} cm/s) is not included in this range. The maximum observed drawdown at GW-455 was only 0.9 ft. Additionally, the only viable solution was based on Theis recovery data alone. This narrow range in Transmissivity values for the deep wells suggests that the zone selectively screened by the deep wells exhibits a low degree of heterogeneity within bedding planes. The correlation further suggests that transmissivity is not depth dependent, but is bedding plane dependent, at this scale of investigation. This also tends to support the hypothesis of an updip and downdip

continuous structural zone, although the hydraulic conductivity of this zone may not be exceptionally high. It is noted that some evidence of transmissivity variation with depth is exhibited by the most shallow deep well GW-477A, which yielded the highest transmissivity of 1.07×10^{-5} ft^2/s.

Deep "A" well storativity values derived from the geometric mean of the Theis (Reference 18) and the Chow (Reference 1) methods ranged from 1.09×10^{-3} in GW-475A to 3.36×10^{-5} in GW-476A. These values are representative of semi-confined to well confined aquifers (Reference 2). The lower value could represent fracture storativity.

The greatest storativity was obtained from GW-475A, which was the only near-field well that did not reach steady state after 24 hours of pumping. The greater storativity and slower drawdown response exhibited by GW-475A, may be attributed to high degree of fracturing within the screened interval and little communication with the pumping well, perhaps indicating a discontinuity in the structure zone between wells GW-473 and GW-475A, or that the well did not adequately monitor the zone that had been stressed by pumping.

Log/time and log/drawdown plots of intermediate wells for the deep test revealed that wells GW-474, GW-475B and GW-476B exhibited a delayed yield response. This response is identified by significant portions of data falling below the Theis curve. This response is a result of the delayed yield due to vertical leakage from strata that overlie the observation wells; therefore, the values derived are not comparative to the deep zone that was more effectively stressed. Transmissivity derived from the intermediate wells ranged from 9.56×10^{-5} ft^2/s in GW-474 to 2.0×10^{-5} ft^2/s in GW-476B. These values are within an order of magnitude of other results (Table 9.2) derived from the shallow pump test.

Bulk Hydraulic Conductivity - Bulk hydraulic conductivity values were estimated from the transmissivities derived from the deep wells and are also presented on Table 9.1. These values were based on an estimated saturated aquifer thickness of 20 feet. This thickness is based on the assumption that the pumping well stresses the aquifer within the bedding plane directions. The screened interval isolates a 20 foot thickness of the aquifer when measured perpendicular to bedding. The 20 foot thickness primarily focuses on the 10^{-5} cm/s zone that is screened by the deep "A" observation wells.

Hydraulic conductivity (K) values (Table 9.1) estimated for the deep wells ("A" wells and deep pumping well) ranged from 1.63×10^{-5} cm/s to 1.0×10^{-5} cm/s. The K derived for the 200 foot open corehole GW-404, is 4.55×10^{-5} cm/s. Although this value is in general agreement with values obtained at other deep observation wells, care should be exercised in comparisons with other results because the corehole is open throughout its entire depth and does not adequately monitor the interval stressed by the pumping well.

The hydraulic conductivity for well GW-455 was calculated as 1.06×10^{-4} cm/s. Because of limited drawdown and the fact that the Theis Recovery method was found to be the only viable analysis performed at this location, the values of transmissivity and hydraulic conductivity calculated are not included in overall geometric means. Additionally, the Neuman delayed results are not included in the overall geometric means as they are not representative of the deep zone aquifer characteristics as previously discussed. The narrow range of hydraulic conductivities derived for deep wells shows only a slight degree of heterogeneity within the bedding. Deep pump test hydraulic conductivity values, in addition to packer test values are presented on section B-B' (Figure 5.2). This

figure illustrates the uniformity of values along bedding and the relatively close comparison of packer test values with pump test values.

Flow Boundaries - Deep pump test semi-log plots (Appendix E-3) were reviewed for the possible presence of impermeable boundaries. Evidence for boundaries is often noted as significant increases in drawdown rates or increases in slope of the semi-log plots. In general, most deep well semi-log plots ("A" wells and deep pumping well in the structural zone) are textbook straight lines, until steady state conditions are approached, thus indicating continuity in the structural zone.

However, well numbers GW-474, GW-475B, GW-476B, GW-477B, GW-478B, and GW-475C, located above the structural zone, did show indications of boundaries. Image well analysis of these possible boundaries did not result in unique definitions of boundary locations. It is believed that these apparent boundaries are due to depletion of groundwater storage in material overlying the structural zone, as shown by rapid increases in drawdown at late times.

Papadopulos Anisotropic Analysis - Non-radial drawdown conditions observed in the deep observation wells during the pump test indicate that the aquifer system is anisotropic and/or heterogeneous; therefore, the Papadopulos anisotropic analysis was applied to derive the values and orientation of the principle values of transmissivity. The results of the deep tracer pump test anisotropic analyses are presented in Table 9.3. Results presented for the deep test only include deep well combinations. The Papadopulos procedure assumes that the rate of drawdown for the wells used in combination be similar. Consequently, well combinations with "B" and "C" wells would violate this assumption. Figure 9.7 shows maximum transmissivity vectors calculated using the Papadopulos

anisotropic analysis. The figure illustrates that the vector orientation does not directly correlate with the direction of strike, although one vector (simulation No. 2) does correlate very closely with a direction perpendicular to strike. More well combinations within the deep zone would be necessary to determine the applicability of the Papadopulos analysis for this particular test.

Gringarten-Witherspoon Anisotropic Analysis - To supplement the information provided by the Papadopulos Anisotropic Analysis, the Gringarten-Witherspoon Analysis was applied to appropriate wells. The Gringarten-Witherspoon method uses an "equivalent reservoir" solution for a anisotropic homogeneous porous medium with a single fracture of higher permeability, to analytically define flow in fractured aquifers (Reference 8).

Both horizontal and vertical fracture models are available. A log-log plot of drawdown data versus time was compared to both horizontal and vertical fracture type curves. The horizontal fracture model proposed by Gringarten-Witherspoon (1972) most closely describes the behavior of the deep system at the tracer/pump test well field, as evidenced by comparisons of observed to type curve data.

Table 9.4 presents the results of the analysis of deep pumping well GW-473. The horizontal fracture model, unlike the vertical fracture model, only provides values of hydraulic conductivity (k) for analyses of the pumping well alone and is not designed to interpret drawdown data from observation wells. The horizontal fracture model, however, does allow for the calculation of a critical distance from the pumping well (ri), beyond which the drawdown is the same as that created by a line-source well in a homogeneous isotropic aquifer under radial flow conditions (Reference 8). This

method can therefore, suggest whether or not drawdown at a given observation well is likely to be significantly influenced by fracture flow effects near the pumping well.

An examination of Table 9.4 indicates that for selected values of storativity ranging from 1.0×10^{-4} to 1.0×10^{-3}, the transmissivity parallel to the principle fracture is about 4.5×10^{-7} ft^2/s. Transmissivity in the vertical (or Z) direction ranges from 4.34×10^{-5} ft^2/s to 4.34×10^{-4} ft^2/s for the same range of storage values.

The range of storativity values used was arrived at by analysis of deep pump test data using the previous mentioned methods. Assuming a saturated thickness of 20 feet, the maximum hydraulic conductivity (parallel to the fracture) calculated is 6.8×10^{-7} cm/s, and the vertical hydraulic conductivity (of the matrix) ranges from 6.6×10^{-5} cm/s to 6.6×10^{-4} cm/s. It is recognized that these values of hydraulic conductivity appear to be reversed. That is, it would be expected that higher hydraulic conductivities would exist parallel to the fracture. This indicates that perhaps the Gringarten model is not well suited for analyses of tests completed in this geologic media.

The critical distance from the pumping well, beyond which observed drawdown is similar to an isotropic homogeneous medium, ranges from 2.36 ft. to 7.46 ft. This would suggest that drawdown at all the observation wells in the tracer/pump test well field would not show the effects of an anisotropic fractured medium equivalent to the single horizontal fracture model suggested by the Gringarten-Witherspoon analysis. Rather, one could expect drawdown at these wells to be quite similar to drawdown observed at a line-source well in a homogeneous isotropic aquifer, suggesting that this drawdown data can be analyzed using standard Theis-type techniques.

9.5 Shallow Tracer Pump Test

General - The shallow tracer pump test was performed to effectively stress the near surface bedrock aquifer overlying the afforementioned structural zone. The open interval of the shallow pumping well is from 26.3 to 44.5 feet and is 23.5 feet above the open interval of the deep test well. As mentioned in section 9.3, intermediate "B" wells and the shallow pump well were completed along a specific stratigraphic and structural horizon. Therefore, these wells decrease in depth to the north, corresponding with the dip of strata (40 to 45 degrees). Shallow "C" wells were screened at the water table. Static conditions observed prior to pumping are discussed in detail in section 9.3. Field data obtained during the shallow pump test is presented in Appendix E4.

9.5.1 Shallow Test - Observed Drawdown Behavior

Arithmetic plots of water level versus time were generated to provide a convenient means of qualitatively evaluating drawdown response to pumping. These plots are presented in Appendix E5 and show that drawdown response in the "B" wells was nearly immediate, a response typical of semi-confined to confined conditions. Intermediate wells continued to exhibit a steady rate of drawdown for approximately the first two hours, after which the drawdown rate sharply declined. This steady rate time period was much shorter than the deep test, indicating greater leakage or recharge from weathered rock and saprolite overlying the tested sequence. The "B" wells approached steady state conditions after approximately 16 to 17 hours, similar to the deep test.

After pumping for 24 hours, the maximum drawdown observed was 16.36 feet in the shallow pump well GW-474. The drawdown pattern observed in the intermediate wells at the end of pumping (24 hours) is presented as Figure 9.8. The drawdown

pattern is fairly radial, in comparison to the more non-radial pattern observed for the deep test. This moderately radial pattern for the zone screened by the "B" wells suggests that the degree of anisotropy is less than that observed for the deep test.

Figure 9.9 presents the maximum drawdown observed in the shallow "C" water table wells after pumping for 24 hours. This figure shows that the drawdown in shallow wells ranged from 0.12 feet to 1.08 feet. The greatest drawdown was experienced in GW-478C, which was the most saturated or deeper penetrating well.

Figure 9.10 presents the drawdown observed in the deep "A" wells after 24 hours of pumping the shallow test wells. The observed drawdown is very minimal, yet uniform, ranging from 0.40 to 0.47 feet. This minor amount of drawdown indicates slight upward vertical leakage from the deeper rock aquifer, and confirms the effect produced by the deep test. The uniform rate of drawdown suggests the lack of major discrete fractures oriented perpendicular to bedding.

9.5.2 Shallow Tracer Pump Test Results

General - Due to the selective nature and partial penetration of the shallow pumping well, only the intermediate ("B") and shallow ("C") wells were considered to represent aquifer characteristics for the shallow pump test. Consequently, only the "B" and "C" results are presented in this section. All calculations on other wells, however, are included in Appendix E6.

Transmissivity (T) and Storativity (S) - Analytical results from the shallow tracer pump test are presented in Table 9.2. The methods used for analysis were the same as those used for the deep test. In general, results of T and S analysis using the different methods were in good agreement. Drawdown and recovery analyses and plots are presented in Appendix E6.

The geometric mean of transmissivity values derived from various methods for the intermediate "B" wells, including the pump well, ranged from 7.36 X 10^{-5} ft^2/s (GW-477B) to 2.62 x 10^{-5} ft^2/s (GW-474) (Table 9.2). These values suggest slight heterogeneity within bedding at the depth range tested.

Intermediate "B" and pump well GW-474 storativity values derived from the geometric mean of the two methods applied (References 8 and 9) ranged from 1.33 x 10^{-4} (GW-475B) to 7.09 x 10^{-4} (GW-477B). These values also show a degree of consistency with respect to the particular stratigraphic and structural zone which was most effectively stressed by the shallow pump well, and is monitored by the "B" wells. These storativity values are representative of a semi-confined to confined aquifer (Reference 2).

Transmissivity values derived from observed drawdown in the shallow "C" wells ranged from 9.08 x 10^{-5} ft^2/s (GW-478C) to 1.58 x 10^{-4} ft^2/s (GW-475C). In general, transmissivities derived from "C" wells were an order of magnitude greater than derived from "B" wells. Values derived from the shallow "C" wells may not be accurate due to their higher stratigraphic location with respect to the pumping well. Therefore, vertical flow components may cause some uncertainty in the results of shallow well results. However, data supporting the reliability of results derived from the "C" wells includes the close correlation of packer test results with pump test results as illustrated on Figure 5.2.

The geometric mean of storativity values derived from the "C" wells ranged from 8.20×10^{-3} (GW-478C) to 7.09×10^{-2} (GW-476C). These values are more representative of an unconfined to semi-confined aquifer system (Reference 2).

Delayed Yield Response - In review of the log/drawdown log/time plots, the pumping well GW-474 exhibited a significant delayed yield response. This response is indicated by the log-log plot falling below the Theis curve, and represents vertical leakage or delayed yield. The Neuman transmissivity value of 1.8×10^{-5} ft^2/s was in good agreement with other methods applied. In general, the Neuman storativity value was somewhat higher than the Theis and Chow results, which again indicates significant delayed yield.

Bulk Hydraulic Conductivity - Bulk hydraulic conductivity values were estimated from the transmissivities derived from the intermediate depth wells and are also presented on Table 9.2. These values were based on an estimated average saturated aquifer thickness of 30 feet, which corresponds to the distance from the water table to the bottom of the pumping well. Hydraulic conductivity (K) values for intermediate wells range from 2.66×10^{-5} cm/s (GW-474) to 7.48×10^{-5} cm/s (GW-477B). K values derived from shallow "C" wells ranged from 9.23×10^{-5} cm/s (GW-478C) to 1.61×10^{-4} cm/s (GW-475C). These values are presented on a cross section (Figure 5.2), along with packer test K values from the adjacent corehole GW-471. The figure illustrates the close correlation in values derived from the two test methods.

Papadopulos Anisotropic Analysis - Slight non-radial drawdown response observed during the shallow pump test indicates that the aquifer system is somewhat anisotropic and/or heterogeneous; therefore, the Papadopulos anisotropic analysis was applied to derive the values and orientation of the principle values of transmissivity. The results of the shallow tracer

pump test anisotropic analyses are presented in Table 9.3 and are illustrated in Figure 9.11. Results presented only include intermediate "B" well combinations. The Papadopulos procedure assumes that the rate of drawdown for the wells used in combination be similar. Consequently, using well combinations that included "A" and "C" wells would violate this assumption.

Figure 9.11 presents magnitude and direction of the maximum transmissivity vectors calculated using the Papadopulos anisotropic analysis for the shallow test. The figure illustrates that the vector orientation does not directly correlate with the direction of strike. More well combinations within the shallow zone would be necessary to determine the applicability of the Papadopulos analysis for this particular test.

Gringarten-Witherspoon Anisotropic Analysis - As was previously mentioned, examination of shallow pump test drawdown data, suggests the existence of fractured anisotropic flow conditions. Thus, the Gringarten-Witherspoon method was applied to pumping well GW-474 in order to supplement the results of the Papadopulos Anisotropic Analysis.

The horizontal fracture model was again the most appropriate for the shallow pump test pumping well. for storage values ranging from 1.0×10^{-4} to 1.0×10^{-3}, maximum transmissivity was calculated as 1.30×10^{-6} ft^2/s and minimum transmissivity (in the vertical direction) ranges from 3.27×10^{-7} ft^2/s to 3.27×10^{-5} ft^2/s, depending on the storativity value used in the calculation.

Assuming a saturated thickness of 30.0 feet, hydraulic conductivity parallel to the principle modeled fracture was calculated as 1.32 x 10^{-6} cm/s and vertical hydraulic conductivity ranges from 3.32 x 10^{-7} cm/s to 3.32 x 10^{-6} cm/s.

The critical distance from the pumping well for homogeneous isotropic drawdown behavior was calculated to range from 41.58 ft. to 131.48 ft. This would suggest that drawdown at all wells would be affected in an anisotropic fractured medium equivalent to the horizontal fracture model suggested by the Gringarten-Witherspoon method. Table 9.4 presents the results of the Gringarten-Witherspoon Analysis for the shallow pump test.

9.6 Summary of Tracer Area Pump Test Results

The design and performance of both a deep and a shallow pumping test in the tracer area enabled the determination of both the vertical and lateral distribution of shallow system (less than 100 feet) bedrock aquifer characteristics. The following includes a summary of the results and interpretations of the tracer area pumping tests:

1. Potentiometric levels measured in the pump/observation multi-level well completions showed a strong upward vertical gradient in the tracer area, ranging from about 0.31 ft.ft. to 0.10 ft/ft.

2. The rate of drawdown in the structural zone in the deep "A" wells during the deep test was constant over a much longer period of time than the intermediate depth "B" wells during the shallow test. Log-log plots indicate this response is a result of greater delayed yield or vertical leakage, probably from above, in the more shallow zone.

3. The maximum drawdown pattern for the deep test (deep wells) exhibited a non-radial pattern elongated along the strike of bedding, which is the expected orientation of maximum transmissivity.

4. Minor to negligible amounts of drawdown observed in shallow and intermediate wells during the deep test illustrated that vertical leakage was minor and that major discrete fractures oriented perpendicular or oblique to bedding are not prevalent.

5. Bulk hydraulic conductivities showed slight heterogeneity in bedding planes. The heterogeneity is more pronounced in the shallow test zone than the deep test zone within the pump test field.

6. Significant drawdown during the deep pump test observed in an open corehole along strike and a bedrock piezometer downdip at distances 105.8 and 150 ft., respectively, along with the absence of boundary effects when reviewing semi-log plots, suggests hydraulic continuity within the structural zone.

7. The results of the Papadopulos anisotropic analysis are inconclusive because of too few appropriate well combinations. The Gringarten-Witherspoon anisotropic results suggest that the aquifer system does not contain significant discrete vertical fractures.

8. Deep pump test and deep "A" well storativity values ranged from 1.09×10^{-3} to 3.36×10^{-5} in comparison to shallow test results that ranged from 1.33×10^{-4} to 7.09×10^{-2}. These results confirm a transition from a confined deep system in the structural interval which dips from depths of 60 feet to over 100 feet in the pump test area, to a semi-confined to unconfined system as the bedrock saprolite interface is approached.

TABLE 9.1

DEEP PUMPTEST/TRACER AREA
SUMMARY OF RESULTS OF
DRAWDOWN AND RECOVERY ANALYSES

WELL NO.	TRANSMISSIVITY (THEIS DRAWDOWN) (SQ FT/SEC)	TRANSMISSIVITY (THEIS RECOVERY) (SQ FT/SEC)	COEF. OF STORAGE (THEIS DRAWDOWN) (DIMENSIONLESS)	TRANSMISSIVITY (NEUMAN METHOD) (SQ FT/SEC) (1)	COEF. OF STORAGE (NEUMAN METHOD) (DIMENSIONLESS)(2)	TRANSMISSIVITY (CHOW'S METHOD) (SQ FT/SEC)	GEOMETRIC MEAN TRANSMISSIVITY (SQ FT/SEC)	COEF. OF STORAGE (CHOW'S METHOD) (DIMENSIONLESS)	AVG. HYDRAULIC CONDUCTIVITY (CM/SEC) (3)
GW-404	2.76E-05	3.20E-05	1.24E-04	NA	NA	3.01E-05	2.98E-05	1.34E-04	4.55E-05
GW-455	NA	6.94E-05	NA	NA	NA	NA	NA	NA	1.06E-04 (5)
GW-471	7.61E-06	8.92E-06	1.47E-04	NA	NA	8.66E-06	8.38E-06	1.18E-04	1.28E-05
GW-473 (PW)	6.48E-06	6.49E-06	NA	NA	NA	6.83E-06	6.60E-06	NA	1.01E-05
GW-474	NA	NA	NA	9.56E-05	3.26E-02	NA	NA	NA	1.46E-04 (4)
GW-475A	1.48E-05	5.08E-06	1.65E-03	NA	NA	7.00E-06	8.07E-06	7.14E-04	1.23E-05
GW-475B	NA	NA	NA	8.01E-05	5.94E-04	NA	NA	NA	1.22E-04 (4)
GW-476A	8.54E-06	7.14E-06	3.60E-05	NA	NA	6.93E-06	7.50E-06	3.13E-05	1.14E-05
GW-476B	NA	NA	NA	2.00E-05	6.06E-04	NA	NA	NA	3.05E-05 (4)
GW-477A	2.25E-05	7.38E-06	1.51E-04	NA	NA	7.35E-06	1.07E-05	6.66E-04	1.63E-05
GW-478A	7.44E-06	6.32E-06	1.62E-04	NA	NA	6.00E-06	6.56E-06	1.69E-03	1.00E-05
OVERALL GEOMETRIC MEAN	1.16E-05	1.10E-05	1.73E-04	5.35E-05	2.27E-03	8.71E-06	9.51E-06	2.71E-04	1.45E-05

NOTE: (1) Represents the geometric mean of two transmissivity values derived using different type curves and/or match points.

(2) Represents the geometric mean of two coefficient of storage values derived using different type curves and /or match points.

(3) Based on the geometric means of the above transmissivity values and assuming a saturated aquifer thickness of 20.00 feet.

(4) K value not used in determination of overall geometric mean since observation well completed in zone immediately above pumped interval.

(5) K value not included in overall geometric mean due to limited drawdown (0.9 feet), and only the Theis recovery method prove to be a viable method of analysis.

(PW) Pumping well

TABLE 9.2

SHALLOW PUMPTEST/TRACER AREA
SUMMARY OF RESULTS OF
DRAWDOWN AND RECOVERY ANALYSES

WELL NO.	TRANSMISSIVITY (THEIS DRAWDOWN) (SQ FT/SEC)	TRANSMISSIVITY (THEIS RECOVERY) (SQ FT/SEC)	COEF. OF STORAGE (THEIS DRAWDOWN) (DIMENSIONLESS)	TRANSMISSIVITY (NEUMAN METHOD) (SQ FT/SEC) (1)	COEF. OF STORAGE (NEUMAN METHOD) (DIMENSIONLESS)(2)	TRANSMISSIVITY (CHOW'S METHOD) (SQ FT/SEC)	GEOMETRIC MEAN TRANSMISSIVITY (SQ FT/SEC)	COEF. OF STORAGE (CHOW'S METHOD) (DIMENSIONLESS)	AVG. HYDRAULIC CONDUCTIVITY (CM/SEC) (3)
GW-474(PW)	5.93E-05	1.45E-05	NA	1.77E-05	5.53E-02	3.11E-05	2.62E-05	NA	2.66E-05
GW-475B	3.66E-05	2.95E-05	1.35E-04	NA	NA	2.09E-05	2.83E-05	1.31E-04	2.88E-05
GW-475C	2.59E-04	2.94E-05	1.20E-02	NA	NA	5.15E-04	1.58E-04	1.27E-02	1.61E-04
GW-476B	7.46E-05	4.69E-05	2.38E-04	NA	NA	7.39E-05	6.37E-05	2.28E-04	6.47E-05
GW-476C	NA	NA	NA	NA	NA	1.12E-04	1.12E-04	7.09E-02	1.14E-04
GW-477B	7.46E-05	1.28E-04	7.92E-04	NA	NA	4.18E-05	7.36E-05	6.35E-04	7.48E-05
GW-477C	4.30E-04	NA	7.55E-02	NA	NA	3.36E-05	1.20E-04	2.25E-02	1.22E-04
GW-478B	3.66E-05	2.54E-05	1.64E-04	NA	NA	4.52E-05	3.48E-05	1.53E-04	3.54E-05
GW-478C	1.46E-04	3.27E-05	8.01E-03	NA	NA	1.57E-04	9.08E-05	8.39E-03	9.23E-05
OVERALL GEOMETRIC MEAN	9.60E-05	3.49E-05	1.63E-03	1.77E-05	5.53E-02	6.71E-05	6.59E-05	2.17E-03	6.69E-05

NOTE: (1) Represents the geometric mean of two transmissivity values derived using different type curves and/or match points.

(2) Represents the geometric mean of two coefficient of storage values derived using different type curves and/or match points.

(3) Based on the geometric means of the above transmissivity values and assuming a saturated aquifer thickness of 30.00 FT.

(PW) Pumping well

TABLE 9.3

DEEP AND SHALLOW TRACER PUMP TEST
PAPADOPULOS ANISOTROPIC ANALYSIS RESULTS

SIMULATION NUMBER	OBSERVATION WELL COMBINATIONS (1)	MAXIMUM TRANSMISSIVITY (SQ FT/SEC)	MINIMUM TRANSMISSIVITY (SQ FT/SEC)	STORAGE COEFFICIENT (DIMENSIONLESS)	ORIENTATION OF MAXIMUM TRANSMISSIVITY (DEGREES) (2)
		DEEP PUMP TEST RESULTS			
1	GW-476A,GW-477A,GW-471	2.63E-05	3.4E-06	3.57E-05	148
2	GW-477A,GW-478A,GW-471	1.3E-05	5.93E-06	1.09E-04	84
		SHALLOW PUMP TEST RESULTS			
1	GW-475B,GW-476B,GW-477B	3.7E-04	1.7E-05	7.68E-05	34
2	GW-475B,GW-477B,GW-478B	2.2E-04	2.2E-05	1.04E-04	37
3	GW-476B,GW-477B,GW-478B	1.7E-04	4.1E-05	2.29E-04	156

NOTES: (1) Well combinations that failed are not listed.
(2) Orientation refers to the direction of the maximum transmissivity measured in degrees counterclockwise from the positive x-axis.

TABLE 9.4
DEEP AND SHALLOW PUMPTEST
SUMMARY OF RESULTS
GRINGARTEN-WITHERSPOON ANALYSIS

WELL NO.	ri (FT)	COEFFICIENT OF STORAGE	Tx (SQ FT/SEC)	Tz (SQ FT/SEC)	Kx (CM/SEC)	Kz (CM/SEC)
GW-473	7.464	1.00E-04	4.50E-07	4.34E-05	6.86E-07	6.61E-05
	5.278	2.00E-04	4.50E-07	8.68E-05	6.86E-07	1.32E-04
	4.309	3.00E-04	4.50E-07	1.30E-04	6.86E-07	1.98E-04
	3.732	4.00E-04	4.50E-07	1.74E-04	6.86E-07	2.65E-04
	3.338	5.00E-04	4.50E-07	2.17E-04	6.86E-07	3.31E-04
	3.047	6.00E-04	4.50E-07	2.60E-04	6.86E-07	3.96E-04
	2.821	7.00E-04	4.50E-07	3.04E-04	6.86E-07	4.63E-04
	2.639	8.00E-04	4.50E-07	3.47E-04	6.86E-07	5.29E-04
	2.488	9.00E-04	4.50E-07	3.91E-04	6.86E-07	5.96E-04
	2.360	1.00E-03	4.50E-07	4.34E-04	6.86E-07	6.61E-04
GW-474	131.487	1.00E-04	1.30E-06	3.27E-07	1.32E-06	3.32E-07
	92.975	2.00E-04	1.30E-06	6.55E-07	1.32E-06	6.65E-07
	75.914	3.00E-04	1.30E-06	9.82E-07	1.32E-06	9.98E-07
	65.743	4.00E-04	1.30E-06	1.31E-06	1.32E-06	1.33E-06
	58.803	5.00E-04	1.30E-06	1.64E-06	1.32E-06	1.67E-06
	53.679	6.00E-04	1.30E-06	1.96E-06	1.32E-06	1.99E-06
	49.697	7.00E-04	1.30E-06	2.29E-06	1.32E-06	2.33E-06
	46.488	8.00E-04	1.30E-06	2.62E-06	1.32E-06	2.66E-06
	43.829	9.00E-04	1.30E-06	2.95E-06	1.32E-06	3.00E-06
	41.580	1.00E-03	1.30E-06	3.27E-06	1.32E-06	3.32E-06

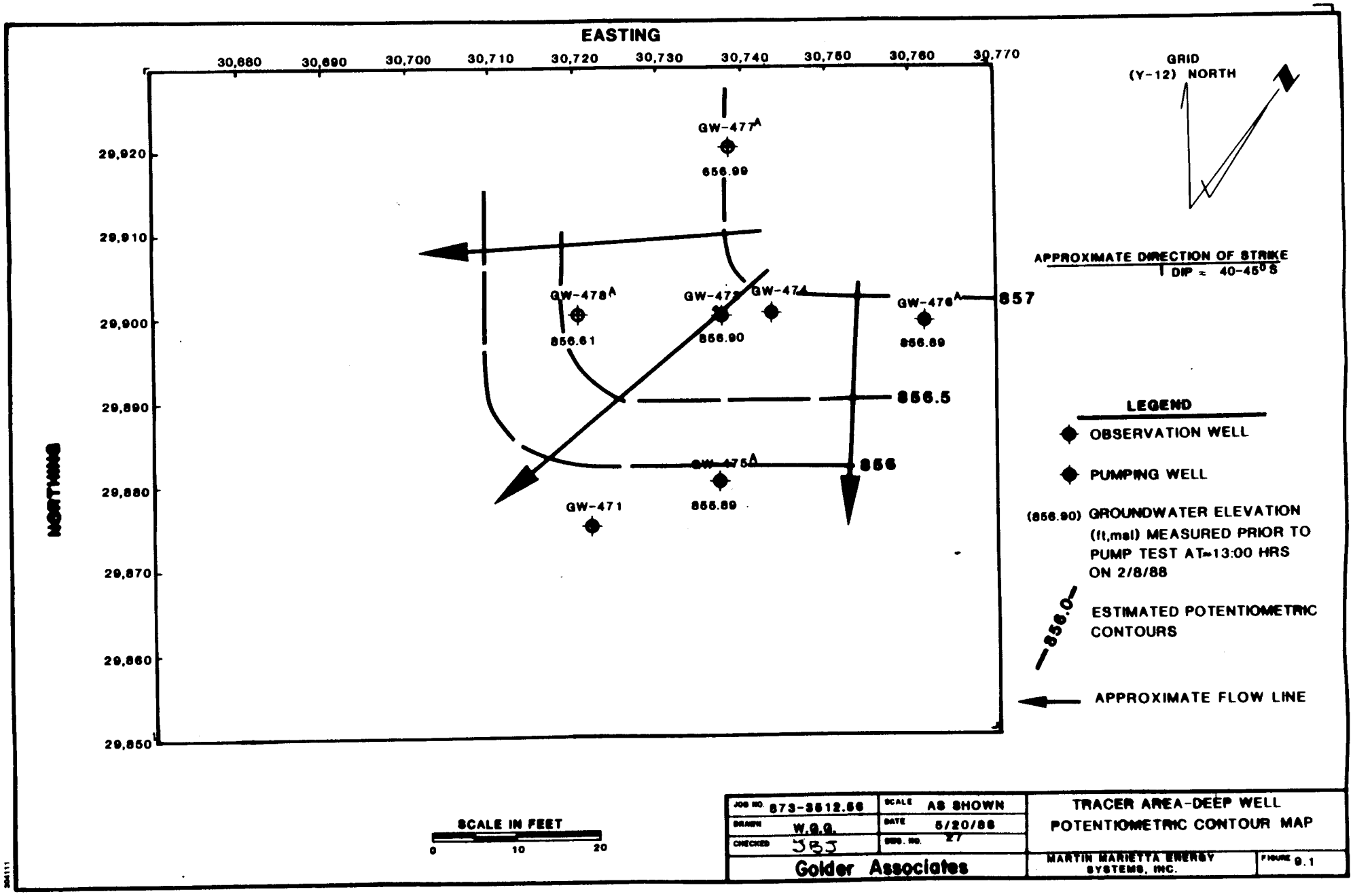
EASTING
30,680
30,690
30,700
30,710
30,720
30,730
30,740
30,750
30,760
30,770
NORTHING
29,920
29,910
29,900
29,890
29,880
29,870
29,860
29,850
GW-477A
856.99
GW-478A
856.61
GW-472
856.90
GW-474
GW-476A
856.89
857
856.5
GW-475A
856
GW-471
856.89
GRID
(Y-12) NORTH
APPROXIMATE DIRECTION OF STRIKE
DIP ≈ 40-45° S
LEGEND
OBSERVATION WELL
PUMPING WELL
(856.90) GROUNDWATER ELEVATION (ft,msl) MEASURED PRIOR TO PUMP TEST AT≈13:00 HRS ON 2/8/88
856.0
ESTIMATED POTENTIOMETRIC CONTOURS
APPROXIMATE FLOW LINE
SCALE IN FEET
0
10
20
JOB NO. 873-3512.56
SCALE AS SHOWN
DRAWN W.G.G.
DATE 5/20/88
CHECKED JBJ
DWG. NO. 27
Golder Associates
TRACER AREA-DEEP WELL
POTENTIOMETRIC CONTOUR MAP
MARTIN MARIETTA ENERGY SYSTEMS, INC.
FIGURE 9.1

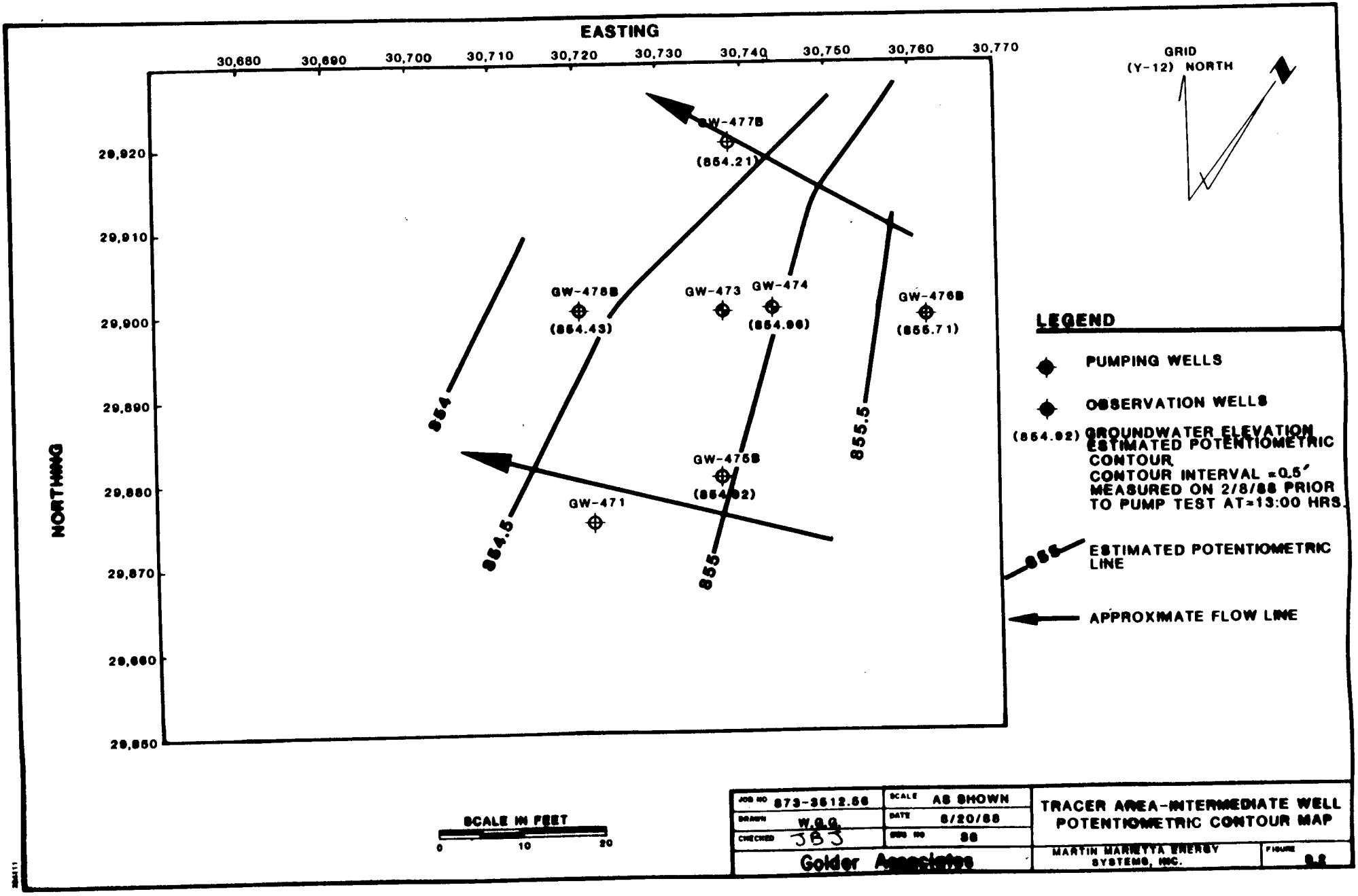
EASTING
30,680
30,690
30,700
30,710
30,720
30,730
30,740
30,750
30,760
30,770
NORTHING
29,920
29,910
29,900
29,890
29,880
29,870
29,860
29,850
GRID
(Y-12) NORTH
GW-477B
(854.21)
GW-478B
(854.43)
GW-473
GW-474
(854.96)
GW-476B
(855.71)
GW-475B
(854.92)
GW-471
854
854.5
855
855.5
LEGEND
PUMPING WELLS
OBSERVATION WELLS
(854.92) GROUNDWATER ELEVATION
ESTIMATED POTENTIOMETRIC CONTOUR
CONTOUR INTERVAL =0.5'
MEASURED ON 2/8/88 PRIOR TO PUMP TEST AT≈13:00 HRS.
ESTIMATED POTENTIOMETRIC LINE
APPROXIMATE FLOW LINE
SCALE IN FEET
0
10
20
JOB NO 873-3512.56
SCALE AS SHOWN
DRAWN W.G.G.
DATE 8/20/88
CHECKED JBJ
DWG NO 88
Golder Associates
TRACER AREA-INTERMEDIATE WELL POTENTIOMETRIC CONTOUR MAP
MARTIN MARIETTA ENERGY SYSTEMS, INC.
FIGURE 9.2

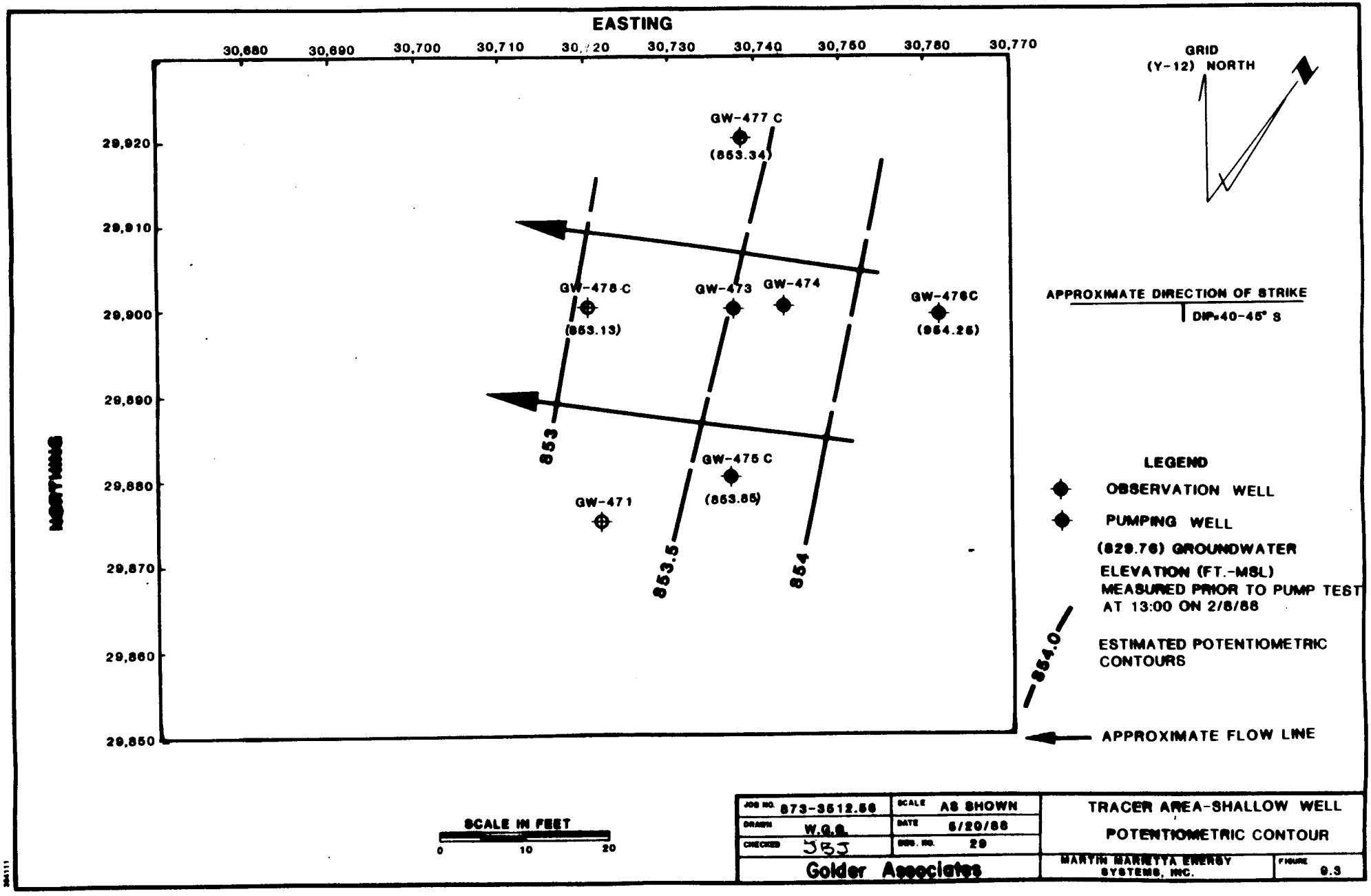
EASTING
30,680
30,690
30,700
30,710
30,720
30,730
30,740
30,750
30,760
30,770
NORTHING
29,920
29,910
29,900
29,890
29,880
29,870
29,860
29,850
GW-477 C
(863.34)
GW-478 C
(863.13)
GW-473
GW-474
GW-476C
(864.26)
GW-475 C
(863.85)
GW-471
853
853.5
854
854.0
GRID
(Y-12) NORTH
APPROXIMATE DIRECTION OF STRIKE
DIP=40-45° S
LEGEND
OBSERVATION WELL
PUMPING WELL
(829.76) GROUNDWATER ELEVATION (FT.-MSL) MEASURED PRIOR TO PUMP TEST AT 13:00 ON 2/8/88
ESTIMATED POTENTIOMETRIC CONTOURS
APPROXIMATE FLOW LINE
SCALE IN FEET
0
10
20
JOB NO. 873-3512.56
SCALE AS SHOWN
DRAWN W.G.S.
DATE 5/20/88
CHECKED JBJ
DWG. NO. 29
Golder Associates
TRACER AREA-SHALLOW WELL
POTENTIOMETRIC CONTOUR
MARTIN MARIETTA ENERGY SYSTEMS, INC.
FIGURE 9.3

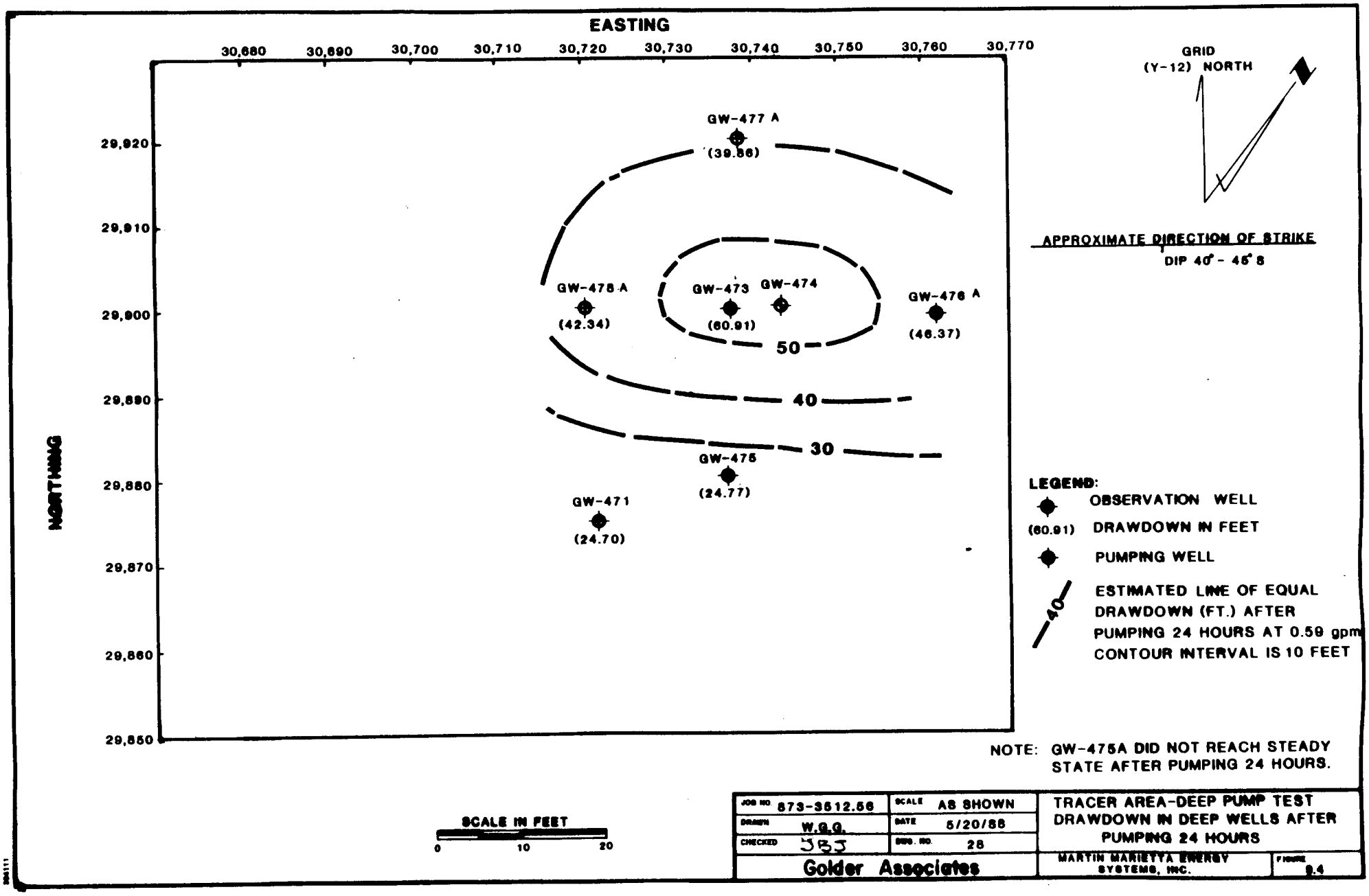
EASTING
30,680
30,690
30,700
30,710
30,720
30,730
30,740
30,750
30,760
30,770
NORTHING
29,920
29,910
29,900
29,890
29,880
29,870
29,860
29,850
GW-477 A
(39.86)
GW-475 A
(42.34)
GW-473
(60.91)
GW-474
GW-476 A
(46.37)
GW-475
(24.77)
GW-471
(24.70)
50
40
30
GRID
(Y-12) NORTH
APPROXIMATE DIRECTION OF STRIKE
DIP 40° - 45° S
LEGEND:
OBSERVATION WELL
(60.91) DRAWDOWN IN FEET
PUMPING WELL
40
ESTIMATED LINE OF EQUAL DRAWDOWN (FT.) AFTER PUMPING 24 HOURS AT 0.59 gpm
CONTOUR INTERVAL IS 10 FEET
NOTE: GW-475A DID NOT REACH STEADY STATE AFTER PUMPING 24 HOURS.
SCALE IN FEET
0
10
20
JOB NO. 873-3512.56
SCALE AS SHOWN
DRAWN W.G.G.
DATE 5/20/88
CHECKED JBJ
DWG. NO. 28
Golder Associates
TRACER AREA-DEEP PUMP TEST
DRAWDOWN IN DEEP WELLS AFTER PUMPING 24 HOURS
MARTIN MARIETTA ENERGY SYSTEMS, INC.
FIGURE 9.4

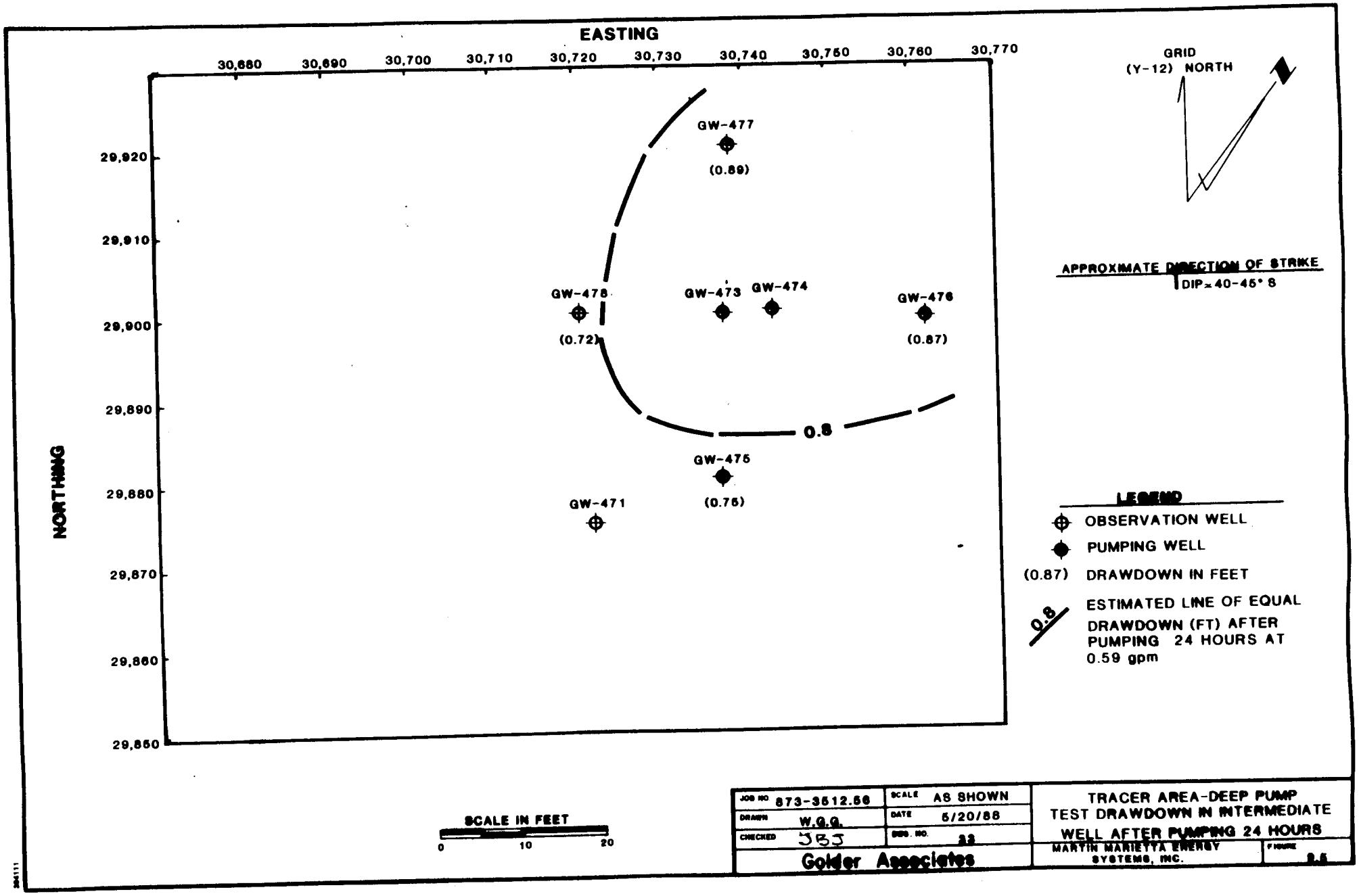
EASTING
30,680
30,690
30,700
30,710
30,720
30,730
30,740
30,750
30,760
30,770
NORTHING
29,920
29,910
29,900
29,890
29,880
29,870
29,860
29,850
GW-477
(0.89)
GW-478
(0.72)
GW-473
GW-474
GW-476
(0.87)
0.8
GW-475
(0.75)
GW-471
GRID
(Y-12) NORTH
APPROXIMATE DIRECTION OF STRIKE
DIP≈40-45° S
LEGEND
OBSERVATION WELL
PUMPING WELL
(0.87) DRAWDOWN IN FEET
0.8 ESTIMATED LINE OF EQUAL DRAWDOWN (FT) AFTER PUMPING 24 HOURS AT 0.59 gpm
SCALE IN FEET
0
10
20
JOB NO 873-3512.56
SCALE AS SHOWN
DRAWN W.G.G.
DATE 5/20/88
CHECKED JBJ
DWG. NO. 33
Golder Associates
TRACER AREA-DEEP PUMP TEST DRAWDOWN IN INTERMEDIATE WELL AFTER PUMPING 24 HOURS
MARTIN MARIETTA ENERGY SYSTEMS, INC.
FIGURE 9.5

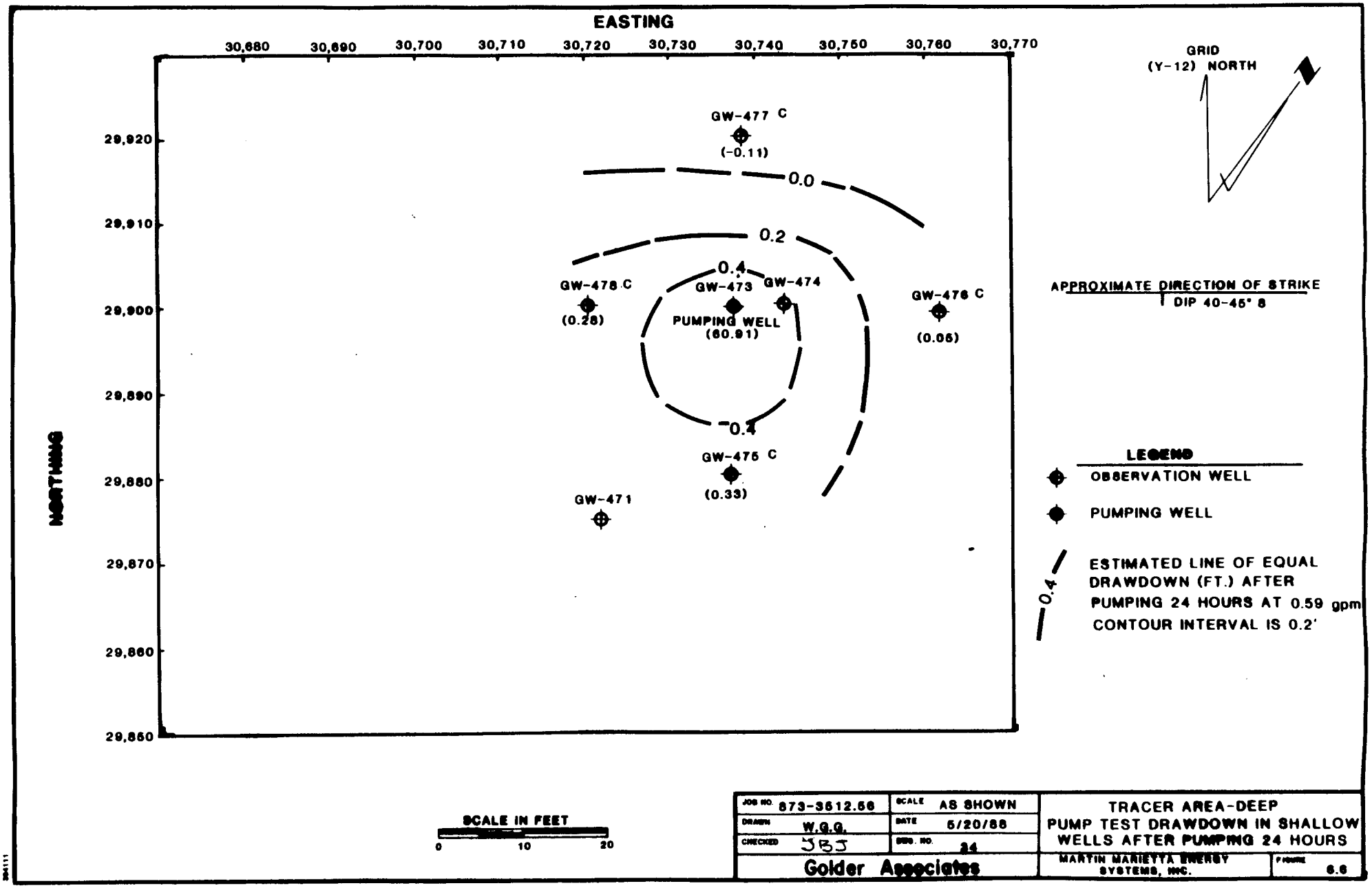
EASTING
30,680
30,690
30,700
30,710
30,720
30,730
30,740
30,750
30,760
30,770
NORTHING
29,920
29,910
29,900
29,890
29,880
29,870
29,860
29,850
GW-477 C
(-0.11)
0.0
0.2
0.4
GW-478 C
(0.28)
GW-473
GW-474
PUMPING WELL
(60.91)
GW-476 C
(0.05)
0.4
GW-475 C
(0.33)
GW-471
GRID
(Y-12) NORTH
APPROXIMATE DIRECTION OF STRIKE
DIP 40-45° S
LEGEND
OBSERVATION WELL
PUMPING WELL
0.4
ESTIMATED LINE OF EQUAL DRAWDOWN (FT.) AFTER PUMPING 24 HOURS AT 0.59 gpm
CONTOUR INTERVAL IS 0.2'
SCALE IN FEET
0
10
20
JOB NO. 873-3612.56
SCALE AS SHOWN
DRAWN W.G.G.
DATE 5/20/88
CHECKED JBJ
DWG. NO. 24
Golder Associates
TRACER AREA-DEEP
PUMP TEST DRAWDOWN IN SHALLOW WELLS AFTER PUMPING 24 HOURS
MARTIN MARIETTA ENERGY SYSTEMS, INC.
FIGURE 6.6

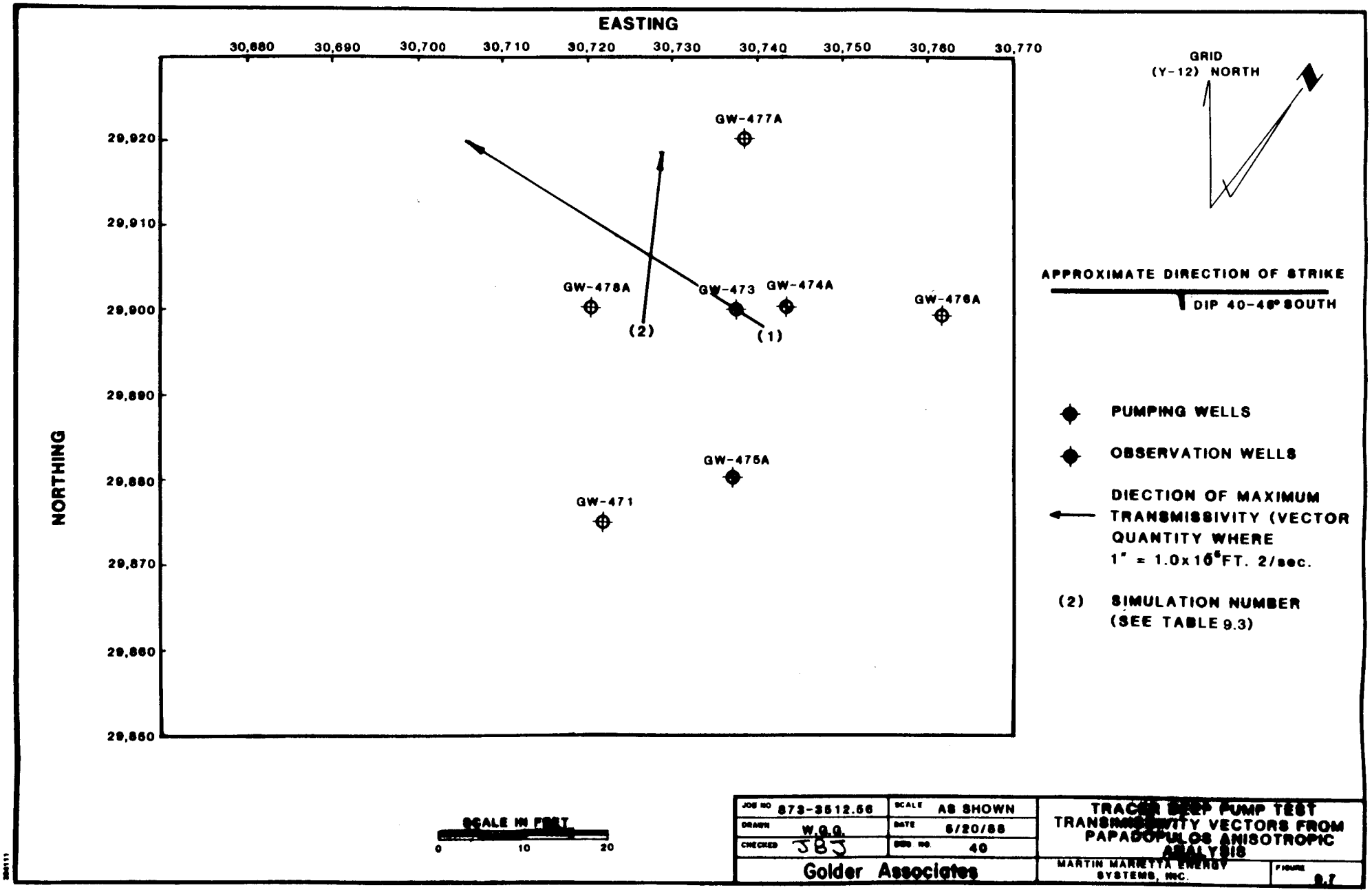
EASTING
30,680
30,690
30,700
30,710
30,720
30,730
30,740
30,750
30,760
30,770
NORTHING
29,920
29,910
29,900
29,890
29,880
29,870
29,860
29,850
GW-477A
GW-478A
GW-473
GW-474A
GW-476A
GW-475A
GW-471
(2)
(1)
GRID
(Y-12) NORTH
APPROXIMATE DIRECTION OF STRIKE
DIP 40-45° SOUTH
PUMPING WELLS
OBSERVATION WELLS
DIECTION OF MAXIMUM TRANSMISSIVITY (VECTOR QUANTITY WHERE 1" = 1.0x10⁻⁵FT. 2/sec.
(2) SIMULATION NUMBER (SEE TABLE 9.3)
SCALE IN FEET
0
10
20
JOB NO 873-3512.56
SCALE AS SHOWN
DRAWN W.G.G.
DATE 5/20/88
CHECKED JBJ
DWG NO. 40
Golder Associates
TRACER DEEP PUMP TEST
TRANSMISSIVITY VECTORS FROM PAPADOPULOS ANISOTROPIC ANALYSIS
MARTIN MARIETTA ENERGY SYSTEMS, INC.
FIGURE 9.7

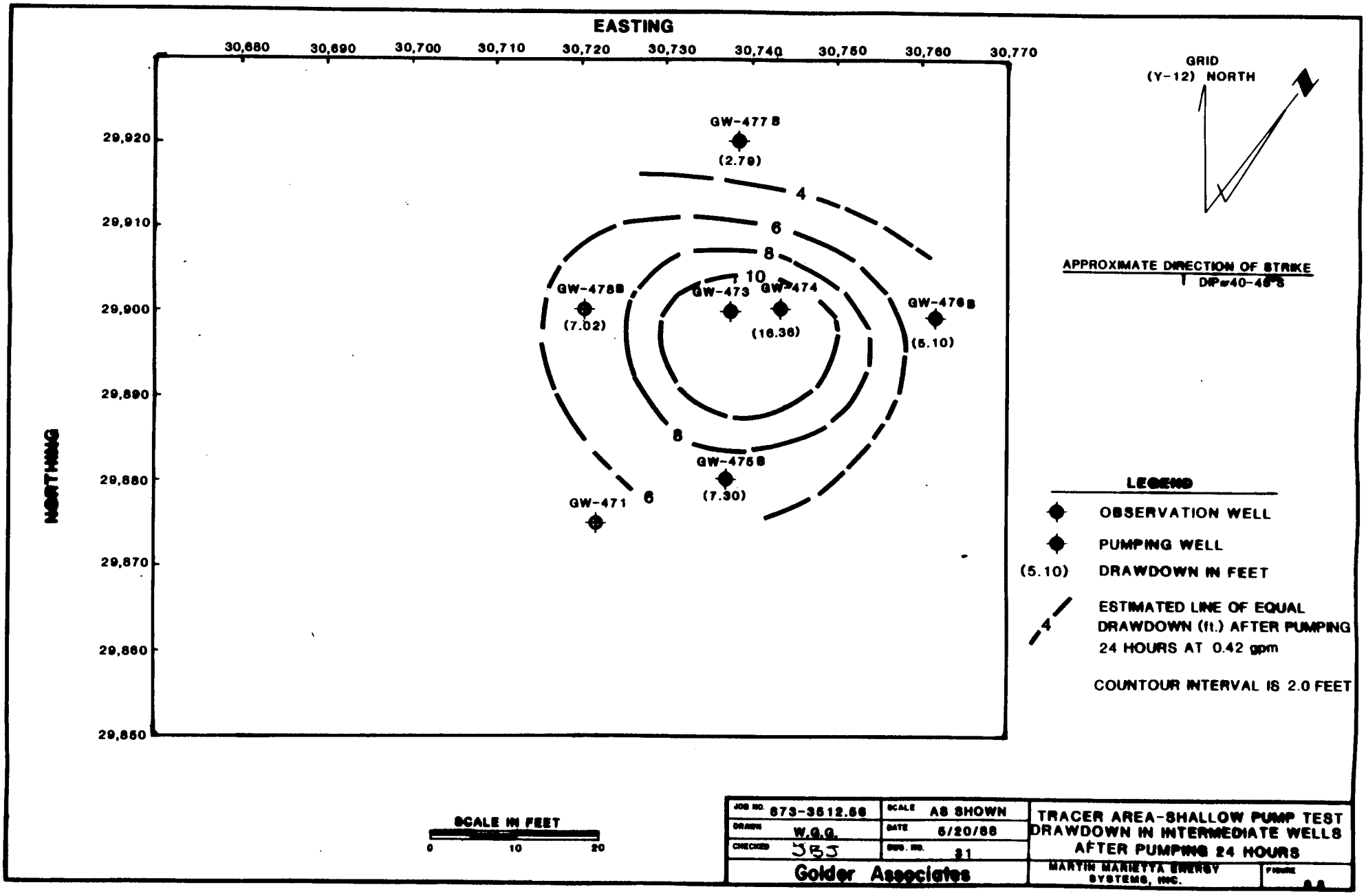
EASTING
30,680
30,690
30,700
30,710
30,720
30,730
30,740
30,750
30,760
30,770
NORTHING
29,920
29,910
29,900
29,890
29,880
29,870
29,860
29,850
GW-477 B
(2.79)
GW-478B
(7.02)
GW-473
GW-474
(16.36)
GW-476B
(5.10)
GW-475B
(7.30)
GW-471
4
6
8
10
8
6
GRID
(Y-12) NORTH
APPROXIMATE DIRECTION OF STRIKE
DIP≈40-45°S
LEGEND
OBSERVATION WELL
PUMPING WELL
(5.10) DRAWDOWN IN FEET
4 ESTIMATED LINE OF EQUAL DRAWDOWN (ft.) AFTER PUMPING 24 HOURS AT 0.42 gpm
COUNTOUR INTERVAL IS 2.0 FEET
SCALE IN FEET
0
10
20
JOB NO. 873-3512.56
SCALE AS SHOWN
DRAWN W.G.G.
DATE 5/20/86
CHECKED JBJ
DWG. NO. 31
Golder Associates
TRACER AREA-SHALLOW PUMP TEST
DRAWDOWN IN INTERMEDIATE WELLS
AFTER PUMPING 24 HOURS
MARTIN MARIETTA ENERGY SYSTEMS, INC.
FIGURE
A.8

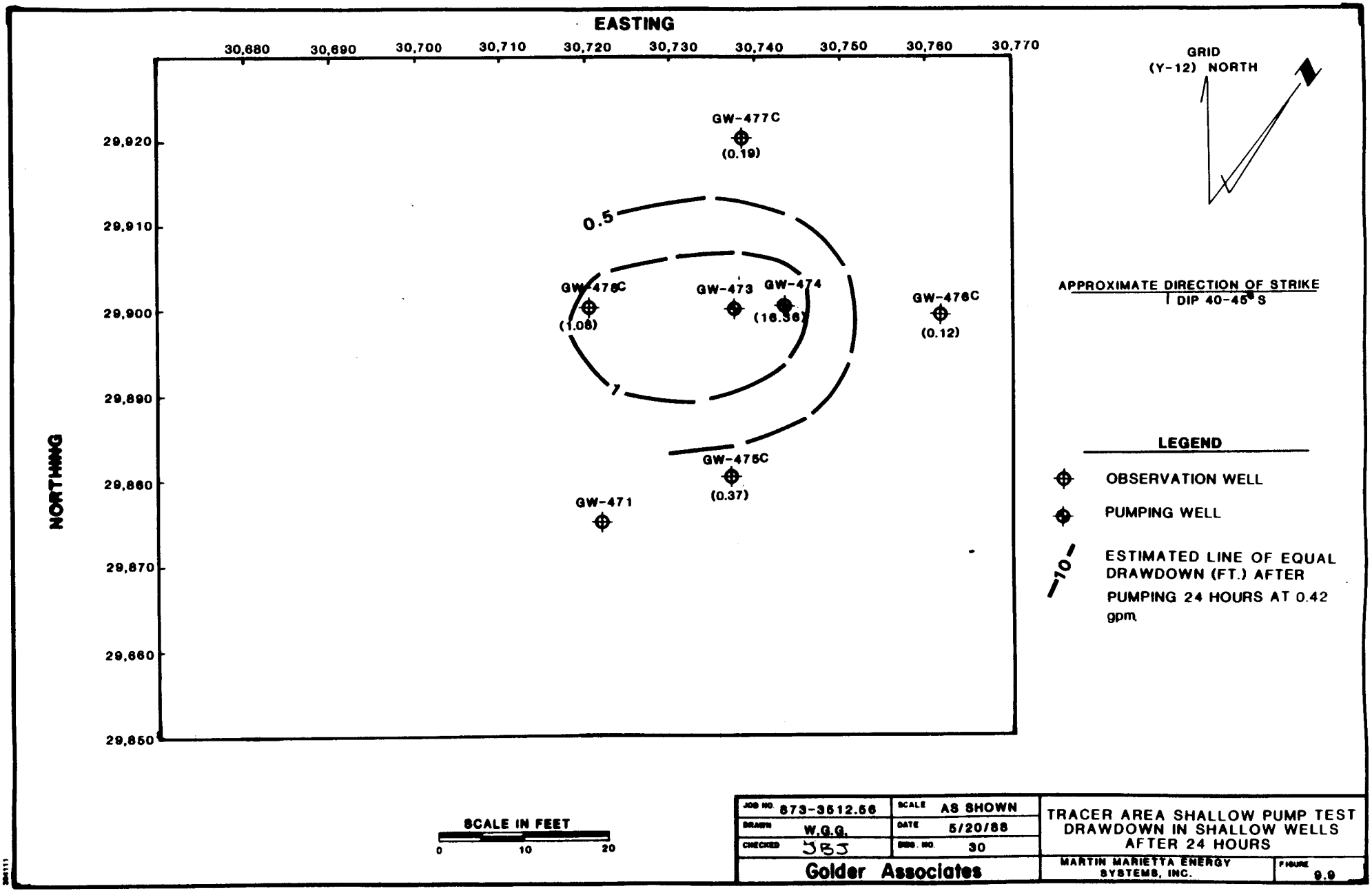
EASTING
30,680
30,690
30,700
30,710
30,720
30,730
30,740
30,750
30,760
30,770
NORTHING
29,920
29,910
29,900
29,890
29,880
29,870
29,860
29,850
GW-477C
(0.19)
0.5
GW-475C
(1.08)
GW-473
GW-474
(16.36)
GW-476C
(0.12)
1
GW-475C
(0.37)
GW-471
GRID
(Y-12) NORTH
APPROXIMATE DIRECTION OF STRIKE
DIP 40-45° S
LEGEND
OBSERVATION WELL
PUMPING WELL
10
ESTIMATED LINE OF EQUAL DRAWDOWN (FT.) AFTER PUMPING 24 HOURS AT 0.42 gpm
SCALE IN FEET
0
10
20
JOB NO. 873-3512.56
SCALE AS SHOWN
DRAWN W.G.G.
DATE 5/20/88
CHECKED JBJ
DWG. NO. 30
Golder Associates
TRACER AREA SHALLOW PUMP TEST
DRAWDOWN IN SHALLOW WELLS
AFTER 24 HOURS
MARTIN MARIETTA ENERGY SYSTEMS, INC.
FIGURE 9.9

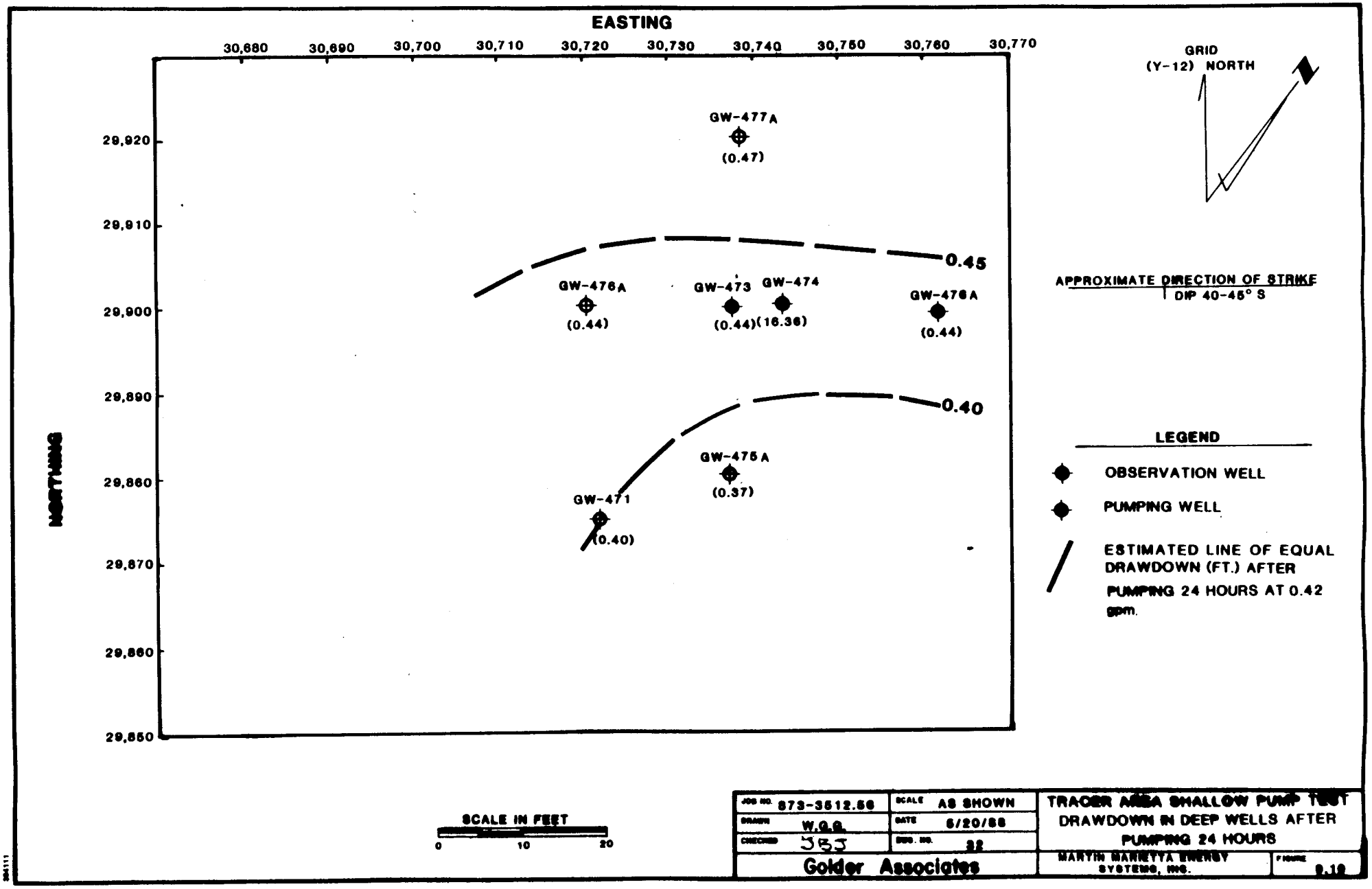
EASTING
30,680
30,690
30,700
30,710
30,720
30,730
30,740
30,750
30,760
30,770
NORTHING
29,920
29,910
29,900
29,890
29,860
29,870
29,860
29,850
GW-477A
(0.47)
0.45
GW-476A
(0.44)
GW-473
(0.44)
GW-474
(16.36)
GW-476A
(0.44)
0.40
GW-475A
(0.37)
GW-471
(0.40)
GRID
(Y-12) NORTH
APPROXIMATE DIRECTION OF STRIKE
DIP 40-45° S
LEGEND
OBSERVATION WELL
PUMPING WELL
ESTIMATED LINE OF EQUAL DRAWDOWN (FT.) AFTER PUMPING 24 HOURS AT 0.42 gpm.
SCALE IN FEET
0
10
20
JOB NO. 873-3512.56
SCALE AS SHOWN
DRAWN W.G.G.
DATE 5/20/88
CHECKED SBS
DWG. NO. 32
Golder Associates
TRACER AREA SHALLOW PUMP TEST
DRAWDOWN IN DEEP WELLS AFTER PUMPING 24 HOURS
MARTIN MARIETTA ENERGY SYSTEMS, INC.
FIGURE 9.19

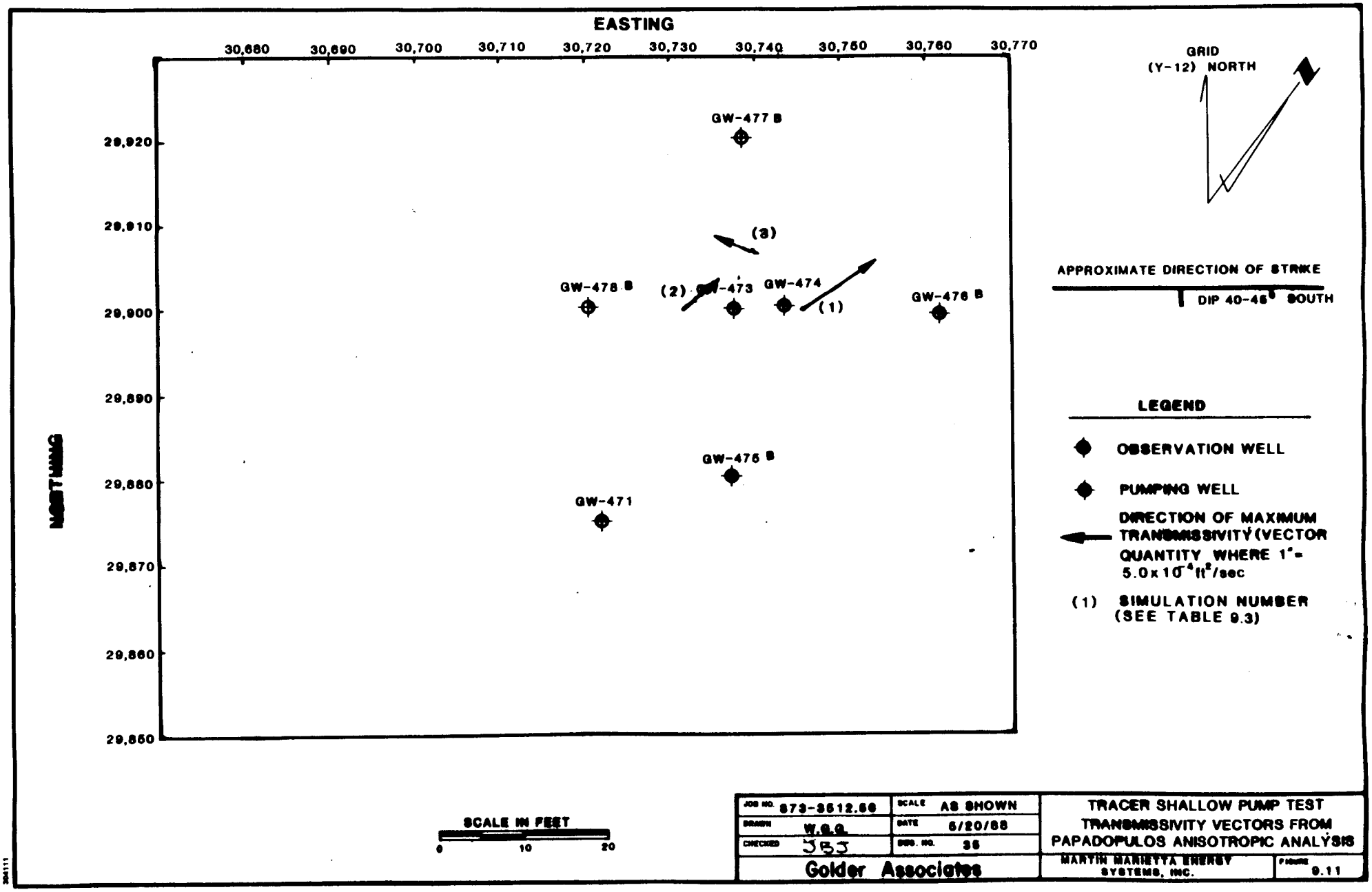
EASTING
30,680
30,690
30,700
30,710
30,720
30,730
30,740
30,750
30,760
30,770
NORTHING
29,920
29,910
29,900
29,890
29,880
29,870
29,860
29,850
GW-477 B
(3)
GW-478 B
(2)
GW-473
GW-474
(1)
GW-476 B
GW-475 B
GW-471
GRID
(Y-12) NORTH
APPROXIMATE DIRECTION OF STRIKE
DIP 40-45° SOUTH
LEGEND
OBSERVATION WELL
PUMPING WELL
DIRECTION OF MAXIMUM TRANSMISSIVITY (VECTOR QUANTITY WHERE 1" = 5.0x10⁻⁴ ft²/sec
(1) SIMULATION NUMBER (SEE TABLE 9.3)
SCALE IN FEET
0
10
20
JOB NO. 873-3512.56
SCALE AS SHOWN
DRAWN W.G.G.
DATE 6/20/86
CHECKED JBJ
DWG. NO. 35
Golder Associates
TRACER SHALLOW PUMP TEST
TRANSMISSIVITY VECTORS FROM
PAPADOPULOS ANISOTROPIC ANALYSIS
MARTIN MARIETTA ENERGY SYSTEMS, INC.
FIGURE 9.11

10.0 FIELD TRACER TEST

10.1 Objectives and Scope

The objective of the field tracer test was to collect field data that could be used to calibrate and validate solute transport models for use in this geologic media. The scope of work included installation of a multi-level monitoring network in discrete geological horizons associated with bedding planes, top of bedrock, water table and the previously described structural zone. In addition, an analytical procedure was developed to detect the tracer, the tracer was injected and tracked through the well field, and a data base was compiled for the tracer migration pathway.

10.2 Test Design and Planning

10.2.1 Injection Depth Selection

As described in section 2.0, the field tracer test was designed to allow the tracer to migrate under natural gradients. Significant consideration was given with regard to the depth at which the tracer should be injected. The initial thoughts, in late 1987, were centered around injecting the tracer into the bedrock and between identifiable low permeability boundaries, such as shale beds or structures, so that boundary conditions could be controlled. A specific objective for this injection would have been to examine the influence of structural zones and fractures in the bedrock. Vadose zone injection, a realistic leak scenario, was discussed, but would have posed significant difficulty with regard to saturated/unsaturated solute transport modeling.

Injection at the water table, an intermediary position between vadose zone and deeper bedrock injection, was also discussed at this time. The debate on injection depth continued for some months prior to final design of the pump test well field. This debate is reflected by the pump well

field design in that the well layout, and tests performed, examined both shallow and deep hydraulic characteristics, and both lithologic and structural phenomena. Vadose zone characteristics were qualitatively examined independently of the pump test by infiltration tests, to be described in the Task 6 report.

After the hydraulics at the tracer area had been better defined by water level measurements and pump testing, and just prior to selection of the actual injection point location, the decision was made to inject at or near the water table. The first reason for this decision was based on the confirmed upward gradient under the site which would allow consideration of using this flow field characteristic as a lower hydraulic-control, i.e. flow would always be vertically upward. The second reason was that, conceptually, the water table injection and upward gradient would cause the tracer to move in a pseudo two dimensional plane, rather than three-dimensionally, within a thin water zone which might be more easily tracked by relatively inexpensive dry augering techniques, ahead of the plume.

10.2.2 Injection Well Location

Significant consideration was also given to the location of the injection point relative to the tracer well field. It was desirable to inject the tracer upgradient of the direction of groundwater flow from the pump test well field. However, tracer injection had to occur close enough to the well field to allow it to migrate through the well field in a reasonable time. In addition, the further upgradient the injection well was placed, the greater the possibility of the tracer moving in an unanticipated direction.

At the time of the decision regarding injection well location, in early April, 1988, concern was raised over the dry atmospheric conditions being encountered in the East Tennessee area. Some evidence existed that, contrary to normal years, the high groundwater peak had passed in February rather than April. Thus, it was considered important that the test be started quickly before the water table dropped significantly. Although survey data for the well field was only just available, and the pump tests had not been fully analyzed, the decision to locate the injection well was made based on preliminary equipotential analyses and preliminary pump test drawdowns. It was also decided that additional shallow water-table wells between pump wells and background wells be installed to refine the well grid in case the tracer did not disperse as much as indicated by preliminary modeling (Section 11.0).

Figure 10.1 illustrates the tracer test well field, including the injection well, background wells, calibration and validation wells. It should be noted that well numbers GW-485 and higher were installed after tracer injection. The injection well was located relative to other wells to cover all options for tracer movement, including the unlikely event of upgradient movement.

10.3 Sampling Equipment and Procedures

The sampling equipment for the tracer test consisted of eight dedicated automatic samplers and dedicated suction lines installed in each well. The automatic samplers are manufactured by ISCO Corporation and essentially consist of a peristaltic pump mounted on a carousel. The sample volume, frequency, and delay can be all be programmed into the sampler's memory. The carousels hold 24 sample bottles and rotate after each successive sample.

Each well was fitted with a 3/8-inch nylon dedicated line. Table 6.1 presents the actual sampling depth for each well. The automatic samplers were programmed to collect about 200-300 ml for each sampling event. The sample was then transferred to new 40 ml glass vials, transported to the on-site laboratory, analyzed for Rhodamine WT concentration, and retained for storage. All wells that were not fitted with automatic samplers were sampled manually using a peristaltic pump. These samples were also transferred to new 40 ml glass vials, analyzed and retained for storage. Upon completion of the tracer test, all samples were delivered to MMES.

The sampling frequency was variable. Initially, samples were collected approximately every 2 hours. Some background wells, however, were only sampled on a daily basis. The actual time of sampling was recorded in the field for each sample. Generally, each sample was analyzed for Rhodomine WT the same day. Weekend samples, however, were generally not analyzed until the following Monday.

10.4 Analytical Procedures and Data Collection

All samples were analyzed using a Perkin Elmer model 5B fluorimeter. The instrument is capable of routinely detecting Rhodamine WT at concentrations as low as 0.1 ppb. The analysis procedure was to transfer a small volume of the sample from the 40-ml sample vial to the optic-cell. The cell was then inserted into the fluorimeter and the concentration of Rhodomine WT was printed directly to a remote printer.

The fluorimeter was zeroed and calibrated daily. Background water from the tracer area wells was used to zero the instrument. Calibration was completed using prepared spikes of 10 ppb or 400 ppb concentrations. It should be noted that the same optic-cell was used for calibrations, zeroing and analyses. This was necessary because each cell was optically

different. If the concentration of the sample was suspected to be greater than about 90 ppb, the fluorimeter was calibrated against the 400 ppb spike. In some cases, the samples were highly concentrated (GW-484, 487, 493) and had to be diluted prior to analysis.

All concentration data was then keyed into a portable microcomputer for plotting and development of breakthrough curves. All entries were checked in Atlanta for typographical entry errors. The printed output from the fluorimeter was maintained for QA/QC purposes.

10.5 Field Data and Results

10.5.1 Tracer Injection

The tracer was injected into well GW-484 (Figure 10.1) on Wednesday, April 20, 1988, from 11:25 AM to 11:37 AM. The tracer injection procedure consisted of evacuating a measured amount of water from the well followed by a slow continuous injection of tracer solution. The well was evacuated using a centrifugal pump, while the tracer injection was completed using a peristaltic pump.

The removal of 10 liters of water from the injection well (GW-484) lowered the water level to within about 1.0 foot of the bottom of the screen. Ten liters of a 40% solution of Rhodamine WT, with a specific gravity of about 1.05, was then injected into the well. After tracer injection, 1 gallon of distilled water was pumped into the well to flush or rinse the injection tube. The tracer injection resulted in a fluid level rise of about 0.5 feet above static. The evacuation/injection procedure resulted in a short inward gradient during the tracer injection process, followed by a slight outward gradient at completion. Immediately after tracer injection, monitoring was initiated. All automatic samplers

were programmed to initially sample on hourly intervals. All field data collected throughout the monitoring phase is presented in Appendix F.

10.5.2 Tracer Detection

During the first 2 to 3 days of detection, extremely small readings (<ppb levels) were measured from many wells. These results are now considered to be false and probably caused by floculants in the well water. The tracer was first detected in observation well GW-481B (Figure 10.3) after 420 minutes following a series of small, but steadily rising numbers. Significant tracer concentrations were then later observed in wells GW-486 after 3 days, GW-487 after 12 days, and GW-493 after 26 days. Based on these results, it was considered the tracer was moving along strike, although the pathway was unknown. Figures 10.2 through 10.6 present an arithmetic plot of tracer concentration verses time for the injection well and these four observation wells. Note that these plots of tracer concentration are not smooth curves. This seemingly erratic response is a result of two factors. First, many of the highly concentrated samples had to be diluted prior to analysis. This dilution may have resulted in slight inaccuracies in the actual concentration. Second, minor precipitation events may have impacted the release of the tracer from well GW-484. However, review of the precipitation data presented in the Task 3 report did not allow any direct quantification of this effect.

Review of the concentrations at well GW-481B indicates that the first arrival of the tracer was detected at about 1.4 ppb about 7 hours after injection. Similarly, observation well GW-486 indicated a first arrival of 13.8 ppb at about 71 hours after injection. The arrival at GW-486 was not as well

defined, however, as it was at GW-481. Well number GW-486 was installed after the tracer was injected. Consequently, no samples were obtained until 54 hours after injection.

The highest observed concentration (with the exception of the injection well) was 9320 ppb in observation well GW-487 at about 28 days after injection. First arrival, however, cannot be estimated at this well because it, too, was drilled after tracer injection. Significant tracer concentrations were also detected in observation well GW-493. The concentration behavior of GW-493 was very similar to GW-487.

Six additional far-field detection wells (GW-495 through GW-499A) were installed downgradient of GW-493, based on the assumption that the tracer was moving discretely along strike with little lateral dispersion. These additional wells, however, have not (as of this writing) shown any evidence of tracer arrival. It was considered that perhaps the tracer had migrated in some unanticipated direction. Consequently, ten additional wells (GW-499G through GW-499P) were installed in an effort to "find" the tracer. Subsequent to the installation of these wells the tracer has been detected in wells GW-499G, GW-499H, GW-499J, GW-499M, GW-499N, GW-499O and GW-499P. The tracer movement appeared to have slowed, but was still moving along strike.

Based on the observed movement of the tracer in the field, the following qualitative conclusions are made:

1. Initially, the tracer migrated from GW-484, the injection well, as an approximate steady state release from a point source. At later times the release rate was much lower, but still rather steady. The release can be approximately described as an exponentially decaying steady state release from a point source. Figure 10.2 illustrates the injection well decay.

2. The tracer migrated in either a narrow fractured zone of limited width or in a weathered bedrock trough caused by weathering of less resistant or fractured rock.

3. The tracer migrated along the top of reasonably competent bedrock from GW-484 at an angle of about 85° West of Y-12 North. This angle approximates lithological strike.

4. There is evidence in the stream bed to the west of the site for the existence of resistant shale beds sandwiching less resistant beds which are consistent with the above mentioned direction of tracer migration.

5. The tracer initially moved at an average velocity of about 2.8 ft./day with little lateral or vertical, mechanical dispersion. The lack of lateral dispersion appears to be controlled by bedding features or by a fracture zone. The lack of vertical dispersion appears caused by the upward hydraulic gradient resulting in little vertical flow components as the tracer was injected near the water table.

6. The slow down in tracer movement is probably caused by a significant drop in the water table, causing a lowering of hydraulic gradient in the horizontal plane of the hydraulic field controlling the tracer migration.

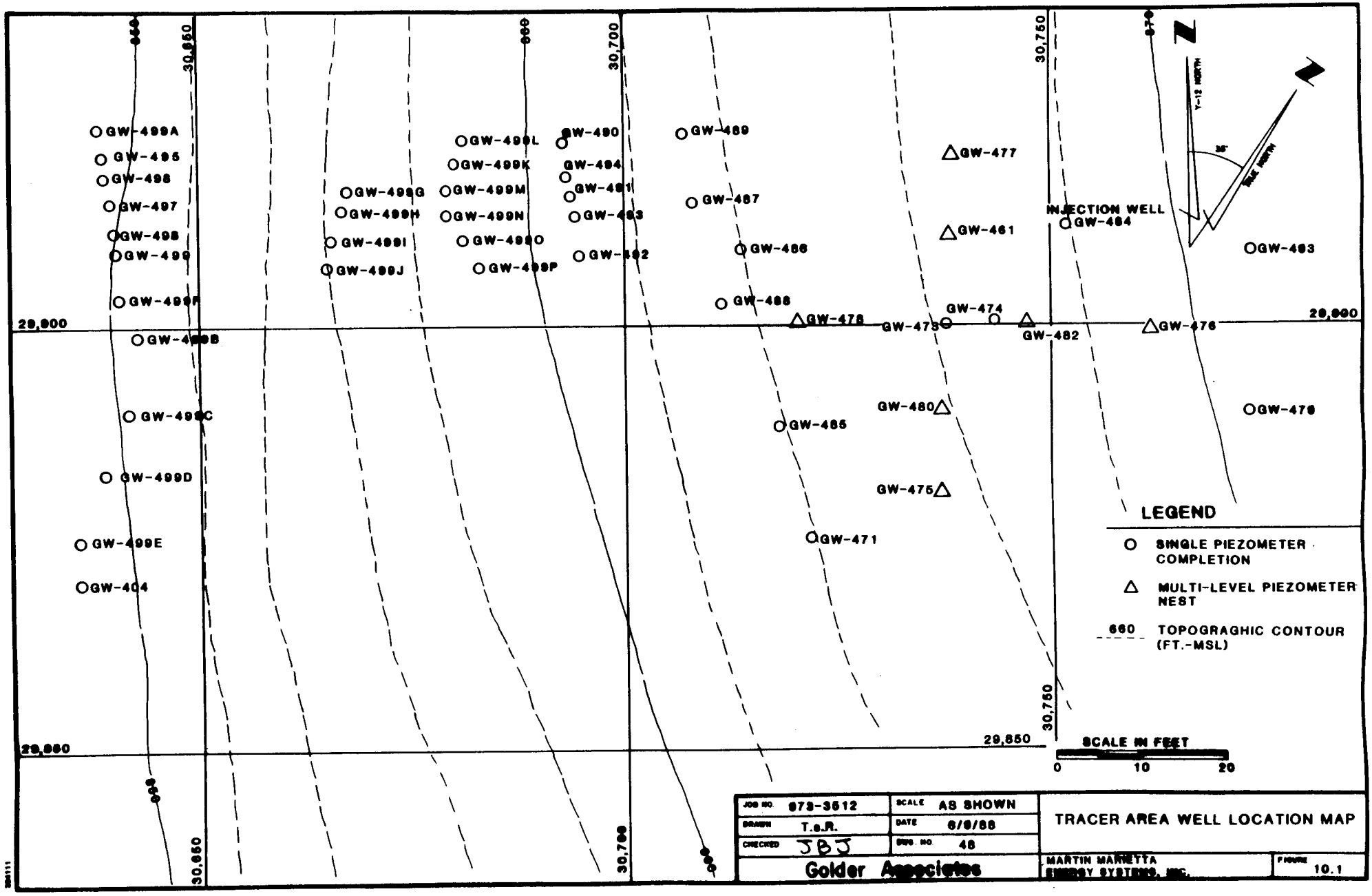
GW-499A
GW-495
GW-498
GW-497
GW-496
GW-499
GW-499F
GW-499B
GW-499C
GW-499D
GW-499E
GW-404
GW-499G
GW-499H
GW-499I
GW-499J
GW-499L
GW-499K
GW-499M
GW-499N
GW-499O
GW-499P
GW-490
GW-494
GW-491
GW-493
GW-492
GW-489
GW-487
GW-486
GW-488
GW-477
GW-461
GW-478
GW-473
GW-474
GW-482
GW-484
INJECTION WELL
GW-480
GW-485
GW-475
GW-471
GW-476
GW-483
GW-479
30,850
30,700
30,750
29,900
29,850
Y-12 NORTH
TRUE NORTH
35°
LEGEND
SINGLE PIEZOMETER COMPLETION
MULTI-LEVEL PIEZOMETER NEST
660 TOPOGRAGHIC CONTOUR (FT.-MSL)
SCALE IN FEET
0
10
20
JOB NO. 873-3512
SCALE AS SHOWN
DRAWN T.s.R.
DATE 6/9/88
CHECKED JBJ
DWG. NO. 48
Golder Associates
TRACER AREA WELL LOCATION MAP
MARTIN MARIETTA ENERGY SYSTEMS, INC.
FIGURE 10.1

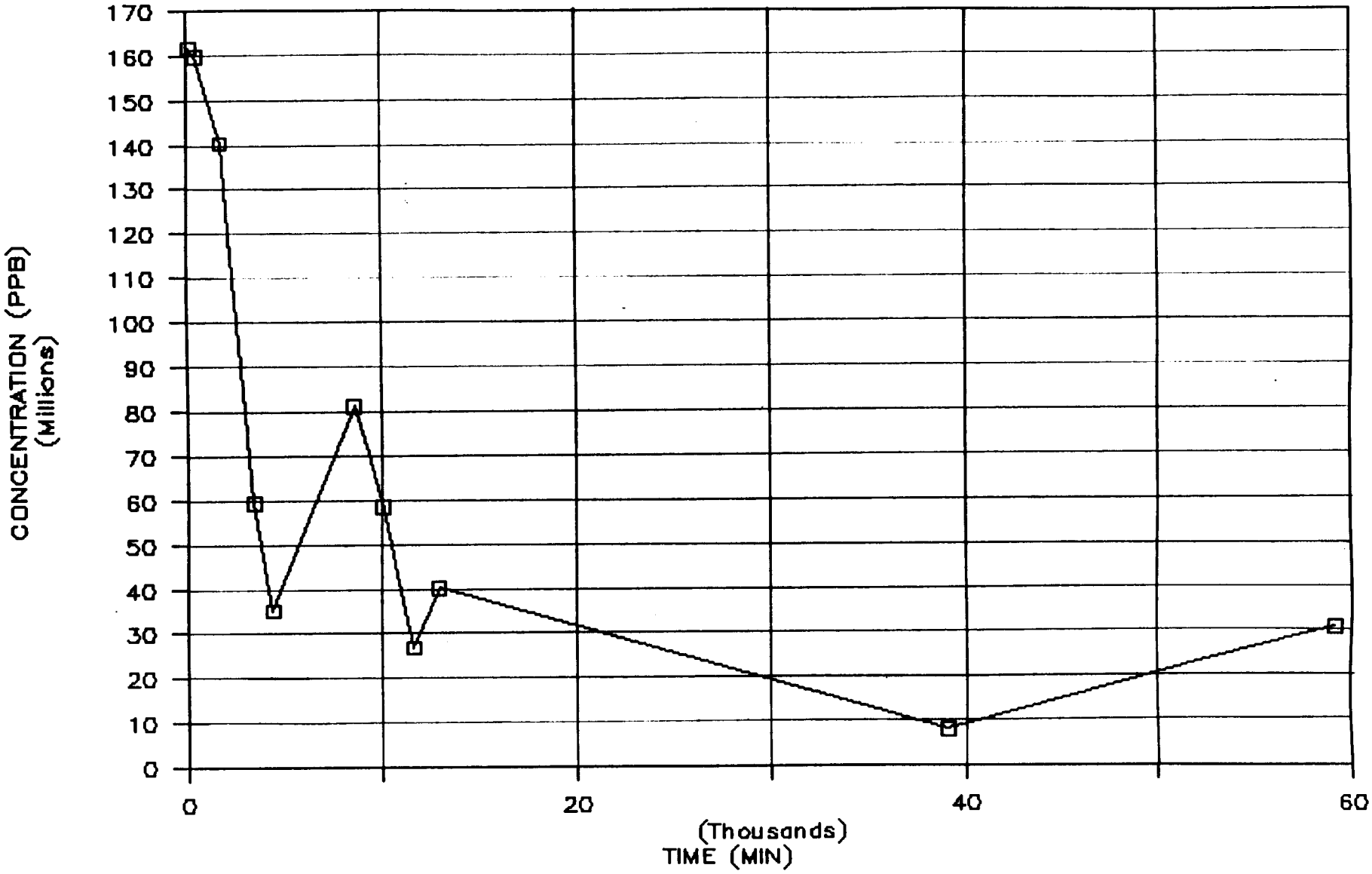

JOB NO 873-3512	SCALE AS SHOWN	Golder Associates	CONCENTRATION OF RHODAMINE-WT IN INJECTION WELL GW-484
DRAWN JLW	DATE 7/22/88		MARTIN MARIETTA ENERGY SYSTEMS, INC.
CHECKED JBJ	DWG NO 49		FIGURE 10.2

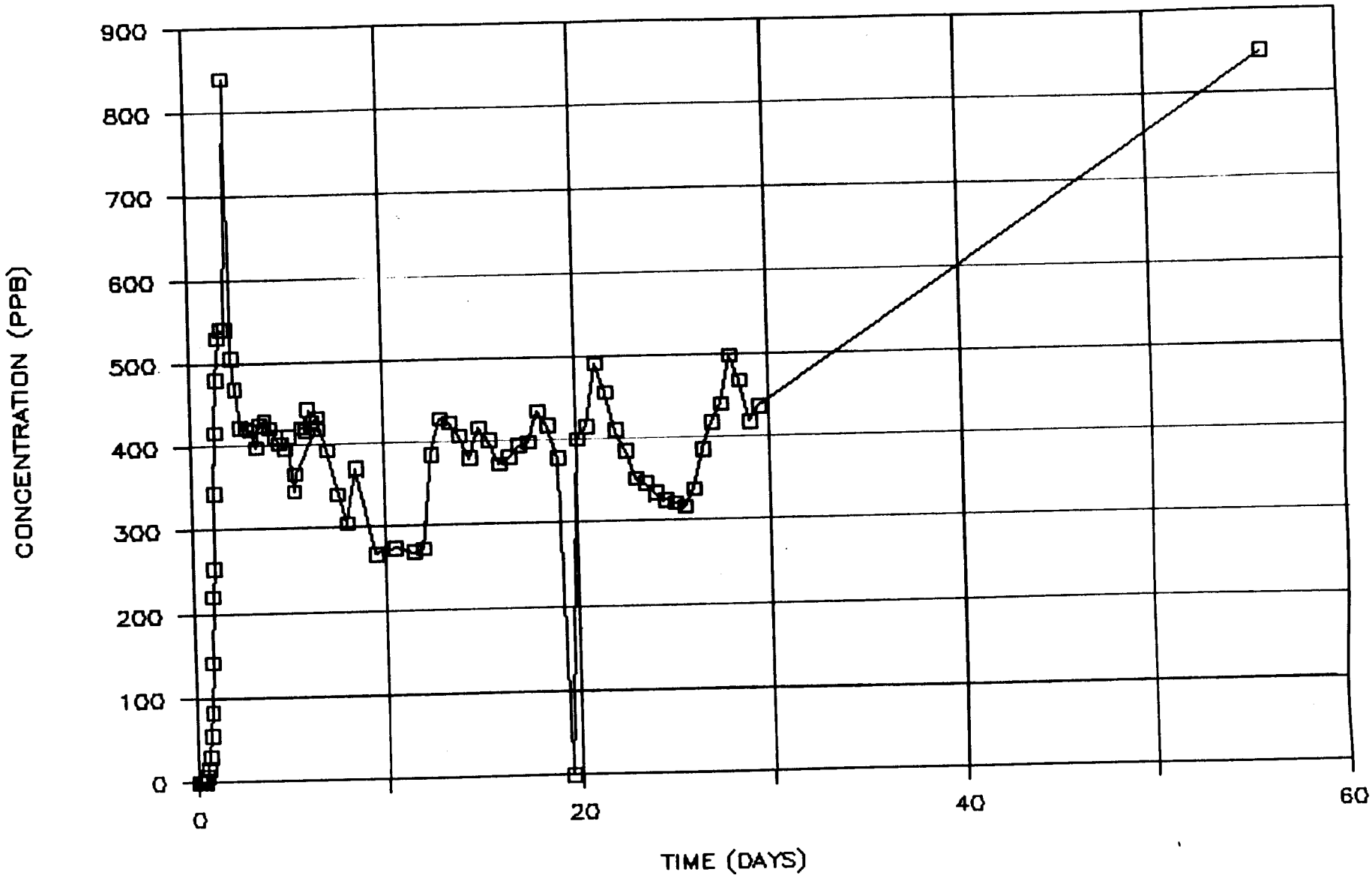

JOB NO 873-3512	SCALE AS SHOWN	Golder Associates	CONCENTRATION OF RHODAMINE-WT IN WELL GW-481B
DRAWN JLW	DATE 7/22/88		MARTIN MARIETTA ENERGY SYSTEMS, INC.
CHECKED JBJ	DWG NO 50		FIGURE 10.3

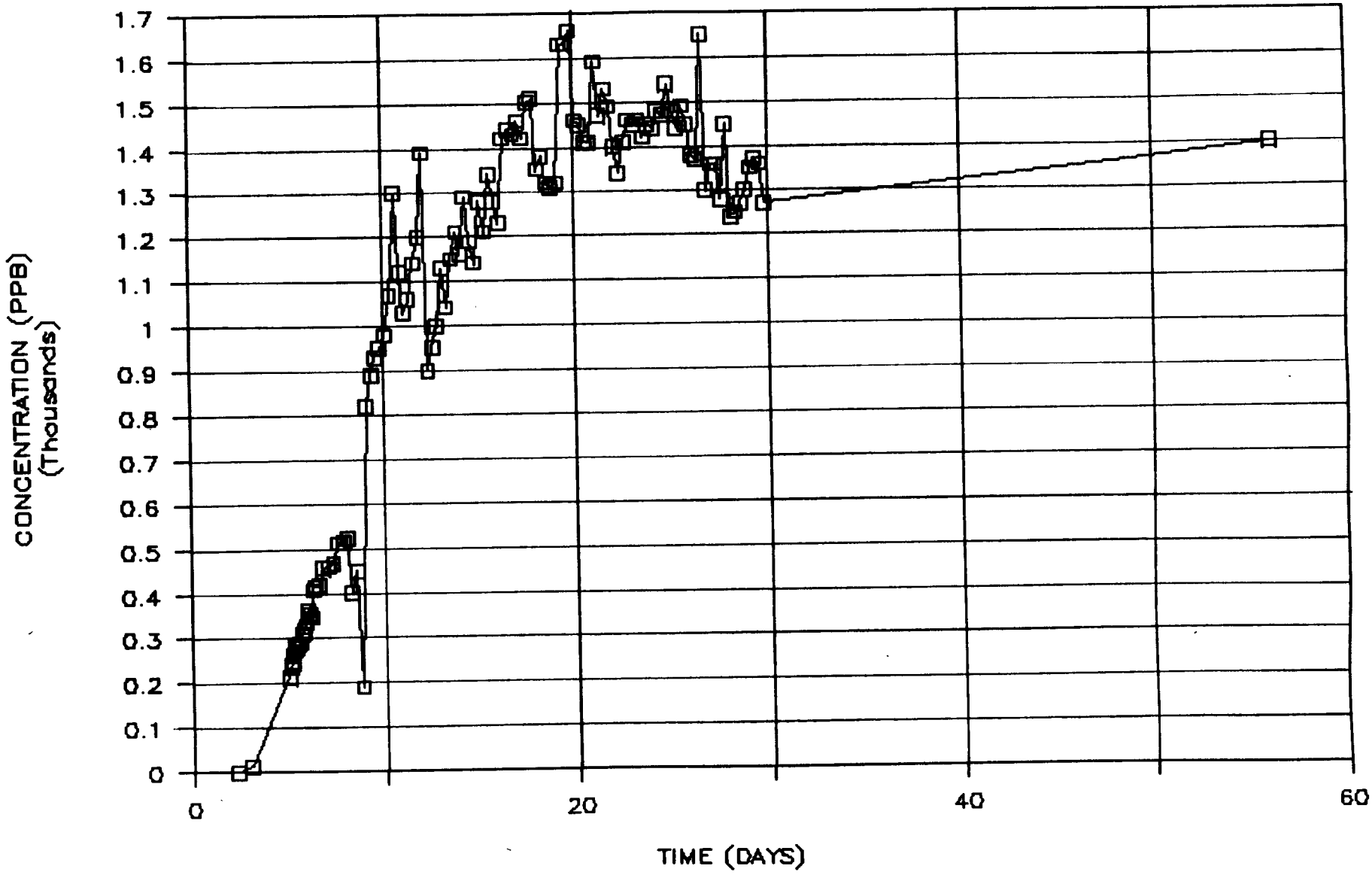

JOB NO 873-3512	SCALE AS SHOWN	Golder Associates	CONCENTRATION OF RHODAMINE-WT IN WELL GW-486
DRAWN JLW	DATE 7/22/88		MARTIN MARIETTA ENERGY SYSTEMS, INC. FIGURE 10.4
CHECKED JBJ	DWG NO 51		

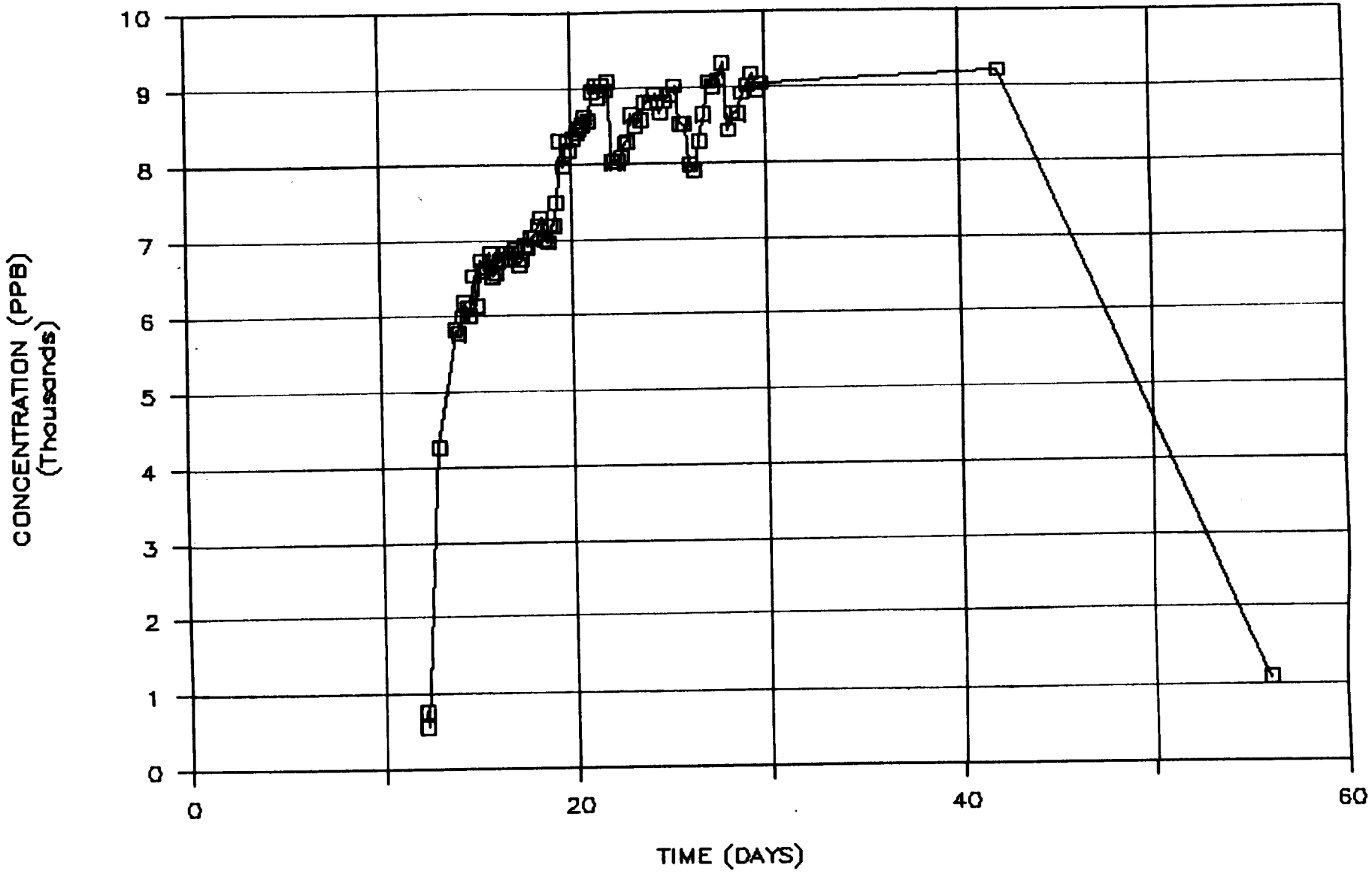

JOB NO 873-3512	SCALE AS SHOWN	Golder Associates	CONCENTRATION OF RHODAMINE-WT IN WELL GW-487
DRAWN JLW	DATE 7/22/88		MARTIN MARIETTA ENERGY SYSTEMS, INC.
CHECKED JBJ	DWG NO 52		FIGURE 10.5

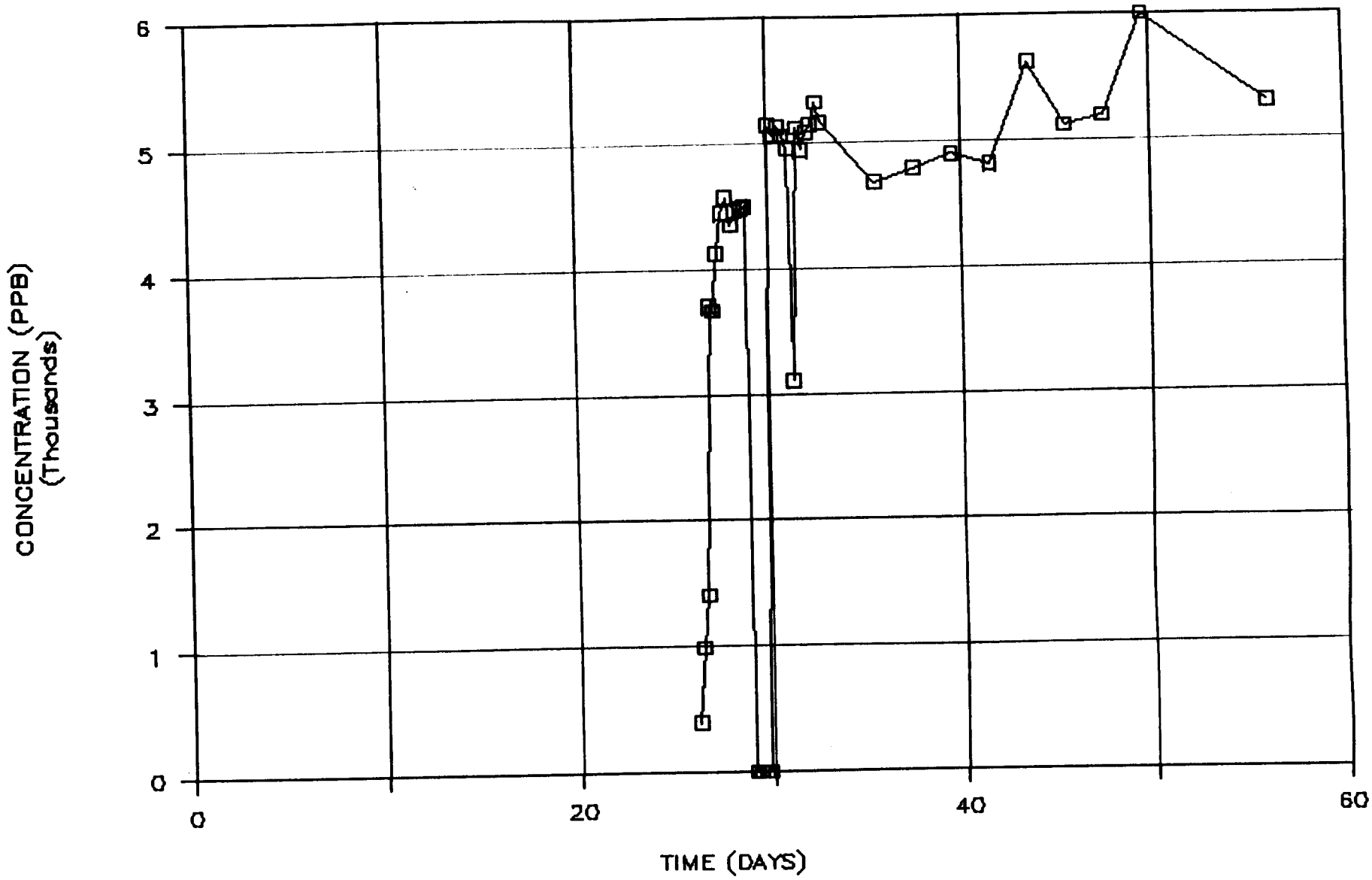

JOB NO 873-3512	SCALE AS SHOWN	Golder Associates	CONCENTRATION OF RHODAMINE-WT IN WELL GW-493
DRAWN JLW	DATE 7/22/88		MARTIN MARIETTA ENERGY SYSTEMS, INC.
CHECKED JBJ	DWG NO 53		FIGURE 10.6

11.0 TRACER AREA GROUNDWATER FLOW AND SOLUTE TRANSPORT MODELING

11.1 Objectives and Scope

The objective of the groundwater flow and solute transport modeling was to evaluate the ability of a model to accurately simulate the migration of contaminants in this type of geologic media. The scope of work included model setup and calibration to an observed steady state flow field, followed by calibration to an observed tracer movement. The calibrated model was then used to predict tracer migration as part of the model validation process.

Groundwater and solute transport modeling of the tracer area utilized the Golder Groundwater Package (Reference 4). The model is a publicly available finite element model capable of simulating a wide variety of groundwater flow and solute transport problems. The code was previously used to complete preliminary modeling for the entire site as part of Task 2. The model was selected for the tracer test because Golder Associates has experience with the model and it had previously been applied to simulate groundwater flow on the site. Other models can be calibrated and perhaps validated using the field data presented in Appendix F. However, the scope of work for this task only included the setup, calibration, and validation of one model.

11.2 Model Setup and Calibration

11.2.1 General

The modeling of the field tracer test was completed in a phased approach. In general, the procedure included mesh generation, groundwater flow calibration, solute transport calibration and simulation runs. The following sections present the modeling process in a somewhat chronological order. However, for reporting convenience and clarification some overlap occurs.

It is important to recognize that the field tracer test (Section 10.0) and solute transport modeling were performed simultaneously. As new data from the field test became available it was used to adjust, modify, and redirect the modeling approach. Once a final decision had been reached in late March 1988, regarding the actual tracer injection point, preliminary modeling commenced. A preliminary working model was developed prior to tracer injection on April 20, 1988.

11.2.2 Mesh Generation

The first step in the process of creating groundwater flow model simulations is the generation of a first order finite element mesh which incorporates those hydrologic and geologic characteristics which appear to control the flow of groundwater within the area of interest. Sources of data utilized in the hydrogeologic characterization of the tracer test area included both the shallow and deep pump tests conducted near the Maryville/Nolichucky contact, core log and packer test data from coreholes GW-404, GW-455, and GW-471, and hydraulic head data collected from wells within and around the tracer area.

The area of interest for which the mesh was created envelopes the pump test/tracer test well field and is bounded to the west by the 848.0 ft. MSL topographic contour line lying within the flood plain of the adjacent creek, and bounded on the east by a line of symmetry dividing the adjacent topographic rise (Plate 1). The study area is further bounded towards Y-12 north by a line running parallel to geologic strike and connecting the before mentioned boundaries, and represents a line of prescribed or interpolated hydraulic head. A more detailed description of the boundaries will be discussed in Section 11.2.3.

The initial finite element grid was set up based on the data and the current understanding of the flow system available at that time. Preliminary interpretation of pump test data suggested a hydraulic gradient and direction of maximum transmissivity of 35° oblique to strike. Consequently, the original mesh was setup with elements oriented so as to exhibit this type of flow behavior. It was later realized that the direction of maximum transmissivity and hydraulic gradient were in fact oriented nearly along strike. The confusion regarding the gradient direction was due to the fact that survey data was not available at the time of preliminary pump test analyses. The misinterpretation regarding the orientation of the maximum transmissivity direction was due to a mistake on the part of Golder Associates regarding the orientation of the well field relative to true north and Y-12 grid north. The original finite element mesh was subsequently modified to more accurately reflect the true observed anisotropy, determined after survey data had been received, and following the realization of the mistake.

In general, the final mesh consisted of a series of interconnected quadrilaterals and triangles. The mesh was fairly coarse near the boundaries and very fine near the well field. The fine mesh near the well field allowed for better resolution of the tracer breakthrough curves of various wells. The final mesh used for the groundwater flow and solute transport model prediction is presented as Plate 2.

11.2.3 Boundary Conditions

The model boundaries were set up using a blowup of a large scale topographic map of the entire site. At a later date, a smaller, more accurate, scale map of the tracer area became available, but had not been used in the modeling exercise.

For the groundwater flow modeling the 848.0 ft.MSL topographic contour which bounds the study area to the west, was assumed to represent a constant head boundary due to its location within the flood plain of the creek. The hydraulic head at all points along this line was estimated at 847.0 ft. MSL. As was previously mentioned, the eastern boundary of the area is a line of symmetry which divides the adjacent topographic high. By symmetry, this line was assumed to represent a no flow boundary. Groundwater flow likely crosses this line of symmetry, however, observations of topography suggest that flow occurring across this boundary is negligible with respect to obtaining a reliable steady state solution.

Hydraulic heads were initially prescribed across the northern boundary of the study area by the generation of a potentiometric map using static water level data from wells within the tracer well field, and by interpolating the water table as a reflection of ground surface in areas of sparse data. Heads along this boundary were subsequently modified slightly during the course of groundwater flow calibration as discussed in more detail in section 11.2.4.

In general, the use of the hydraulic boundary conditions described above proved to be a good first approximation of head distribution within the tracer area as evidenced by initial model calibration runs.

11.2.4 Groundwater Flow Calibration

The groundwater flow model calibration procedure commenced following the entry of the digitized finite element mesh and boundary conditions into the FPM program of the Golder Groundwater Package. Estimates of maximum hydraulic conductivity, the degree of anisotropy, and direction of maximum

hydraulic conductivity were obtained by analysis of pump test data and by observations of the ongoing tracer test and were also input to the FPM program.

Model calibration was an iterative process of trial and error, whereby modifications in prescribed heads, maximum and minimum hydraulic conductivity magnitudes and directions, and changes in material property across the site were made in order to match generated to observed potentials at those nodes in the finite element grid corresponding to wells in the tracer field.

Proper calibration was deemed to have been achieved when a reasonable match of generated to observed head potentials (differences on the order of 1 to 3 feet) was obtained, and when interactive runs with the solute transport model indicated plume travel times and directions which were consistent with field observations of the tracer test. The following is a chronological description of the calibration process.

Calibration Runs Prior To Test Start

The first two model runs used a grid possessing elements generally oriented at a 35 degree angle from strike. This orientation was selected based upon preliminary interpretatoons of drawdown potentiometric maps from the shallow tracer pump test. Directions of maximum hydraulic conductivity (K) and maximum transmissivity (T) were oriented at this angle and a hydraulic conductivity (K) of 0.567 ft/day in the direction of maximum T was used for the entire grid i.e. the system was initially set up as a homogenous, anisotropic system since heterogeneity indications from the shallow pump test were not significant. This K value was arrived at by calculating the geometric mean of all K values obtained by all possible methods for the shallow tracer pump test. The

minimum K was estimated by initially assuming a degree of anisotropy of 10:1, or one order of magnitude, based on the pump tests performed by Golder Associates in Bear Creek in 1986 (Reference 14). Boundary conditions were as described in Section 11.2.3.

After the results of the initial simulations were examined in detail, adjustments were made along the prescribed head boundary and in the degree of anisotropy.

The prescribed head and anisotropy were selected for adjustment because very little information was available on the actual distribution of heads along the northern boundary, and the actual degree of anisotropy in the shallow system was rather uncertain. The seventh simulation run, "RUN7", (available from Golder Associates) was of particular interest because it possessed the best calibration to observed heads of the first 8 simulations. Calculated heads were generally within 1.5 to 2.5 feet of observed hydraulic potentials. This calibration, although not perfect, was considered to represent a good first approximation of the shallow flow system and would serve as a good basis for preliminary solute transport runs. All of the preliminary simulations thus far discussed were created prior to the execution of the actual tracer test, and with the incorrect maximum transmissivity direction, previously mentioned in Section 11.2.2.

Calibration Runs After Test Start

The boundary conditions and mesh geometry utilized in the "RUN7" simulations were used throughout the initial simulation phase. Changes were made in the degree of anisotropy and maximum K direction when the tracer movement direction became known. Most notably, tracer movement seemed to be taking place in an along strike direction. This was not consistent with preliminary pump test interpretations which suggested

that maximum K and T directions were actually at a 35 degree angle from strike. Changes were then made in the model direction of maximum K in order that subsequent solute transport modeling would more accurately reflect the tracer movement.

The calibration was not improved by changing the maximum K direction to approximate strike, and increasing the degree of anisotropy; in fact, the calibration become worse. In general, it was found that smaller degrees of anisotropy, and larger angles from strike for maximum K, typically tended to increase the values of hydraulic head at wells in the tracer field thereby improving the hydraulic head calibration. The sensitivity of the model to changes in the hydraulic gradient along the prescribed head boundary, however, were typically less dramatic. This was likely due to the fixed conditions to the east and west of the study area.

In an attempt to obtain a better hydraulic head calibration and at the same time use a direction of maximum K along strike, it was considered that the concept of a homogeneous anisotropic flow field was inappropriate. Therefore, a second material property of low K, just south of the tracer area, was added. It was desirable to model the groundwater flow system and simulate observed tracer flow without the use of such a low K material, as this was recognized at the time as perhaps being an unjustified scenario. Attempts were made to model tracer movement with a region of K values representative of pump test results, and a region of equivalent or slightly lower K immediately south of the tracer path. Not only did calibration to observed heads worsen, but simulated tracer movement did not behave consistently with field observations. It was now realized that the orientation of elements in the grid, originally designed for an anisotropic flow direction 35 degrees from strike, was part of the cause of plume drift and poor calibration under the above described

conditions. New interpretations of shallow pump test drawdown data, based on the actual survey data, suggested a 1.5:1 to 2:1 level of anisotropy with a maximum T and K direction parallel to strike. Further, it was realized that mesh modification to some degree would be necessary.

A second phase of model simulations was embarked upon utilizing an adaption of the original finite element mesh. It was felt that a reworking of only the immediate tracer area, west of the injection point, would be the most expedient and cost effective approach to the problem. This area of the grid was reworked by the creation of uniform squares about 10 feet on a side, which were bisected to form triangles. The bisection directions of the triangles was setup in two directions to facilitate the up or down movement of the material property boundary guiding the tracer flow. The use of "RUN7" prescribed and constant head boundary conditions continued for the Phase II runs. The orientation of these new elements was established by drawing a line between wells GW-484 (injection point) and GW-493 (observation well at approximate plume center). This line was used to represent the axis of the approximate plume center, and all elements were oriented in this fashion. Sometime later, near the conclusion of the tracer test when official surveyor's data was received for the new wells drilled after the tracer test start, it was discovered that the location of GW-493 used in the new model grid was in error. The original line drawn was 10° from strike, and the redrawn line, using surveyed locations data was at about N56^{o}E, directly along strike.

A lower degree of anisotropy of 2:1 was utilized in Phase II runs and maximum K directions were oriented at about 5° to strike, parallel to the proposal plume axis locations.

Although various scenarios were simulated it was realized, once again, that the only way to model tracer flow with this grid would be to use a low K region to restrict tracer migration to the observed line of travel, in an attempt to simulate the apparent structure controlling the tracer plume.

Rationalization and justification for introducoing a degree of heterogenity into the model with the use of a low K "boundary" was sought. Field personnel were instructed to examine the stream bed along strike from the test area. They reported the presence of alternating resistant shale and weathered limestone beds in the location, with spacing between beds of about 3-5 feet. In addition, core logs and packer testing from wells GW-404, GW-471 and GW-455 demonstrated variability in both lithologic and hydraulic properties which indicated the presence of low (10^{-7} cm/s) to high (10^{-4} cm/s) hydraulic conductivities.

It is recognized that, in general, the packer spacings were too large to differentiate hydraulic conductivity variations on the order of 3 to 5 feet. However, small scale variation in hydraulic conductivity at the tracer area is evident from packer tests completed in GW-471. The packers were moved downhole 3.4 feet which resulted in a change in hydraulic conductivity from 5.39×10^{-6} cm/s to 7.1×10^{-5} cm/s. Additional justification for the low K boundary was based on review of boring logs for all water table wells which indicated the potential for the existence of bedrock highs and lows which could be associated with resistant (low K) and weathered (high K) units. Thus, it was felt very reasonable, based on the above evidence, to input a low K unit to the model.

The solute transport phase of the modeling will be discussed in greater detail in Section 11.3. However, it is now obvious that it was not sufficient to merely calibrate the groundwater flow model and then move unidirectionally into solute transport modeling. Rather, it was necessary to move back and forth between groundwater flow and solute transport simulations. If simulated solute transport did not agree with field observations it was sometimes necessary to move back to groundwater flow simulations and make changes in K magnitude and/or direction, material properties, and/or the degree of anisotropy. The groundwater flow model would then need to be recalibrated and a new solute transport solution was created for further comparison to field observations.

Final Calibration

A potentiometric surface map of the final calibrated model run appears as Plate 4. The final calibration incorporated two material types. The maximum hydraulic conductivity for material 1 for the final run was 5.6×10^{-1} ft/day (2×10^{-4} cm/s) and the minimum hydraulic conductivity used was 4.0×10^{-1} ft./day (1.4×10^{-4} cm/s) which are consistent both in magnitude and in degree of anisotropy with geometric means derived from the shallow pump test and with higher values derived from packer tests. The maximum and minimum hydraulic conductivity for material 2 were 5.0×10^{-3} ft/day (1.8×10^{-6} cm/s) and 5.0×10^{-4} ft/day (1.8×10^{-7} cm/s), respectively, which are consistent with lower values from packer tests. While the evidence to support the presence of such a low hydraulic conductivity regime at shallow depth, described above, might be debated since there are no measurements at the water table horizon, the configuration of the potentiometric surface within the region of tracer flow, and the calibration of model predicted potentials at the tracer

area wells appeared to be quite consistent with field observations and, thus, was expected to yield a reasonable prediction of tracer flow.

Qualitatively, the evidence to support the two material system may be the alternating resistant and less resistant shale beds that can be seen in the creek, west of the tracer area. In defending the two material system, it is recognized that the results of pump test analyses represent an average bulk permeability. The actual hydraulic conductivity of the more resistant shale beds is much lower. If the tracer indeed is moving through a "slot" of less resistant limestone sandwiched between two more resistant shale beds, the introduction of a low permeability "Wall" is appropriate. For modeling convenience, this scenario was modeled using a 2-layer system rather than a series of alternating layers. The net effect of this simplification is to alter the overall flow field vectors, especially to the south, however, the hydraulics of the flow field at or near the material boundary are unchanged.

The direction of maximum hydraulic conductivity for materials 1 and 2 was along a line of N 56°E (almost parallel to strike) which was consistent with field observations of tracer movement, the direction of anisotropy indicated by analysis of the shallow pump test, and observations of fracture sets from related coring data.

The calibration to potentials at shallow system wells in the tracer field was generally within 1 to 1.5 feet of observed static levels. A well by well comparison of generated versus observed potentials appears in Table 11.1.

11.3 Solute Transport Modeling

Data from the calibrated groundwater flow model, in conjunction with longitudinal and transverse dispersivity, porosity, and retardation estimates were used as input into the SOLTR program of the Golder Groundwater Package in order to obtain solute transport solutions over time for a given initial injection concentration and location.

11.3.1 Initial and Boundary Conditions

The finite element mesh was constructed so as to ensure that a nodal point would exactly coincide with the actual location of the injection well GW-484 to enable precise concentrations to be injected mathematically into the model to simulate injection in the field.

After observing the slow decay of the tracer in well GW-484 in the field, it was determined that a prolonged simulated injection would be more appropriate than a slug type of injection. An initial concentration of 7.36 kg/ft^3 was theoretically injected at node 282 at time 0.0 days prior to the solute transport solution phase. This concentration of 7.36 kg/ft^3 is equivalent to the 260,000 ppm injection of Rhodamine WT at well GW-484 in the field. Node 282 (injection point) was allowed to vary naturally over time in accordance with the steady state solution achieved during the groundwater flow modeling phase. The model predicted concentration decay at the injection well is in excellent agreement with the field observed decay, as depicted in Figure 10.2.

All boundary nodes were assigned an initial and constant concentrations of 0.0 kg/ft^3, except for nodes 271-281 and node 283 which lie in the general path of solute flow. These latter nodes were given an initial concentration of 0.0 kg/ft^3, but were allowed to vary naturally over time, thus allowing the travel of solute out of the modeled system, as

would be expected in the natural system. This prevented the backup of solute along the boundary at later time steps in the solute transport solution process.

11.3.2 Solute Transport Calibration

General

The calibration of the solute transport model essentially involved the same basic procedure as the calibration of the groundwater flow model. Adjustments in longitudinal and transverse dispersivity, and porosity were made in conjunction with interactive runs with the groundwater flow model in order to coordinate model simulated arrival times and concentrations with field observations. These comparisons of simulated to observed arrival times and concentrations were made at points in the finite element mesh that were interpolated to coincide with actual wells in the tracer field.

It was necessary to adjust calibration, in part, by making changes in the groundwater flow model, recalibrating the model, and then subsequently using the new steady state solution for a new solute transport solution phase. Therefore, calibration of the solute transport model, like calibration of the groundwater flow model, was an interactive and iterative process.

Calibration of the solute transport model was deemed complete when the groundwater flow model had been successfully calibrated to observed hydraulic heads, and when concentration breakthrough curves based on field data provided a reasonable match with model generated breakthrough curves.

Initial Solute Transport Calibration Runs

Initial runs of the solute transport model made use of longitudinal and transverse dispersivity and porosity values obtained from a pump test with tracers performed in October 1986 by Golder Associates in Bear Creek Valley within the Nolichucky Shale (Reference 14). The initial longitudinal dispersivity was 10 feet and the ratio of transverse dispersivity was varied from 1:1 to 10:1. The latter ratio tended to yield a more unidirectional (not dispersed in all directions) and reasonable plume slope. The porosity used (0.005, Reference 14) and retardation factor (0.67, Reference 16), were kept constant for the initial runs. A concentration of 1 kg/ft^3 was injected into the model in lieu of a known injection concentration in order to yield a proportional and not an absolute response in tracer migration. Both slug and protracted-type decay schemes were used. These preliminary runs were completed before actual tracer injection.

As was previously mentioned, tracer migration was anticipated to be oblique to strike, at an angle of about 35 degrees. However, soon after the actual tracer was injected, it became apparent that tracer was present only at wells in a more or less along strike directions from GW-484 (injection point). When this observation was compared with the 35 degree direction of anisotropy concept, it was speculated that the tracer plume might be following a somewhat "S-shaped" travel path.

A number of scenarios capable of explaining these phenomena were developed. It was possible that tracer flow was being controlled structurally by fracture sets or weathered zones in the upper portion of the bedrock. It was also conceivable that tracer flow was being controlled by variations in bedrock topography.

Therefore, in order to reconcile the model with field observations and theories of probable tracer behavior based upon known site data, a tentative approach of modeling a lower K region to the immediate south of the apparent line of tracer travel was embarked upon as a first step to a final model calibration. Progressively lower K's were used for this zone while the bulk pump test K value of 0.567 ft/day was retained for that part of the grid where the tracer was actually travelling. The direction of maximum K was initially left the same, and then was progressively decreased until it was along a line concurrent with strike. While both the "S-shaped" and along-strike scenarios were both achieved, head calibration was still a problem. It was realized that the low K region did not fully describe the layered nature of the medium, however, attempts to model the area as a relatively homogeneous, isotropic aquifer did not yield results that were consistent with observed tracer behavior.

It was becoming apparent that the tracer was being controlled by a structure with small width proportions, and that the limitations in modeling these structures with the existing grid might present a potential problem in producing a believable, defendable model. The low K used (.005 ft/day, 1.8×10^{-6} cm/s) was the only way to create a "wall" representing fracture or high bedrock control. It was also finally conceded that maintaining a 35 degree from strike direction of maximum K, despite the use of a low K "wall", was not conducive to simulating observed tracer movement.

Complicating the above issues was the absence of survey data for wells drilled and completed subsequent to the initiation of the tracer test. As it would later be discovered, this level of uncertainty as to true well location was to cause otherwise avoidable errors in the modeling process.

The next stage of modeling consisted of simulations which made use of along-strike directions of maximum K and T. Additionally, it was desirable to model these situations without the use of a retention or "wall" of low values of hydraulic conductivity. Attempts were made to model the observed tracer movement with a region of K values representative of pump test results, and a region of equivalent or slightly lower K immediately south of the tracer path. There were numerous problems with this approach. First, the plume was consistently too dispersed, despite the use of very low transverse dispersivity values. Next, the plume would consistently travel southward from strike despite the change in maximum K direction, unless very low K numbers were used, as in previous runs. Additionally, the plume was still moving too rapidly to be able to calibrate to field observations. It is believed that the orientation of elements in the grid originally designed for 35 degree from strike anisotropy, was the cause of some of the plume drift to the south. It was further realized that a reworking of the grid to at least some degree would be necessary.

Reworked Calibration Runs

For the final phase of model development it was decided that the finite element mesh in use needed to undergo refinement in order to be responsive to subtle changes in material property boundaries south of the apparent line of tracer travel. The idea of an "S-shaped" plume was abandoned as unlikely, and the theory of along-strike structural control seemed to be a more plausible approach to the problem.

As was mentioned earlier, it was felt that a reworking of the grid in the immediate tracer test area, west of the injection point, would be the most expedient and cost effective approach to the problem. As described in Section 11.3.1, this area of the grid was reworked by the creation of uniform

squares about 10 feet on a side, which were bisected to form triangles. The bisection directions of the triangles were setup in two directions to facilitate the up or down movement of the material property boundary guiding the tracer flow.

Since the highest concentration of tracer outside of the injection well was observed at GW-493, and survey data was not yet available on this well at the time, locations were approximated using pace and compass techniques. A line was drawn between wells GW-484 (injection well) and GW-493. This line was intended to represent the axis of the approximate center of the plume. This line made an angle approximately 85 degrees west to Y-12 North. This was used as the direction of maximum K for runs in this stage of the modeling process. Additionally, the degree of anisotropy was reduced to a 2:1 ratio, which was a reflection of refined pump test drawdown analysis made possible by the provision of current survey data.

Despite the fact that extremely high ratios of longitudinal to transverse dispersivity values were used (1000:1) the model plume was not narrow enough to satisfy field observations which indicated the actual plume width to be on the order of 5 to 6 ft.

Attempts were also being made to calibrate observed and generated concentrations of tracer as well as to accurately model plume shape. Porosity was increased over previous runs to decrease seepage velocity and thereby to slow the solute mass down. However, if porosity was sufficiently high to allow the necessary concentrations at the injection point, and longitudinal dispersivity was high enough to obtain concentrations at a given time that were consistent with observations made at wells along strike, then the dispersed front of the plume was too far ahead and first arrivals came too soon. It was recognized that a balance between porosity

and longitudinal dispersivity would allow sufficient solute to remain near the injection point to corroborate observations there, while allowing the plume front to disperse enough to reach nodal points which would match field arrival time observations.

The grid refinement described above was modified to allow a smooth line at an angle of 85 degrees west of Y-12 North, to be established as a material property boundary, immediately south of the observed tracer flow. After numerous simulations using alternative methods it was realized, as described earlier, that the only way to model tracer flow with this grid would be to use a low K region to prevent tracer migration away from the observed line, thereby simulating the structural control which was now obviously controlling tracer movement.

Final model calibration was made with groundwater flow and solute transport runs "FPM7" and "SOLTR7" respectively, (available at Golder Associates). Calibration was performed at nodes which most closely corresponded to the actual well locations, with respect to both approximate arrival time and concentration sometime after arrival. Specifically, concentration calibrations were made after 27 days at nodes corresponding to wells GW-493, GW-487, and GW-484. When factors such as head calibration and plume arrival time had been satisfied, the model concentrations at calibration nodes were converted into field units (ppb & ppm) and a dilution factor was calculated from GW-487 by taking model concentration and dividing it by observed concentration.

This dilution factor of 555 was applied to the model concentration at GW-493 and a result closely matching the field value was obtained. This calculation of a dilution factor was necessary to account for the effect of tracer dilution in the field by resident water in the observation wells. The

dilution factor, however, was not used for model concentrations at the injection point since all the water in well GW-484 was removed prior to the introduction of the tracer, therefore, direct comparisons between model and observed concentrations could be made at the injection point.

After the calibration phase was completed the model was run with the same parameters to simulate tracer migration 40 days into the future. When the concentration of the tracer had reached high enough concentrations to be visible at a node on the flood plain of the creek, a prediction was made as to the approximate arrival or occurrence time of that concentration at that location. Five observation wells were drilled in a line perpendicular to the direction of tracer movement at this location in the field for the purpose of validating the model.

Two valuable conclusions were made at the end of this phase of the modeling. First, the grid used for these 2 runs had elements getting progressively smaller towards the creek and along the material property boundary in the Material 1 zone. The plume in this region demonstrated a decisive "thinning" trend (ie. it pinched in) apparently demonstrating the effect a finer element mesh coupled with small transverse dispersivities could have on the plume shape. Perhaps if a finer mesh were used such small values of transverse dispersivity might not be necessary.

Additionally, if the entire grid were reworked to reflect the new maximum K direction and structural features obviously controlling the tracer migration, then more reasonable values of K might be used, as well as more reasonable boundaries for various material properties.

The second conclusion became evident after the receipt of accurate survey data for the tracer observation wells drilled during the test. It was apparent that the actual monitoring well locations differed somewhat from what had been originally estimated by pace and compass survey. For example, GW-493 was found to be nearly along-strike from GW-484. Consequently, the simulations made with tracer flow directed at 5 degrees from strike were somewhat in error, as were the placements of validation wells. Additionally, calibration to the wrong nodes was performed due to the mislocation of observation wells on the finite element grid.

Final Solute Transport Calibration

The final calibrated model used a longitudinal and transverse dispersivity of 10.0 ft. and 4.0 x 10^{-5} ft., respectively, for materials 1 and 2. The retardation factor for the tracer was 0.67 or 33% retardation, and the porosity used for both materials was 3.0 x 10^{-2}. The longitudinal dispersivity of 10 ft. is consistent with results obtained from the pump test with tracers performed in the Nolichucky Shale in 1986 (Reference 14). The extremely small value of transverse dispersivity was necessary in order to simulate the fracture or structure controlled dispersion behavior observed in the field. The retardation factor was arrived at based upon absorption characteristics of the Rhodamine WT, as reported in Reference 17.

Figures 11.1 through 11.3 present the results of the final model calibration in terms of model predicted verses field observed tracer breakthrough curves. The well by well comparison of observed versus calculated concentrations after 27 days appears as Table 11.2. This comparison was used as the final calibration of the solute transport model at the 27 day time step. The contour map of simulated concentration at 27 days appears as Plate 5.

11.4 Model Validation

The calibrated model was used to predict tracer arrival at the line of wells GW-495 through GW-499A (Figure 10.1). It is noted that the dilution factor of 555 was applied to the model predicted results at wells GW-495 through GW-499A.

Golder Associates' prediction for tracer arrival at these wells was presented to MMES in a telecopy transmittal dated May 19, 1988, as follows:

a. The tracer arrival, as defined as a measurement of about 1300 ppb will arrive at a point located 55 feet west of GW-493, along the direction of tracer migration, on Wednesday, May 25, 1988.

b. The predicted tracer concentration at observation well number GW-493 on Wednesday, May 25, 1988, is about 6500 ppb.

c. Once the tracer enters the flood plain at the above location, we expect it will become more dispersed as it moves to the stream in the flood plain materials. The tracer will probably enter the stream as a somewhat more laterally dispersed front.

Field monitoring of the six model validation wells continued through June 15, 1988. At the time of this writing, no tracer has been detected based on visual observations in any of these six wells. Consequently, in an effort to "find" the tracer, ten additional wells were installed between the six validation wells and GW-493. On July 11, 1988, tracer was detected in observation wells GW-499G, GW-499H, GW-499J, GW-499M, GW-499N, GW-499O, GW-499P, at levels of 130, 11, 10, 69, 234, 114, and 77 parts-per-billion, respectively. No additional analyses have been completed since July 11, 1988.

TABLE 11.1

GROUNDWATER FLOW MODEL HYDRAULIC HEAD CALIBRATION (2)

WELL NO.	NEAREST MESH NODE NO.	MODEL PREDICTED HYDRAULIC HEAD (FT MSL)	OBSERVED HYDRAULIC HEAD (3/25 to 3/26) (FT MSL)
GW-474	193	852.54	854.80
GW-475B	249	850.82	854.89
GW-475C	249	850.82	853.52
GW-476B	119	853.47	855.48
GW-476C	119	853.47	854.68
GW-477B	160	853.38	854.19
GW-477C	160	853.38	854.50
GW-478B	195	851.54	854.50
GW-478C	195	851.54	852.99
GW-480B	212	851.62	853.40
GW-480C	212	851.62	853.24
GW-481B	179	853.37	854.25
GW-481C	179	853.37	854.02
GW-482B	192	852.91	854.50
GW-482C	192	852.91	854.80
GW-483	86,121 (1)	855.00 (1)	855.88
GW-484	282	853.88	854.46

NOTES: (1) Actual well location is between listed nodes, therefore, in these cases the geometric mean of predicted heads is used for calibration.

(2) Comparisons between model predicted and actual head in intermediate (B) wells were considered to be more representative of the hydrogeologic system controlling tracer flow.

TABLE 11.2

SOLUTE TRANSPORT MODEL CALIBRATION
AFTER 27 DAYS

WELL NO.	NEAREST MESH NODE NO.	MODEL PREDICTED CONCENTRATION (1) (PPB)		OBSERVED CONCENTRATION (PPB)
GW-4818	179	1.74E+04		418
GW-484 (Injection)	282	5.60E+06	(2)	8.30E+06
GW-487	163,182	8,270	(3)	8,290
GW-493	183,184	4,049	(3)	~4,000

NOTES: (1) Model predicted concentrations shown were corrected for dilution factor of 555.
(2) Concentration shown was not corrected for dilution due to removal of all water in well prior to injection.
(3) Model concentration shown was interpolated from contour map between nodes listed.

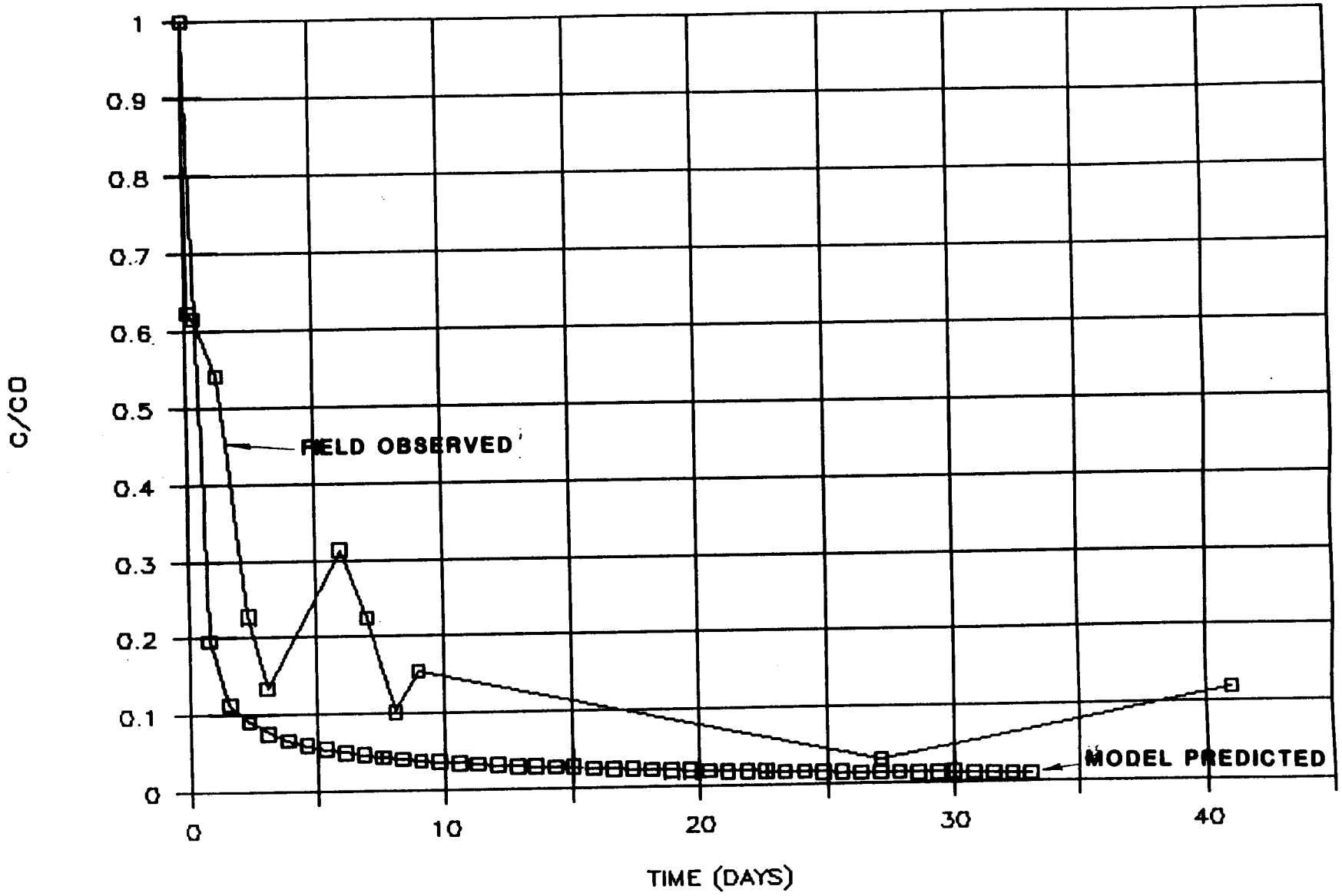

JOB NO 873-3512	SCALE AS SHOWN	Golder Associates	FIELD OBSERVED VERSUS MODEL PREDICTED BREAK-THROUGH CURVES, WELL NO: GW-484
DRAWN JLW	DATE 7/23/88		MARTIN MARIETTA ENERGY SYSTEMS, INC.
CHECKED JBJ	DWG NO 54		FIGURE 11.1

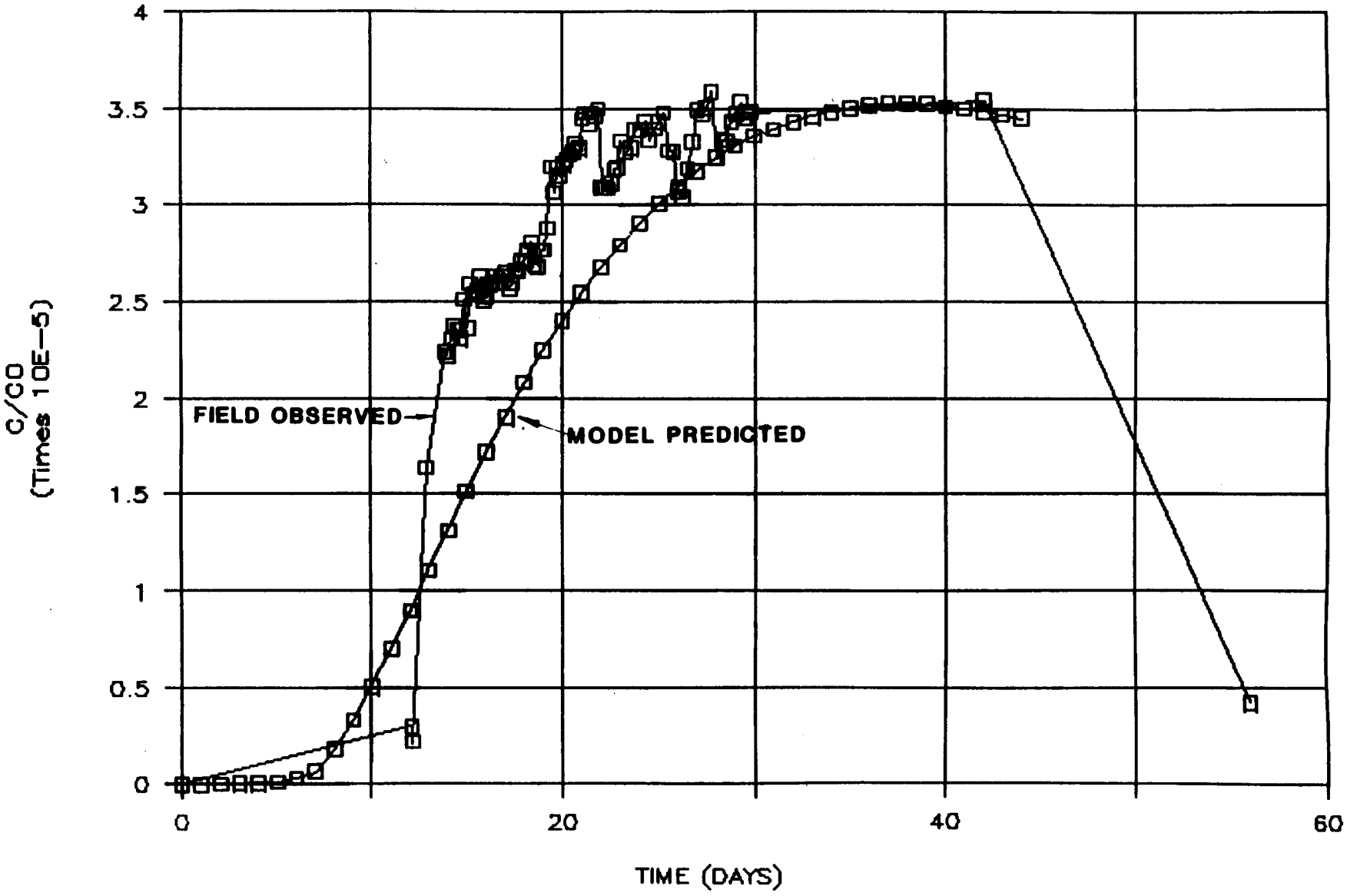

JOB NO 873-3512	SCALE AS SHOWN	Golder Associates	FIELD OBSERVED VERSUS MODEL PREDICTED BREAK-THROUGH CURVES, WELL NO: GW-487
DRAWN JLW	DATE 7/23/88		MARTIN MARIETTA ENERGY SYSTEMS, INC.
CHECKED JBJ	DWG NO 55		FIGURE 11.2

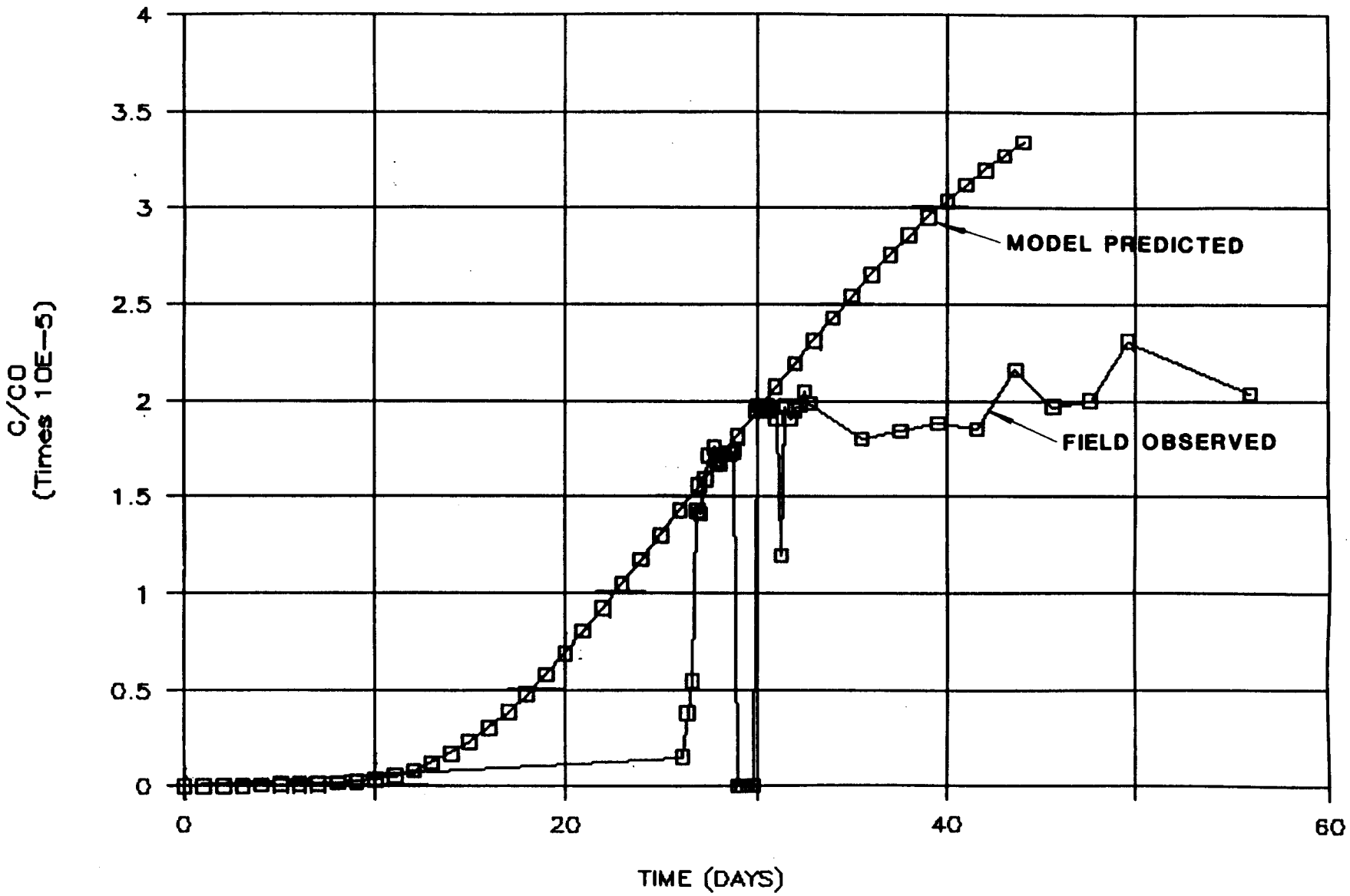

JOB NO 873-3512	SCALE AS SHOWN	Golder Associates	FIELD OBSERVED VERSUS MODEL PREDICTED BREAK-THROUGH CURVES, WELL NO: GW-493
DRAWN JLW	DATE 7/23/88		MARTIN MARIETTA ENERGY SYSTEMS, INC.
CHECKED JBJ	DWG NO 56		FIGURE 11.3

12.0 DISCUSSION OF RESULTS AND CONCLUSIONS

12.1 Final Model Validation

Model predicted verses field measured concentrations at observation well GW-481B (Table 11.2) indicated very poor calibration with regard to lateral migration. Modeling solute transport using finite element techniques, is known to be very sensitive to the fineness (or coarseness) of the mesh. Part of the problem was thus attributed to the coarseness of the finite element mesh relative to the tracer plume, which appeared very narrow; about 5-6 feet in width. In addition, much of the lateral dispersion depicted in Plate 5 is probably a by-product of a mesh that is too coarse to accurately simulate a narrow plane. Because of initial lack of success in validating the solute transport model, attempts were made to improve the model calibration.

In an attempt to produce a better calibration, a new finite element grid was developed. The revised grid was again coarse near boundaries, but was much finer in the area of the tracer well field. The new grid contained about 7400 elements and 7400 nodal points as compared to 281 nodes and 393 elements for the original mesh. The nodal spacing near the tracer well field was reduced from about 10 feet to one foot.

An initial run was made using the new mesh for debugging purposes only. Due to the size of the new grid, it was necessary to now make all runs on a VAX mainframe computer. It was recognized, however, that further development would delay final reporting. It was mutually decided with MMES that no additional simulations would be completed using the new grid.

This decision was also based on the realization that the flow field at the tracer area was clearly in a non-steady state due to drought conditions, which resulted in a dropping water table. Even if the new grid would result in a better calibration, it would not have resulted in a successful validation. A transient model would have to be developed for the possibility of a successful model validation.

12.2 Model Uncertainties and Deficiencies

At this point, the single-most important model deficiency is that the model was not built or run to simulate the non-steady flow conditions that were obviously controlling the tracer movement. As stated in Section 10.2.2, initial concerns were expressed regarding the unusually dry conditions that were being experienced in East Tennessee. These early concerns proved to be warranted, as the drought conditions resulted in a dropping water table and significantly decreased the driving hydraulic gradient at the tracer area.

Long term hydraulic head monitoring of the tracer area was completed using transducers and datalogger systems. The water level was monitored in wells GW-475B, GW-476B, GW-477B, GW-478A, GW-478B, and GW-478C. Plots of these water levels over time presented in the Task 3 report showed steadily declining water levels.

Table 12.1 presents a summary of water levels obtained at the tracer area. Figures 12.1 and 12.2 present the potentiometric surface at the tracer area on April 18, 1988, just prior to tracer injection and June 17, 1988, respectively. In general, the water table dropped about 3 feet during the period from tracer injection (4/20/88) through June 17, 1988. This resulted in a decreasing lateral hydraulic gradient throughout the test. The average driving gradient, as measured

between potentiometric contours (assuming a linear gradient) at the time of tracer injection was 0.08 ft/ft. This average gradient was reduced to 0.004 ft/ft as measured on June 17, 1988. Clearly the flow field was in a non-steady state.

The reduced gradient probably resulted in a slow-down of tracer migration. The breakthrough curves, presented in Section 11.0, indicate that the model appeared to be well calibrated for the first 30 days or so. However, as the hydraulics in the field changed, the steady state flow model, not surprisingly, resulted in poor calibration at longer times. It would be possible to calibrate many other models to the early field data. However, unless the models were designed to simulate the transient flow system resulting from drought conditions, it is highly unlikely that any of the models would result in a successful model validation.

One final point of model uncertainty lies in the treatment of the apparent structural trough of tracer migration. The effect of structure on groundwater flow is best illustrated by the potentiometric maps, Figures 12.1 and 12.2. Figure 12.1 shows the interpretation made for flow direction in the early days of the test. Figure 12.2 shows the data obtained, and new interpretation, after the test had run over 40 days. Not only had the gradient changed, but the increase in data points had revealed that the heads are also controlled by apparent structures. To simulate tracer migration along such structural troughs, a low hydraulic conductivity layer was imposed on the lower half of the grid. In reality, the entire tracer area at the bedrock horizon and perhaps in the overlying saprolite consists of interbedded layers of high and low hydraulic conductivity. As stated earlier, this alternating system was modeled, for convenience, as a two-layer system. The net effect was to alter the overall, model predicted, potentiometric surface at the tracer area.

However, the hydraulics of the flow system at the two-layer interface are unchanged. Perhaps a more rigorous approach, although not necessarily more accurate, would be to simulate the entire system as alternating layers of high and low hydraulic conductivity.

With regard to the applicability of modeling this system using a porous media approach rather than a discrete fracture network model, the porous media approach appears to be adequate. However, the porous media model must be able to simulate both heterogeneity and anisotropy and, most importantly, non-steady flow fields. The Golder Groundwater Package, a porous media model, can be used to simulate these conditions. With the benefit of hindsight, perhaps a time-variant flow field should have been used. However, at the time of model prediction, the model seemed to be accurately simulating the tracer movement. It was not until late in the test that it was obvious that the reduced gradient had significantly slowed the tracer migration. Although subsequent runs could have been made, it would have violated the essence of model predictions. That is, a prediction after collecting the field data would be mute.

12.3 Conclusions

The following is a list of the major conclusions made as a result of this effort:

- The field methods, including the use of Rhodamine WT, automatic samplers, and on site analytical tools, in conjunction with dry auger drilling techniques for plume tracking, were extremely successful for this test.
- The porous media finite element approach, when both heterogeneity and anisotropy were included, proved to be adequate in terms of developing a calibrated model to match the early time tracer results.
- A steady state flow field was not appropriate to simulate late time tracer results.

- Difficulties were caused in test interpretation and modeling, mainly due to inadequate definition of physical properties in the vicinity of the water table.

GOLDER ASSOCIATES INC.

John B. Johnston
Hydrogeologist

William B. Lozier, P.E.
Project Engineer

Ray Pearson, P.Eng.
Associate

WBL/WGG/RP:rcs

SEPTEMBER 1988 873-3512

TABLE 12.1

PAGE 1 OF 2

SUMMARY OF TRACER AREA
WATER LEVEL DATA

WELL NO.	MEAS. POINT ELEV.	4/18/88 DEPTH	4/18/88 ELEV.	6/17/88 DEPTH	6/17/88 ELEV.	6/30/88 DEPTH	6/30/88 ELEV.
GW-471	865.18	6.35	858.83	10.89	854.29	15.12	850.06
GW-473	868.93	11.55	857.38	13.81	855.12	14.65	854.28
GW-474	870.03	14.68	855.35	17.03	853	17.98	852.05
GW-475A	870.2	13.81	856.39	15.72	854.48	16.39	853.81
GW-475B	870.7	15.26	855.44	17.62	853.08	18.7	852
GW-475C	870.83	16.37	854.46	18.75	852.08	19.39	851.44
GW-476A	871.86	14.3	857.56	16.67	855.19	17.59	854.27
GW-476B	872.72	16.68	856.04	19.17	853.55	19.94	852.78
GW-476C	873.45	18.88	854.57	DRY		DRY	
GW-477A	870.13	12.58	857.55	14.97	855.16	15.83	854.3
GW-477B	870.75	16.03	854.72	18.15	852.6	19.02	851.73
GW-477C	871.39	16.75	854.64	18.42	852.97	19.03	852.36
GW-478A	865.2	8.17	857.03	10.45	854.75	11.25	853.95
GW-478B	865.4	10.36	855.04	12.69	852.71	13.54	851.86
GW-478C	865.55	11.91	853.64	13.76	851.79	14.41	851.14
GW-479	873.04	17.87	855.17	20.13	852.91	21.04	852
GW-480A	871.28	16.68	854.6	18.81	852.47	19.63	851.65
GW-480B	871.93	17.73	854.2	19.87	852.06	20.72	851.21
GW-480C	871.84	18.16	853.68	DRY		DRY	
GW-481A	871.13	15.97	855.16	18.33	852.8	19.15	851.98
GW-481B	870.5	15.62	854.88	18.71	851.79	--	
GW-481C	870.87	16.33	854.54	DRY		DRY	
GW-482A	871.18	15.87	855.31	18.14	853.04	18.93	852.25
GW-482B	871.46	16.34	855.12	18.58	852.88	19.41	852.05
GW-482C	871.96	17.86	854.1	DRY		DRY	

TABLE 12.1

PAGE 2 OF 2

SUMMARY OF TRACER AREA
WATER LEVEL DATA

WELL NO.	MEAS. POINT ELEV.	4/18/88 DEPTH	4/18/88 ELEV.	6/17/88 DEPTH	6/17/88 ELEV.	6/30/88 DEPTH	6/30/88 ELEV.
GW-485	864.3	--	--	12.75	851.55	14.18	850.12
GW-486	866.32	--	--	14.67	851.65	15.59	850.73
GW-487	865.25	--	--	13.38	851.87	14.4	850.85
GW-488	866.81	--	--	15.37	851.44	16.06	850.75
GW-489	867.27	--	--	15.7	851.57	16.57	850.7
GW-490	863.83	--	--	12.35	851.48	13.37	850.46
GW-491	864.69	--	--	13.02	851.67	14.09	850.6
GW-492	862.85	--	--	11.76	851.09	12.82	850.03
GW-493	863.99	--	--	12.27	851.72	13.31	850.68
GW-494	863.75	--	--	12.1	851.65	13.2	850.55
GW-495	855.08	--	--	7.91	847.17	8.38	846.7
GW-496	854.68	--	--	7.61	847.07	8.03	846.65
GW-497	854.57	--	--	6.06	848.51	6.78	847.79
GW-498	854.48	--	--	5.42	849.06	6.12	848.36
GW-499	854.85	--	--	6.62	848.23	7.16	847.69
GW-499A	854.69	--	--	7.47	847.22	7.92	846.77
GW-499G	859.76	--	--	7.08	852.68	10.01	849.75
GW-499H	859.77	--	--	9.03	850.74	10.01	849.76
GW-499I	859.75	--	--	10	849.75	10	849.75
GW-499J	859.6	--	--	8.78	850.82	9.96	849.64

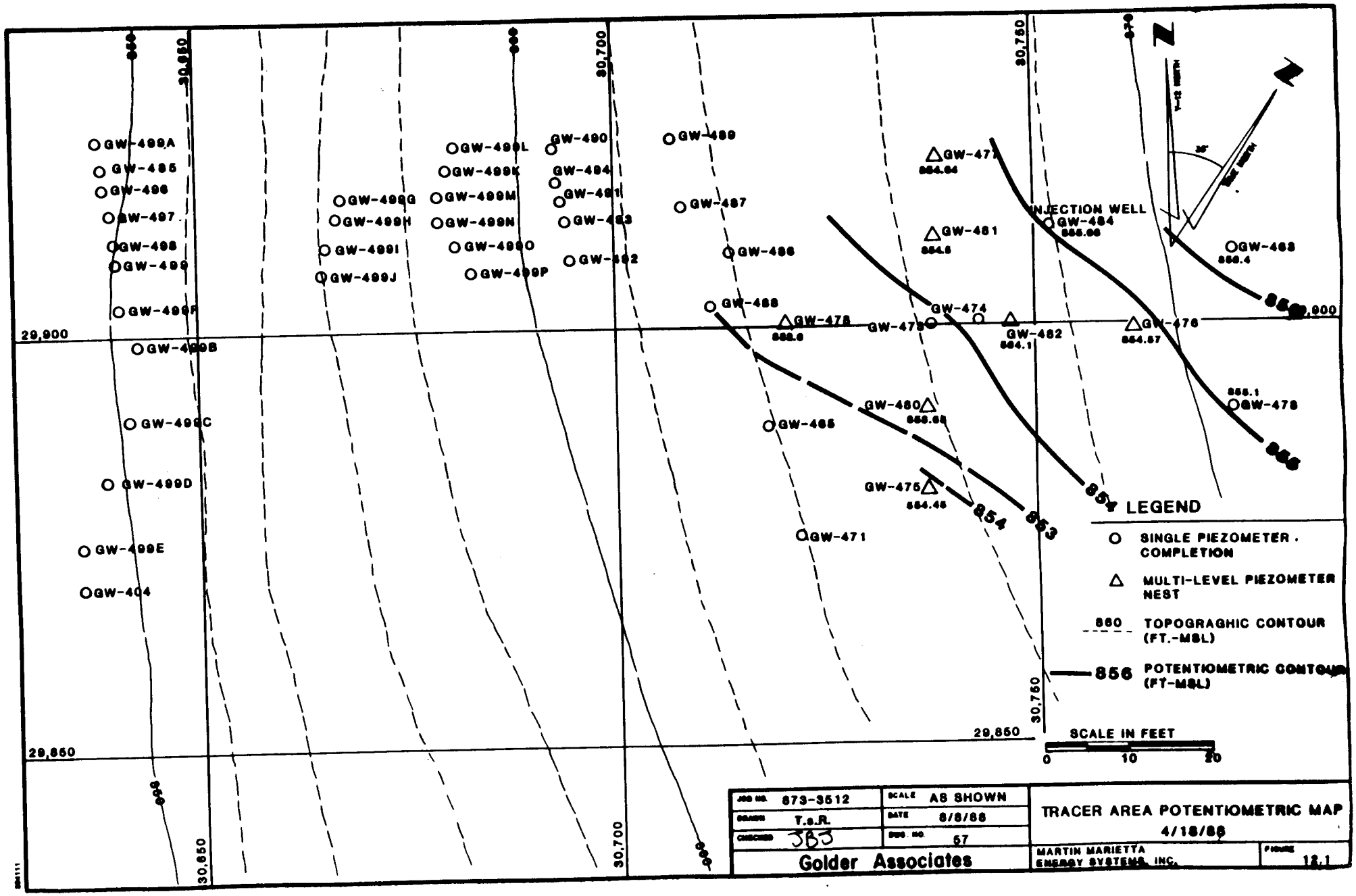
GW-499A
GW-485
GW-496
GW-497
GW-498
GW-499
GW-499F
GW-499B
GW-499C
GW-499D
GW-499E
GW-404
GW-499G
GW-499H
GW-499I
GW-499J
GW-499L
GW-499K
GW-499M
GW-499N
GW-499O
GW-499P
GW-490
GW-494
GW-491
GW-493
GW-492
GW-489
GW-487
GW-486
GW-488
GW-465
GW-471
GW-478
GW-479
GW-474
GW-482
GW-480
GW-475
GW-481
GW-484
INJECTION WELL
GW-463
GW-476
GW-477
854.64
854.5
555.06
554.4
554.1
554.57
555.1
554.45
29,900
29,850
30,650
30,700
30,750
N
LEGEND
SINGLE PIEZOMETER COMPLETION
MULTI-LEVEL PIEZOMETER NEST
860 TOPOGRAGHIC CONTOUR (FT.-MSL)
856 POTENTIOMETRIC CONTOUR (FT-MSL)
SCALE IN FEET
0
10
20
JOB NO. 873-3512
SCALE AS SHOWN
DRAWN T.S.R.
DATE 8/8/88
CHECKED JBJ
DWG. NO. 57
Golder Associates
TRACER AREA POTENTIOMETRIC MAP
4/18/88
MARTIN MARIETTA ENERGY SYSTEMS, INC.
FIGURE 12.1

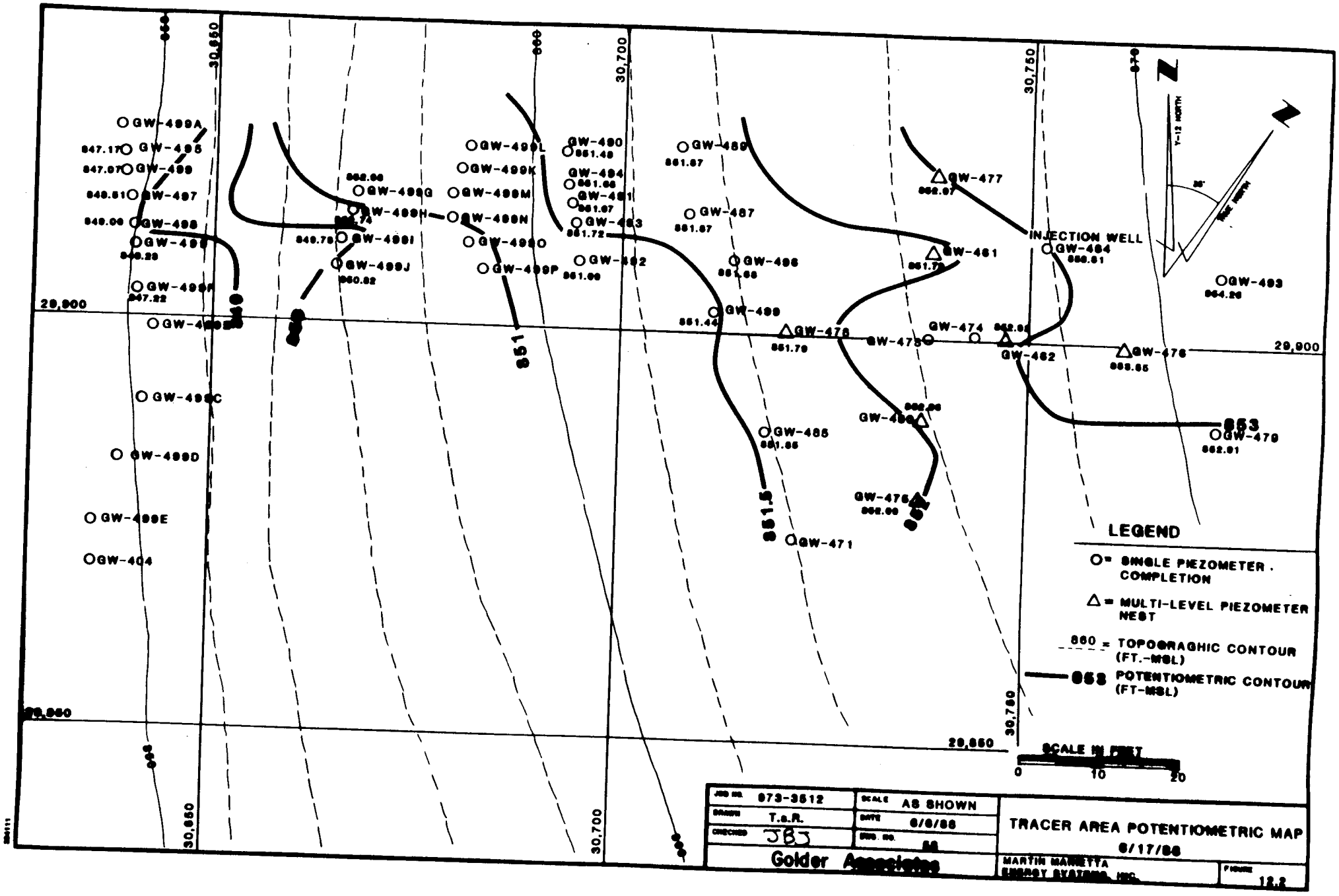
LEGEND
O = SINGLE PIEZOMETER COMPLETION
Δ = MULTI-LEVEL PIEZOMETER NEST
860 = TOPOGRAPHIC CONTOUR (FT.-MSL)
863 POTENTIOMETRIC CONTOUR (FT-MSL)
SCALE IN FEET
0 10 20
INJECTION WELL
GW-484
GW-477
GW-461
GW-474
GW-475
GW-462
GW-476
GW-479
GW-493
GW-471
GW-485
GW-487
GW-489
GW-490
GW-494
GW-491
GW-483
GW-492
GW-496
GW-499
GW-499A
GW-495
GW-499
GW-497
GW-498
GW-499B
GW-499F
GW-499C
GW-499D
GW-499E
GW-404
GW-499L
GW-499K
GW-499G
GW-499M
GW-499H
GW-499N
GW-499I
GW-499O
GW-499J
GW-499P
851
851.5
863
29,900
29,850
30,650
30,700
30,750
30,780
Golder Associates
TRACER AREA POTENTIOMETRIC MAP
6/17/86
MARTIN MARIETTA ENERGY SYSTEMS, INC.
FIGURE 12.2

REFERENCES

1. Chow, V.T., On the Determination of Transmissivity and Storage Coefficient from Pumping Test Data, Trans. Amer. Geophysical Union, Vol. 33, 1952.

2. Freeze, R.A. and J.A. Cherry, Groundwater, Prentice Hall, Inc., Englewood Cliffs, New Jersey, 1979.

3. Gierke, William G., Lozier, William B., Pearson, R., "Task 2, Well Logging and Geohydrologic Testing, Site Characterization and Groundwater Flow Computer Model Application, Contract No. 30X-SA706C," Oak Ridge National Laboratory, Oak Ridge, Tennessee, May, 1988, ORNL/SUG/-30X-SA706C..

4. Golder Associates, Groundwater Computer Package, Golder Associates, Inc., Seattle, WA, 1979.

5. Golder Associates, Quarterly Technical Progress Report Geohydrologic Site Characterization and Groundwater Flow Computer Model, Contract No. 30X-SA706C, for Martin-Marietta Energy Systems, Inc., December, 1987.

6. Golder Associates, Second Quarterly Progress Report Geohydrologic Site Characterization and Groundwater Flow Computer Model, Contract No. 30X-SA706C, for Martin-Marietta Energy Systems, Inc., March, 1988.

7. Gringarten, A.C., D.P. Bourdet, P.A. Landell, and V.J. Kniazeff., A Comparison Between Different Skin and Wellbore Storage Type Curves for Early-Time Transient Analysis, Presented at the SPE-AIME 54th Annual Fall Technical Conference and Exhibition, Las Vegas, Nevada, Sept. 23-26; Society of Petroleum Engineers Reprint SPE-8205, 1979.

8. Gringarten, A.C. and Witherspoon, P.A. A Method of Analyzing Pump Test Data From Fractured Aquifers. Proc. Symposium on Percolation Through Fissured Rock, Stuttgart, Inst. Soc. Rock Mechanics and Intl. Assn. Engineering Geol, T#-B-1 to T#-B-8, 1972.

9. Horner, D.R., Pressure Build-Up in Wells, Proceedings, Third World Petroleum Congress, The Hague Section II, 503-523, 1951. Also Reprint Series No. 9 Pressure Analysis Methods, Society of Petroleum Engineers of AIME, Dallas, 1967, P. 25-43.

10. Hvorslev, M.J., Time Lag and Soil Permeability in Groundwater Observations, Bulletin No. 36, Waterways Experiment Station, Corps of Engineers, Vicksburg, Miss., 1951.

11. Johnston, John B., Pearson, R., Task 3, Hydraulic Head Data Collection, Geohydrological Site Characterization and Groundwater Flow Computer Model Application, Contract No. 30X-SA706C, Oak Ridge National Laboratory, Oak Ridge, Tennessee, September, 1988, ORNL/Sub/30X-SA706C.

12. Kruseman, G.P. and N.A. De Ridder, Analysis and Evaluation of Pumping Test Data, International Institute for Land Reclamation and Improvement, Wageningen, The Netherlands, 1983.

13. Lozier, W.B., Spiers, C.A., Pearson, R., Aquifer Pump Test With Tracers, Oak Ridge National Laboratory, Oak Ridge, TN, 1986, ORNL/Sub/86-32136/2.

14. Neuman, S.P. Analysis of Pumping Test Data From Anisotropic Uniconfined Aquifers Considering Delayed Gravity Response. Water Resources Research, Vol. II, No. 2, pp. 329-342, 1975.

15. Papadopulos, I.S. Nonsteady Flow to a Well in an Infinite Anisotropic. Hydrology of Fractured Rocks, Proceedings of Dubrovnik Symposium, Vol. I, 1965.

16. Smart, P.L. and Laidlaw, I.M.S., 1976, An Evaluation of Some Fluorescent Dyes for Water Tracing, Water Resources Research, AGU, Vol. 13, No. 1, pp 15-33.

17. Strickland, Donald J., Pearson, R., Task 4, Groundwater Geochemical Sampling and Analysis - Site Characterization and Groundwater Computer Model Application, Contract No. 30X-SA706C, Oak Ridge National Laboratory, Oak Ridge, Tennessee, September, 1988, ORNL/Sub/30X-SA706C.

18. Theis, C.V., The Relation Between the Lowering of the Piezometric Surface and the Rate and Duration of Discharge of a Well Using Groundwater Storage, Trans. Am. Geophys. Un., 16th annual meeting, pt. 2, pp. 519-524, 1935.